Duke Energy℠

H. B. Barron
Vice President

March 19, 2002

U.S. Nuclear Regulatory Commission
ATTN: Document Control Desk
Washington, DC 20555

Subject: McGuire Nuclear Station, Units 1 and 2
                Docket Nos. 50-369, 50-370
                Reactor Cavity Neutron Measurement Program

During Cycle 12 of reactor operation, a reactor cavity measurement program was instituted at each McGuire unit to provided continuous monitoring of the beltline region of the reactor vessel. The use of the cavity measurement program coupled with available surveillance capsule measurements provides a plant specific data base that enables the evaluation of the vessel neutron exposure and the uncertainty associated with that exposure over the licensed life of the unit.

The results of the reactor cavity measurement program for McGuire Unit 1 are contained in WCAP-15253, "Duke Power Company Reactor Cavity Neutron Measurement Program for William B. McGuire Unit 1 Cycle 12" (attached). Similarly, the results for McGuire Unit 2 are contained in WCAP-15334, "Duke Power Company Reactor Cavity Neutron Measurement Program for William B. McGuire Unit 2 Cycle 12" (also attached).

By letter dated June 13, 2001, Duke Energy Corporation (DEC) submitted an Application to Renew the Facility Operating Licenses of McGuire Nuclear Station and Catawba Nuclear Station (Application). In a letter dated January 28, 2002, the staff provided requests for additional information (RAIs) based on its review of the reactor coolant system portion of the Application. Both of the above WCAPs will be referenced in some of the Duke responses to these staff RAIs, which will be submitted on or about April 15, 2002. WCAP-15253 and WCAP-15334 may also be referenced in future licensing submittals pertaining the McGuire reactor vessels and neutron exposure.

If there are any questions concerning this submittal, please contact either Kay Crane at (704) 875-4306 or Bob Gill at (704) 382-3339.

[signature]

H. B. Barron

Attachments

A001

cc: R. E. Martin
        U. S. Nuclear Regulatory Commission
        Office of Nuclear Reactor Regulation
        Washington, D.C. 20555

        Rani L. Franovich
        U. S. Nuclear Regulatory Commission
        License Renewal and Environmental Impacts Program
        Office of Nuclear Reactor Regulation
        Washington, D.C. 20555

        Luis A. Reyes
        U. S. Nuclear Regulatory Commission
        Atlanta Federal Center
        61 Forsyth St., SW, Suite 23T85
        Atlanta, GA 30303

        Scott Shaeffer
        Senior Resident Inspector
        McGuire Nuclear Station

U. S. Nuclear Regulatory Commission
Document Control Desk
March 19, 2002
Page 3

bxc: ELL
        RGC File
        Master File
        Bob Gill

◆ ◆ ◆ ◆ ◆ ◆ ◆ ◆ ◆ ◆ ◆

**WCAP - 15334
Revision 0**

Duke Power Company Reactor Cavity Neutron Measurement Program for William B. McGuire Unit 2 Cycle 12

Westinghouse Electric Company LLC

WCAP-15334

Duke Power Company
Reactor Cavity Neutron Measurement Program
for
William B. McGuire Unit 2 Cycle 12

Arnold H. Fero
Radiation Engineering and Analysis

November 1999

Approved:
G. A. Brassart, Manager
Radiation Engineering and Analysis

Prepared by Westinghouse for the Duke Power Company
Purchase Order No. MN19501
Work performed under Shop Order No. DIPP450

TABLE OF CONTENTS

LIST OF TABLES

LIST OF TABLES (Continued)

LIST OF TABLES (Continued)

LIST OF TABLES (Continued)

LIST OF FIGURES

EXECUTIVE SUMMARY

All of the calculations and dosimetry evaluations presented in this report have been based on the BUGLE-96 nuclear cross-section data library derived from ENDF/B-VI. The analysis presented in this report is consistent with the NRC approved methodology detailed in WCAP-14040-NP-A[1].

During Cycle 12 of reactor operation, a reactor cavity measurement program was instituted at McGuire Unit 2 to provide continuous monitoring of the beltline region of the reactor vessel. The use of the cavity measurement program coupled with available surveillance capsule measurements provides a plant specific data base that enables the evaluation of the vessel exposure and the uncertainty associated with that exposure over the service life of the unit.

To date, reactor cavity dosimetry has been evaluated at the conclusion of Cycle 12, in addition to the six internal surveillance capsules withdrawn following Cycle 1, 5, 7, 8 and 10, resulting in the following projected best estimate fast neutron fluence levels at the inner radius of the reactor vessel wall:

MIDPLANE/MAXIMUM Φ (E > 1.0 MeV) [n/cm^2]

Azimuth	EOC 10	EOC 12
0°	3.32E+18	3.97E+18
15°	4.96E+18	5.93E+18
30°	4.67E+18	5.64E+18
45°	5.28E+18	6.36E+18

The maximum exposure location occurs at the axial core midplane. Since the intermediate and lower shell forgings are joined by a circumferential weld that is located at essentially the same location, all of these materials see approximately the same neutron exposure.

Based on the continued use of an average (Cycles 10–12) low leakage fuel loading pattern, the projected maximum fast neutron exposure of the vessel beltline materials at 21, 34, and 51 effective full power years of operation is summarized as follows:

	Φ (E > 1.0 MeV) [n/cm^2]		
Reactor Vessel Beltline Material	**21 EFPY**	**34 EFPY**	**51 EFPY**
Intermediate Shell Forging - 526840 Circumferential Weld – W05 Lower Shell Forging - 411337	1.07E+19	1.68E+19	2.47E+19
Circumferential Weld – W04 Lower Transition Shell Forging - 527428	4.37E+18	6.86E+18	1.01E+19

As further data are accumulated from subsequent irradiations, the neutron environment in the vicinity of the Unit 2 reactor vessel will become better characterized and the uncertainties in the vessel exposure projections will be reduced. Thus, the measurement program will permit the assessment of vessel condition to be based on realistic exposure levels with known uncertainties and will eliminate the need for any unnecessary conservatism in the determination of vessel operating parameters.

1 OVERVIEW OF THE PROGRAM

The Reactor Cavity Neutron Measurement Program initiated at McGuire Unit 2 at the onset of reactor operation was designed to provide a mechanism for the long term monitoring of the neutron exposure of those portions of the reactor vessel and vessel support structure which may experience radiation induced increases in reference nil ductility transition temperature (RT_{NDT}) over the nuclear power plant lifetime. When used in conjunction with dosimetry from internal surveillance capsules[2], the reactor cavity neutron dosimetry provides an extensive plant specific measurement data base that can be used with the results of neutron transport calculations to provide best estimate neutron exposure projections for the reactor vessel with a minimum uncertainty. Minimizing the uncertainty in the neutron exposure projections will, in turn, help to assure that the reactor can be operated in the least restrictive mode possible with respect to

1. 10CFR50 Appendix G pressure/temperature limit curves for normal heatup and cooldown of the reactor coolant system.
2. Emergency Response Guideline (ERG) pressure/temperature limit curves.
3. Pressurized Thermal Shock (PTS) RT_{PTS} screening criteria.

In addition, an accurate measure of the neutron exposure of the reactor vessel and support structure can provide a sound basis for requalification should operation of the plant beyond the current design and/or licensed lifetime prove to be desirable.

In the assessment of the state of embrittlement of light water reactor vessels, an accurate evaluation of the neutron exposure of the materials comprising the beltline region of the vessel is required. This exposure evaluation must, in general, include assessments not only at locations of maximum exposure at the inner diameter of the vessel, but, also, as a function of axial, azimuthal, and radial location throughout the vessel wall.

A schematic of the beltline region of the McGuire Unit 2 reactor vessel is provided in Figure 1-1. In this case, the beltline region is constructed of three ring forgings and two circumferential welds. Each of these five materials must be considered in the overall embrittlement assessments of the reactor vessel.

In order to satisfy the requirements of 10CFR50 Appendix G for the calculation of pressure/temperature limit curves for normal heatup and cooldown of the reactor coolant system, fast neutron exposure levels must be defined at depths within the vessel wall equal to 25 and 75 percent of the wall thickness for each of the materials comprising the beltline region. These locations are commonly referred to as the ¼T and ¾T positions in the vessel wall. The ¼T exposure levels are also used in the determination of upper shelf fracture toughness as specified in 10CFR50 Appendix G.

In the determination of values of RT_{PTS} for comparison with applicable pressurized thermal shock screening criteria for plates, longitudinal welds, and circumferential welds, maximum neutron exposure levels experienced by each of the beltline materials are required. These maximum levels will, of course, occur at the vessel inner radius.

In the event that a probabilistic fracture mechanics evaluation of the reactor vessel is performed, or if an evaluation of thermal annealing and subsequent material re-embrittlement is undertaken, a complete embrittlement profile is required for the entire volume of the reactor vessel beltline. The determination of this embrittlement profile would, in turn, necessitate the evaluation of neutron exposure gradients throughout the entire beltline.

The methodology used to provide these required best estimate neutron exposure evaluations for the McGuire Unit 2 reactor vessel is based on the underlying philosophy that, in order to minimize the uncertainties associated with vessel exposure projections, plant specific neutron transport calculations must be supported by benchmarking of the analytical approach, comparison with industry wide power reactor data bases of surveillance capsule and reactor cavity dosimetry, and, ultimately, by validation with plant specific surveillance capsule and reactor cavity dosimetry data bases. That is, as a progression is made from the use of a purely analytical approach tied to experimental benchmarks to an approach that makes use of industry and plant specific power reactor measurements to remove potential biases in the analytical method, knowledge regarding the neutron environment applicable to a specific reactor vessel is increased and the uncertainty associated with vessel exposure projections is minimized.

With this overall methodology in mind, the Reactor Cavity Measurement Program was established to meet the following objectives:

1. Provide a measurement data base sufficient to:
   a. remove biases that may be present in analytical predictions of neutron exposure; and
   b. support the methodology for the projection of exposure gradients through the thickness of the reactor vessel wall.
2. Establish uncertainties in the best estimate fluence projections for the reactor vessel wall.
3. Provide a long term continuous monitoring capability for the beltline region of the reactor vessel.

This report provides the results of neutron dosimetry evaluations performed subsequent to the completion of Cycle 12. Fast neutron exposure in terms of fast neutron fluence (E > 1.0 MeV) and dpa is established for all measurement locations in the reactor cavity. The analytical formalism describing the relationship among the measurement points and locations within the reactor vessel wall is described and used to project the exposure of the vessel itself.

Results of exposure evaluations from surveillance capsule dosimetry withdrawn at the end of Cycles 1, 5, 7, 8, and 10 as well as cavity dosimetry results from Cycle 12 are incorporated to provide the integrated exposure of the reactor vessel from plant startup through the end of Cycle 12. Also, uncertainties associated with the derived exposure parameters at the measurement locations and with the projected exposure of the reactor vessel are provided.

In addition to the evaluation of the current exposure of the reactor vessel beltline materials, projections of the future exposure of the vessel are also provided. Current evaluations and future projections are provided for each of the beltline weldments as well as for the forgings comprising the intermediate, lower, and transition shells.

All of the calculations and dosimetry evaluations presented in this report have been based on the BUGLE-96 nuclear cross-section data library derived from ENDF/B-VI.
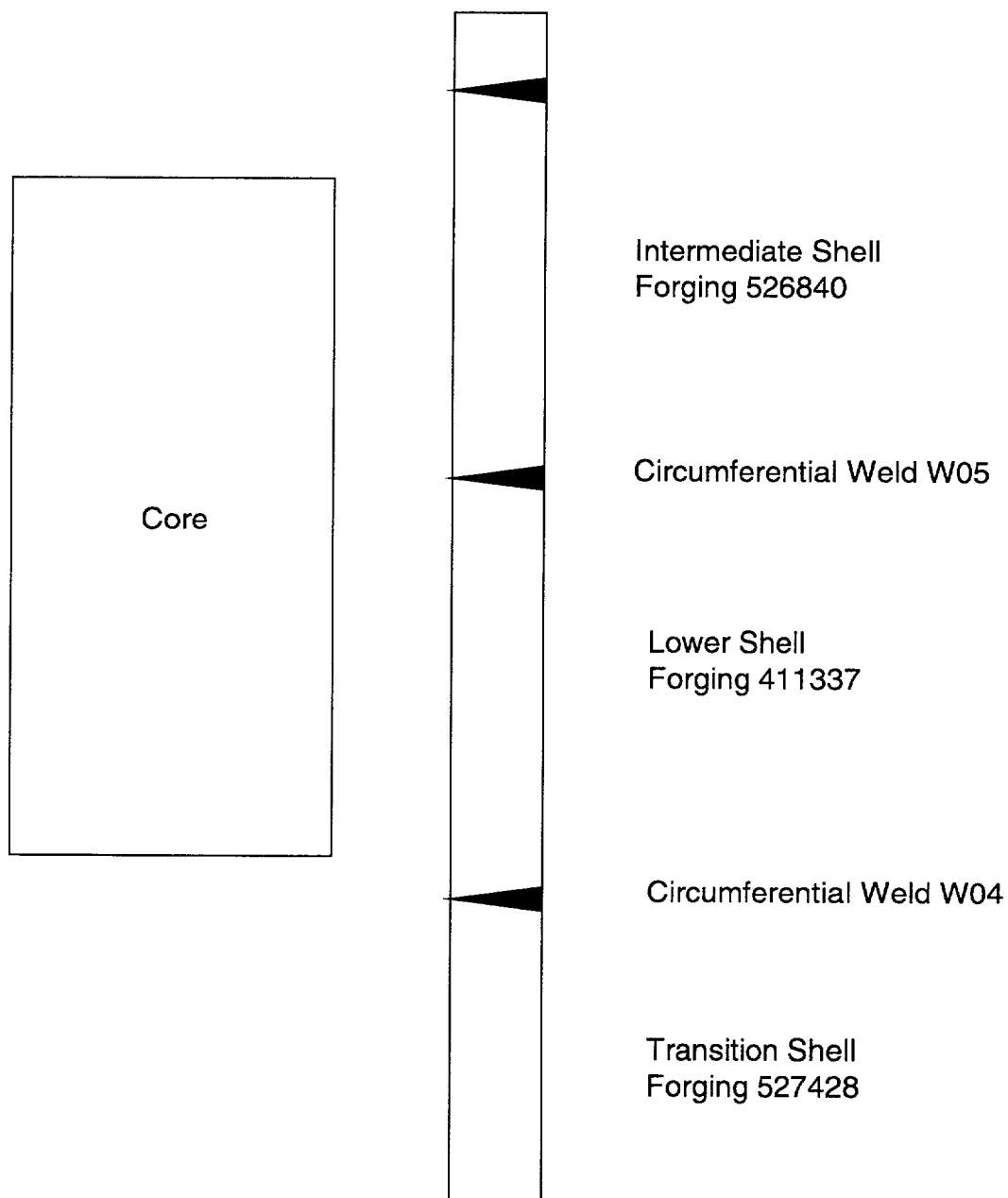
Figure 1-1 Description of Reactor Vessel Beltline Materials

2   DESCRIPTION OF THE MEASUREMENT PROGRAM

2.1   DESCRIPTION OF REACTOR CAVITY DOSIMETRY

To achieve the goals of the Reactor Cavity Neutron Measurement Program, comprehensive multiple foil sensor sets consisting of radiometric monitors (RM) were installed at several locations in the reactor cavity to characterize the neutron energy spectra within the beltline region of the reactor vessel. In addition, gradient chains were used in conjunction with the encapsulated sensors to complete the azimuthal and axial mapping of the neutron environment over the regions of interest.

Placement of the multiple foil sensor sets was such that spectra evaluations could be made at four azimuthal locations at an axial elevation representative of the midplane of the reactor core. The intent here was to determine changes in spectra caused by varying amounts of water located between the core and the reactor vessel. Due to the irregular shape of the reactor core, water thickness varies significantly as a function of azimuthal angle. In addition to the four midplane sensor sets, two multiple foil packages were positioned opposite the top and bottom of the active core at the azimuthal angle corresponding to the maximum neutron flux. Here the intent was to measure variations in neutron spectra over the core height; particularly near the top of the fuel where backscattering of neutrons from primary loop nozzles and vessel support structures could produce significant perturbations. At each of the four azimuthal locations selected for core midplane spectra measurements, gradient chains extended over a thirteen foot height centered on the core midplane.

2.1.1   Sensor Placement in the Reactor Cavity

The placement of the individual multiple foil sensor sets and gradient chains within the reactor cavity is illustrated in Figures 2.1-1 and 2.1-2. In Figure 2.1-1 plan views of the azimuthal locations of the four strings of sensor sets are depicted. The strings were located at azimuthal positions of 0.5, 14.5, 29.5, and 44.5 degrees relative to the core cardinal axis. The sensor strings were hung in the annular gap between the reactor vessel insulation and the primary biological shield at a nominal radius of 101.75 inches relative to the core centerline.

In Figure 2.1-2, the axial extent of each of the sensor set strings is illustrated along with the locations of the multiple foil holders used during the Cycle 12 irradiation. At the 44.5° azimuth, multiple foil sets were positioned at the core midplane as well as opposite the top and bottom of the active fuel. At each of the remaining azimuthal locations, multiple foil sets were positioned only opposite the core midplane. In all cases, stainless steel gradient chains extended ± 6.5 feet relative to the midplane of the active core.

The sensor sets and gradient chains were suspended from a support bar that hung underneath the Bravo Loop hot leg nozzle. The support bar was suspended from support plates welded to the liner plate at El. 746'+10½". The top edge of the support bar was positioned 10 inches above the top of the active fuel. The sensor sets and gradient chains were retained and supported at the bottom by chain clamps attached to the mounting plates bolted to the bioshield wall in the sump area below the reactor vessel. The design of the dosimetry support bar along with the

gradient chains and stops ensured correct axial and azimuthal positioning of the dosimetry relative to well known reactor features.

2.1.2   Description of Irradiation Capsules

The sensor sets used to characterize the neutron spectra within the reactor cavity were retained in 3.87 inch x 1.00 inch x 0.50 inch rectangular Type 6061 aluminum capsules such as that shown in Figure 2.1-3. Each capsule included three compartments to hold the neutron sensors. The top compartment (position 1) was intended to accommodate bare radiometric monitors, whereas, the two remaining compartments (positions 2 and 3) were meant to house cadmium shielded packages. The separation between positions 1 and 2 was such that cadmium shields inserted into position 2 did not introduce perturbations in the thermal flux in position 1. Type 6061 aluminum was selected for the dosimeter capsules in order to minimize neutron flux perturbations at the sensor set locations as well as to limit the radiation levels associated with post-irradiation shipping and handling of the capsules. A summary of the contents of the multiple foil capsules used during the Cycle 12 irradiation is provided in the appendices to this report.

2.1.3   Description of Gradient Chains

Along with the multiple foil sensor sets placed at discrete locations within the reactor cavity, gradient chains were employed to obtain axial variations of fast neutron exposure along each of the four traverses. Subsequent to irradiation these gradient chains were removed from the cavity and segmented to provide neutron reaction rate measurements at one-foot intervals over the height of the axial traverses. When coupled with a chemical analysis, the stainless steel gradient chains yielded activation results for the $^{54}Fe(n,p)^{54}Mn$, $^{58}Ni(n,p)^{58}Co$, and $^{59}Co(n,\gamma)^{60}Co$ reactions. The high purity iron, nickel, and cobalt-aluminum foils contained in the multiple foil sensor sets irradiated during Cycle 12 established a direct correlation with the measured reaction rates from the stainless steel chain and are used to confirm the composition of the 18-8 stainless steel gradient chain.
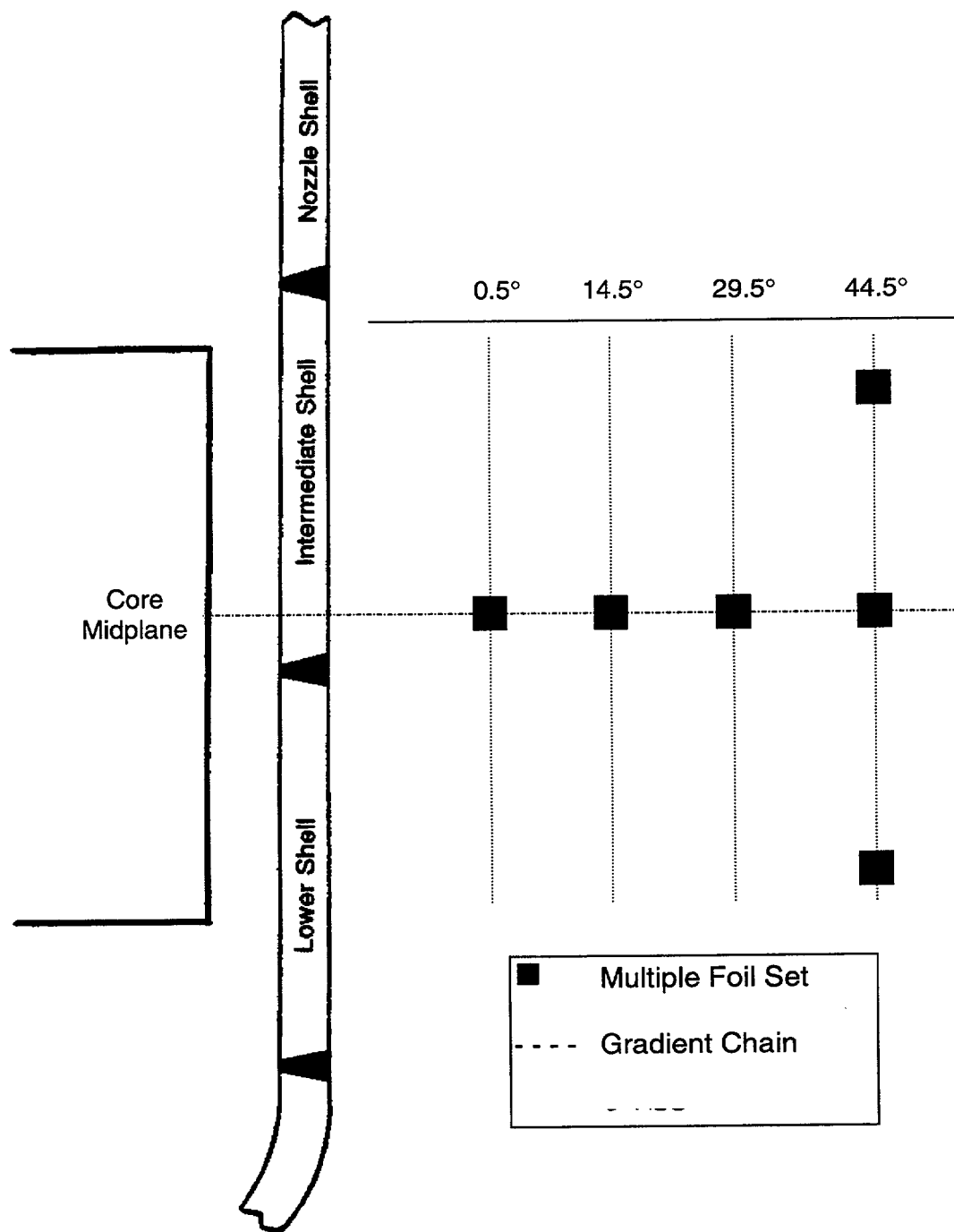
Figure 2.1-1 Axial Location of Multiple Foil Sensor Sets

Pos. 1-Bare
Fe Foil
Co Foil

Pos. 2-Cd
Fe Foil
Ni Foil
Cu Foil
Ti Foil
Co Foil

Pos. 3-Cd
U-238 RM
Np-237 RM
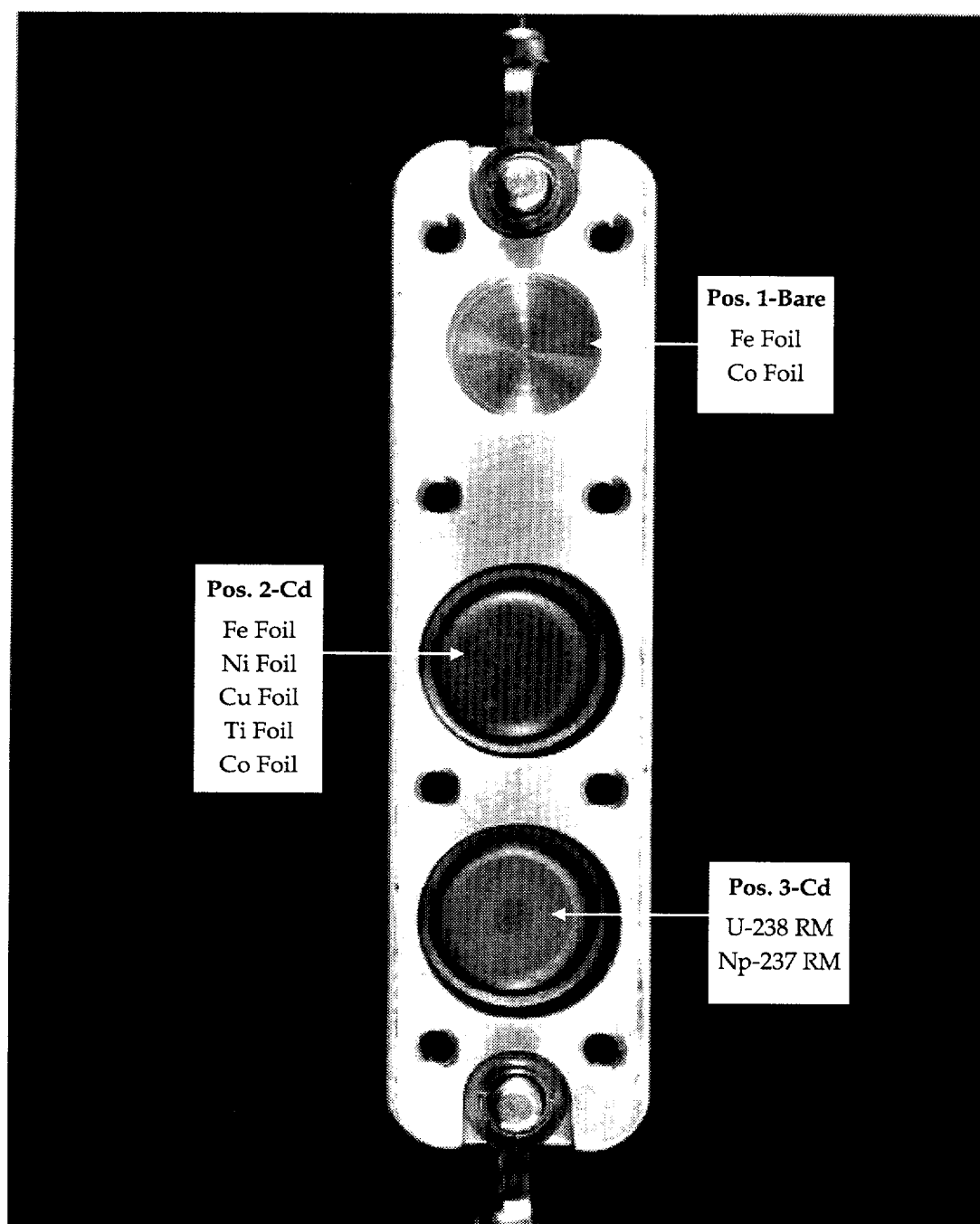
Figure 2.1-2 Irradiation Capsule for Cavity Sensor Sets

2.2 DESCRIPTION OF SURVEILLANCE CAPSULE DOSIMETRY

At the conclusion of the first fuel cycle at McGuire Unit 2, the first material surveillance capsule was withdrawn from its position between the neutron pad and the reactor vessel. The second internal surveillance capsule was withdrawn at the conclusion of Cycle 5, a third capsule was withdrawn at the end of Cycle 7, two more were withdrawn following Cycle 8, and the sixth and final capsule was withdrawn after Cycle 10. The neutron dosimetry contained within these capsules provided a measure of the integral exposure received by the capsules during their respective irradiation periods; i.e., Cycle 1, Cycles 1 through 5, Cycles 1 through 7, Cycles 1 through 8, and Cycles 1 through 10.

The type and location of the neutron sensors included in the materials surveillance program are described in some detail in Reference 2; and, are illustrated schematically in Figure 2.2-1 of this report.

Relative to Figure 2.2-1, copper, iron, nickel, and cobalt-aluminum monitors, in wire form, were placed in holes drilled in spacers at several axial levels within each capsule. The cadmium-shielded uranium and neptunium fission monitors were accommodated within a dosimeter block located near the center of the capsule. Specific information pertinent to the individual sensor sets included in Capsules V, X, U, Y, Z, and W is provided in the appendices to this report.
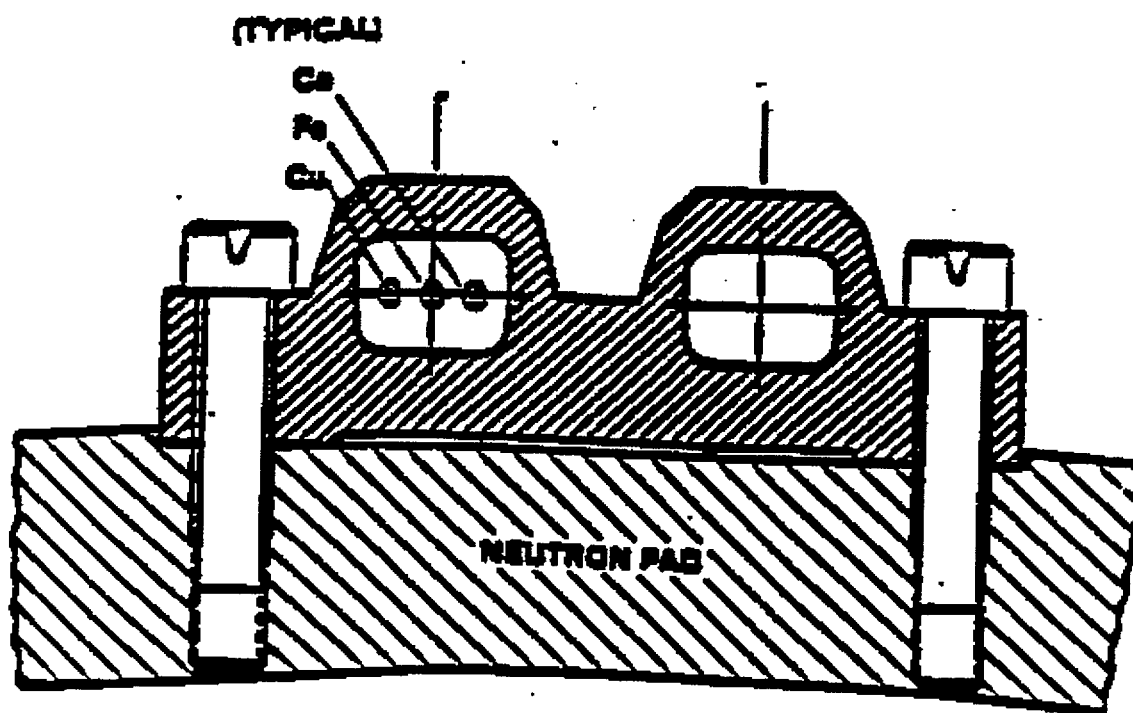
Figure 2.2-1 Neutron Sensor Locations within Internal Surveillance Capsules

3 NEUTRON TRANSPORT AND DOSIMETRY EVALUATION METHODOLOGIES

As noted in Section 1.0 of this report, the best estimate exposure of the reactor vessel was developed using a combination of absolute plant specific neutron transport calculations and plant specific measurements from the reactor cavity and internal surveillance capsules. In this section, the neutron transport and dosimetry evaluation methodologies are discussed in some detail and the approach used to combine the calculations and measurements to produce the best estimate vessel exposure is presented.

3.1 NEUTRON TRANSPORT ANALYSIS METHODS

Fast neutron exposure calculations for the reactor and cavity geometry were carried out using both forward and adjoint discrete ordinates transport techniques. A single forward calculation provided the relative energy distribution of neutrons for use as input to neutron dosimetry evaluations as well as for use in relating measurement results to the actual exposure at key locations in the reactor vessel wall. A series of adjoint calculations, on the other hand, established the means to compute absolute exposure rate values using fuel cycle specific core power distributions; thus, providing a direct comparison with all dosimetry results obtained over the operating history of the reactor.

In combination, the absolute cycle specific data from the adjoint evaluations together with relative neutron energy spectra distributions from the forward calculation provided the means to:

1. Evaluate neutron dosimetry from reactor cavity and surveillance capsule locations.
2. Enable a direct comparison of analytical prediction with measurement.
3. Determine plant specific bias factors to be used in the evaluation of the best estimate exposure of the reactor vessel.
4. Establish a mechanism for projection of reactor vessel exposure as the design of each new fuel cycle evolves.

3.1.1 Reference Forward Calculation

A plan view of the reactor geometry at the core midplane elevation is shown in Figure 3.1-1. Since the reactor exhibits $1/8^{th}$ core symmetry only a 0-45 degree sector is depicted. In addition to the core, reactor internals, reactor vessel, and the primary biological shield, the model also included explicit representations of the surveillance capsules, the reactor vessel cladding, and the mirror insulation located external to the vessel.

A description of a dual surveillance capsule holder attached to the neutron pad is shown in Figure 3.1-2. From a neutronic standpoint, the inclusion of the surveillance capsules and associated support structures in the analytical model is significant. Since the presence of the capsules and structure has a marked impact on the magnitude of the neutron flux as well as on the relative neutron energy spectra at dosimetry locations within the capsules, a meaningful

comparison of measurement and calculation can be made only if these perturbation effects are properly accounted for in the analysis.

In contrast to the relatively massive stainless steel and carbon steel structures associated with the internal surveillance capsules, the small aluminum capsules used in the reactor cavity measurement program were designed to minimize perturbations in the neutron flux and, thus, to provide free field data at the measurement locations. Therefore, explicit modeling of these small capsules in the forward transport model was not required.

The forward transport calculation for the reactor model depicted in Figures 3.1-1 and 3.1-2 was carried out in r,θ geometry using the DORT two-dimensional discrete ordinates transport theory code[3] and the BUGLE-96 cross-section library[4]. The BUGLE-96 library is a 47-neutron-energy-group, ENDF/B-VI based, data set produced specifically for light water reactor applications. In these analyses, anisotropic scattering was treated with a P_3 expansion of the scattering cross-sections and the angular discretization was modeled with an S_8 order of angular quadrature. The reference forward calculation was normalized to a core midplane power density characteristic of operation at a thermal power level of 3411 MWt. The 3411 MWt power level represents the rated operating power for the McGuire Unit 2 reactor.

The spatial core power distribution utilized in the reference forward calculation was derived from statistical studies of long-term operation of Westinghouse four-loop plants. Inherent in the development of this reference core power distribution was the use of an out-in fuel management strategy; i.e., fresh fuel on the core periphery. Furthermore, for the peripheral fuel assemblies, a 2σ uncertainty derived from the statistical evaluation of plant to plant and cycle to cycle variations in peripheral power was used.

Due to the use of this bounding spatial power distribution, the results from the reference forward calculation establish conservative exposure projections for reactors of this design operating at the rated power of 3411 MWt. Since it is unlikely that actual reactor operation would result in the implementation of a power distribution at the nominal $+2\sigma$ level for a large number of fuel cycles and, further, because of the widespread implementation of low leakage fuel management strategies, the fuel cycle specific calculations for this reactor result in exposure rates well below these conservative predictions. This difference between the conservative forward calculation and the fuel cycle specific best estimate computations is illustrated by a comparison of the analytical results given in Section 4.0 of this report.

3.1.2 Cycle Specific Adjoint Calculations

All adjoint analyses were also carried out using an S_8 order of angular quadrature and the P_3 cross-section approximation from the BUGLE-96 library. Adjoint source locations were chosen at each of the azimuthal locations containing cavity dosimetry as well as at several key azimuths on the reactor vessel inner radius. In addition, adjoint calculations were carried out for sources positioned at the geometric center of capsules located at 31.5 and 34.0 degrees relative to the core cardinal axes.

Again, these calculations were run in r,θ geometry to provide neutron source distribution importance functions for the exposure parameter of interest, in this case, ϕ (E > 1.0 MeV).

The importance functions generated from these individual adjoint analyses provided the basis for all absolute exposure projections and comparison with measurement. These importance functions, when combined with cycle specific neutron source distributions, yielded absolute predictions of neutron exposure at the locations of interest for each of the fuel cycles to date; and, established the means to perform similar predictions and dosimetry evaluations for all subsequent fuel cycles.

Having the importance functions and appropriate core source distributions, the response of interest can be calculated as:

$$R(r,\theta) = \int_r \int_\theta \int_E I(r,\theta,E)\, S(r,\theta,E)\, r\, dr\, d\theta\, dE$$

where:

R(r,θ) = ϕ (E > 1.0 MeV) at radius r and azimuthal angle θ.

I(r,θ,E)=   Adjoint source importance function at radius r, azimuthal angle θ, and neutron source energy E.

S(r,θ,E)=   Neutron source strength at core location r,θ and energy E.

It is important to note that the cycle specific neutron source distributions, S(r,θ,E), utilized with the adjoint importance functions, I(r,θ,E), permitted the use not only of fuel cycle specific spatial variations of fission rates within the reactor core, but, also allowed for the inclusion of the effects of the differing neutron yield per fission and the variation in fission spectrum introduced by the build-in of plutonium isotopes as the burnup of individual fuel assemblies increased.

Although the adjoint importance functions used in these analyses were based on a response function defined by the threshold neutron flux (E > 1.0 MeV), prior calculations[5] have shown that, while the implementation of low leakage loading patterns significantly impact the magnitude and the spatial distribution of the neutron field, changes in the relative neutron energy spectrum are of second order. Thus, for a given location the exposure parameter ratios such as [dpa/sec] / [ϕ (E > 1.0 MeV)] are insensitive to changing core source distributions. In the application of these adjoint importance functions to the current evaluations, therefore, calculation of the iron atom displacement rates (dpa/sec) and the neutron flux (E > 0.1 MeV) were computed on a cycle specific basis by using the appropriate [dpa/sec] / [ϕ (E > 1.0 MeV)] and [ϕ (E > 0.1 MeV)] / [ϕ (E > 1.0 MeV)] ratios from the reference forward analysis in conjunction with the cycle specific ϕ (E > 1.0 MeV) solutions from the individual adjoint evaluations.

In particular, after defining the following exposure rate ratios,

$$R_1 = \frac{[dpa/ \sec]}{\phi(E > 1.0\, MeV)}$$

$$R_2 = \frac{\phi(E > 0.1\, MeV)}{\phi(E > 1.0\, MeV)}$$

the corresponding fuel cycle specific exposure rates at the adjoint source locations were computed from the following relations:

$$dpa/\sec = [\,\phi(E > 1.0\,MeV)]\,R_1$$

$$\phi(E > 0.1\,MeV) = [\,\phi(E > 1.0\,MeV)]\,R_2$$

All absolute calculations were also normalized to the current rated power level for McGuire Unit 2, 3411 MWt.
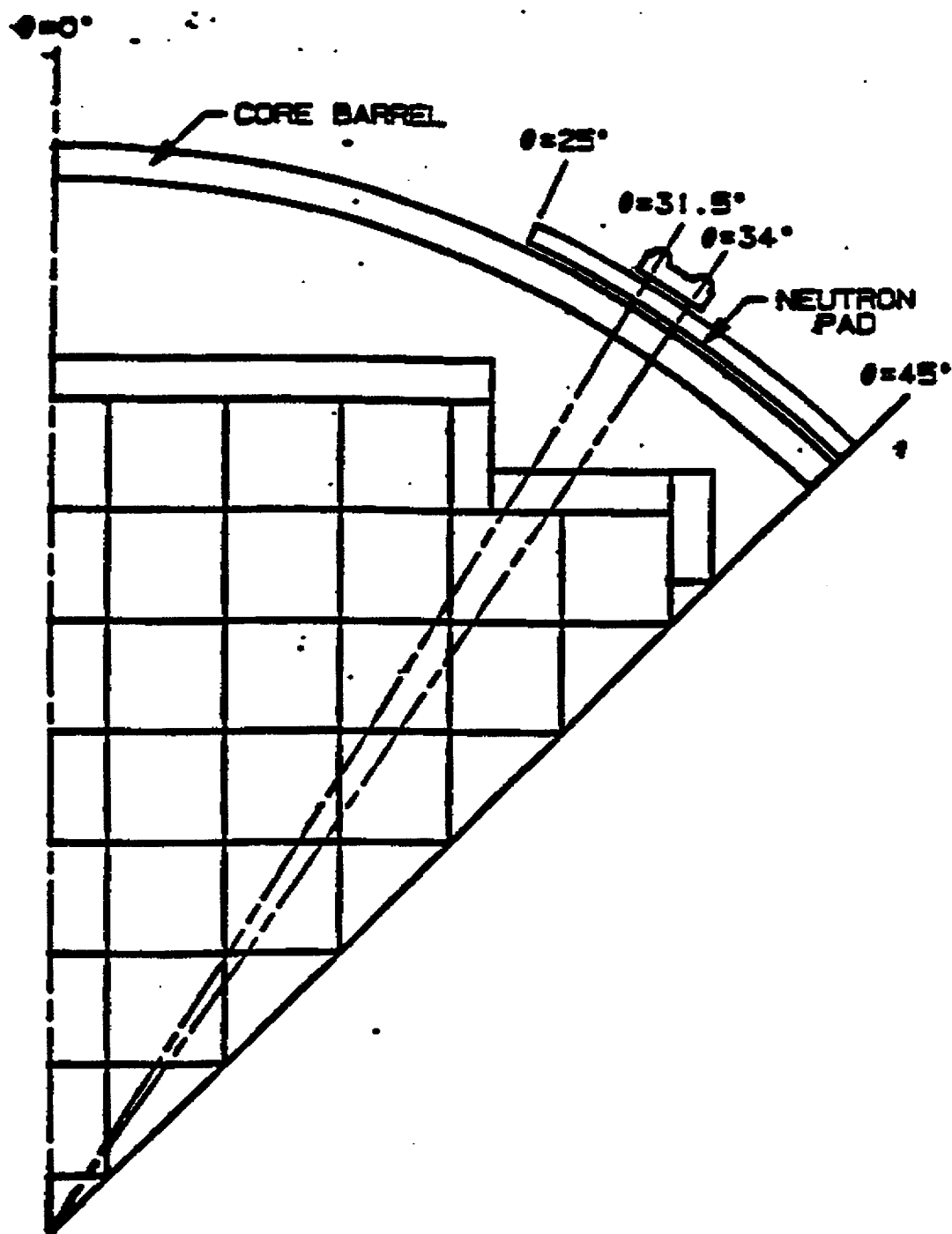
Figure 3.1-1 Reactor Geometry Showing A 45° R,Θ Sector

CHARPY SPECIMEN

NEUTRON PAD
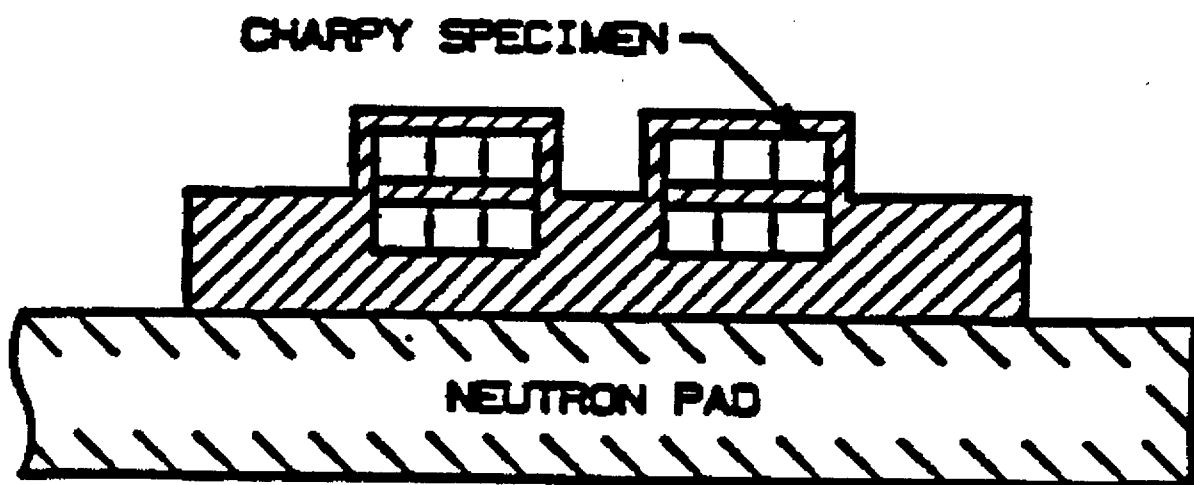
Figure 3.1-2 Internal Surveillance Capsule Geometry

3.2   NEUTRON DOSIMETRY EVALUATION METHODOLOGY

The use of passive neutron sensors such as those included in the internal surveillance capsule and reactor cavity dosimetry sets does not yield a direct measure of the energy dependent neutron flux level at the measurement location. Rather, the activation or fission process is a measure of the integrated effect that the time- and energy-dependent neutron flux has on the target material over the course of the irradiation period. An accurate assessment of the average flux level and, hence, time integrated exposure (fluence) experienced by the sensors may be developed from the measurements only if the sensor characteristics and the parameters of the irradiation are well known. In particular, the following variables are of interest:

1 - The measured specific activity of each sensor
2 - The physical characteristics of each sensor
3 - The operating history of the reactor
4 - The energy response of each sensor
5 - The neutron energy spectrum at the sensor location

In this section the procedures used by Westinghouse to determine sensor specific activities, to develop reaction rates for individual sensors from the measured specific activities and the operating history of the reactor, and to derive key fast neutron exposure parameters from the measured reaction rates are described.

These procedures apply to all of the evaluations provided in this report. For McGuire Unit 2, the measurement of specific activities was performed by Westinghouse or a qualified supplier and Westinghouse carried out the evaluation of all measured data. Thus, the measurement and evaluation procedures were consistent for all surveillance capsule and cavity dosimetry evaluations.

3.2.1   Determination of Sensor Reaction Rates

Following irradiation, the multiple foil sensor sets along with reactor cavity gradient chains were recovered and transported to Pittsburgh for evaluation. Analysis of all radiometric foils and gradient chains was performed at the Westinghouse Waltz Mill Facility by Antech Ltd.

3.2.1.1 Radiometric Sensors

The specific activity of each of the radiometric sensors and gradient chain segments was determined using established ASTM procedures[6 through 16]. Following sample preparation and weighing, the specific activity of each sensor was determined by means of a lithium drifted germanium, Ge(Li), gamma spectrometer. In the case of the surveillance capsule and cavity multiple foil sensor sets, these analyses were performed by direct counting of each of the individual foils or wires; or, as in the case of ^{238}U and ^{237}Np fission monitors from internal surveillance capsules, by direct counting preceded by dissolution and chemical separation of cesium from the sensor. For the stainless steel gradient chains used in the cavity irradiations, individual sensors were obtained by cutting the chains into a series of segments to provide data points at one foot intervals over an axial span encompassing $\pm$ 6 feet relative to the reactor core midplane.

The irradiation history of the reactor over its operating lifetime was obtained from NUREG-0020, "Licensed Operating Reactors Status Summary Report" and from data supplied by utility personnel[17]. For the sensor sets utilized in surveillance capsule and reactor cavity irradiations, the half-lives of the product isotopes are long enough that a monthly histogram describing reactor operation has proven to be an adequate representation for use in radioactive decay corrections for the reactions of interest in the exposure evaluations.

Having the measured specific activities, the operating history of the reactor, and the physical characteristics of the sensors, reaction rates referenced to full power operation at 3411 MWt were determined from the following equation:

$$R = \frac{A}{N_o FY \sum_j \frac{P_j}{P_{ref}} C_j [1 - e^{-\lambda t_f}] e^{-\lambda t_d}}$$

where:

A = measured specific activity (dps/gm)

R = reaction rate averaged over the irradiation period and referenced to operation at a core power level of P_{ref} (rps/nucleus).

N_o = number of target element atoms per gram of sensor.

F = weight fraction of the target isotope in the sensor material.

Y = number of product atoms produced per reaction.

P_j = average core power level during irradiation period j (MW).

P_{ref} = maximum or reference core power level of the reactor (MW).

C_j = calculated ratio of ϕ (E > 1.0 MeV) during irradiation period j to the time weighted average ϕ (E > 1.0 MeV) over the entire irradiation period.

λ = decay constant of the product isotope (sec⁻¹).

T_f = length of irradiation period j (sec).

T_d = decay time following irradiation period j (sec).

and the summation is carried out over the total number of monthly intervals comprising the total irradiation period.

In the above equation, the ratio P_j/P_{ref} accounts for month by month variation of power level within a given fuel cycle. The ratio C_j is calculated for each fuel cycle using the adjoint transport methodology and accounts for the change in sensor reaction rates caused by variations in flux level due to changes in core power spatial distributions from fuel cycle to fuel cycle. For a single cycle irradiation C_j = 1.0. However, for multiple cycle irradiations, particularly those employing low leakage fuel management the additional C_j must be utilized.

3.2.1.2 Corrections to Reaction Rate Data

Prior to using the measured reaction rates in the least squares adjustment procedure discussed in Section 3.2.2 of this report, additional corrections were made to the ^{238}U foil measurements to account for the presence of ^{235}U impurities in the sensors as well as to adjust for the build-in of plutonium isotopes over the course of the irradiation. These corrections were location and fluence dependent and were derived from calculations.

In addition to the corrections made for the presence of ^{235}U in the ^{238}U fission sensors, corrections were also made to both the ^{238}U and ^{237}Np sensor reaction rates to account for gamma ray induced fission reactions occurring over the course of the irradiation. These photofission corrections were, likewise, location dependent and were based on the reference transport calculations described in Section 3.1.1.

For the reactor cavity fission monitors, corrections were also made to the ^{238}U and ^{237}Np reactions for the vanadium encapsulated oxide detectors. Since these sensors are counted directly with the Ge(Li) detector, a correction has to be made to account for self-absorption of the fission fragment gamma rays by the UO_2 or NpO_2 oxide material and by the vanadium tubing. These correction factors were determined by J. M. Adams, et al and are reported in a recent paper[18]. For the three fission product nuclides measured the correction factors are:

Daughter	Correction
^{95}Zr	1.048
^{103}Ru	1.073
^{137}Cs	1.055

3.2.2 Least Squares Adjustment Procedure

Values of key fast neutron exposure parameters were derived from the measured reaction rates using the FERRET least squares adjustment code[19]. The FERRET approach used the measured reaction rate data, sensor reaction cross-sections, and a calculated trial spectrum as input and proceeded to adjust the group fluxes from the trial spectrum to produce a best fit (in a least squares sense) to the measured reaction rate data. The best estimate exposure parameters along with the associated uncertainties were then obtained from the best estimate spectrum. This methodology is fully consistent with that described in Reference 1.

In the FERRET evaluations, a log-normal least squares algorithm weights both the *a priori* values and the measured data in accordance with the assigned uncertainties and correlations. In general, the measured values, *f*, are linearly related to the flux, ϕ, by some response matrix, A:

$$f_i^{(s,\alpha)} = \sum_g A_{ig}^{(s)} \phi_g^{(\alpha)}$$

where i indexes the measured values belonging to a single data set s, g designates the energy group, and α delineates spectra that may be simultaneously adjusted. For example,

$$R_i = \sum_g \sigma_{ig} \, \phi_g$$

relates a set of measured reaction rates, R_i, to a single spectrum, ϕ_g, by the multigroup reaction cross-section, σ_{ig}. The log-normal approach automatically accounts for the physical constraint of positive fluxes, even with large assigned uncertainties.

In the least squares adjustment, the continuous quantities (i.e., neutron spectra and cross-sections) were approximated in a multi-group format consisting of 53 energy groups. The trial input spectrum was converted to the FERRET 53 group structure using the SAND-II code[20]. This procedure was carried out by first expanding the 47 group calculated spectrum into the SAND-II 620 group structure using a SPLINE interpolation procedure in regions where group boundaries do not coincide. The 620-point spectrum was then re-collapsed into the group structure used in FERRET.

The sensor set reaction cross-sections, obtained from the ENDF/B-VI dosimetry file[21], were also collapsed into the 53-energy group structure using the SAND-II code. In this instance, the trial spectrum, as expanded to 620 groups, was employed as a weighting function in the cross-section collapsing procedure. Reaction cross-section uncertainties in the form of a 53 × 53 covariance matrix for each sensor reaction were also constructed from the information contained on the ENDF/B-VI data files. These matrices included energy group to energy group uncertainty correlations for each of the individual reactions. However, correlations between cross-sections for different sensor reactions were not included. The omission of this additional uncertainty information does not significantly impact the results of the adjustment.

Due to the importance of providing a trial spectrum that exhibits a relative energy distribution close to the actual spectrum at the sensor set locations, the neutron spectrum input to the FERRET evaluation was taken from the center of the surveillance capsule modeled in the reference forward transport calculation. While the 53 × 53 group covariance matrices applicable to the sensor reaction cross-sections were developed from the ENDF/B-VI data files, the covariance matrix for the input trial spectrum was constructed from the following relation:

$$M_{gg'} = R_n^2 + R_g \, R_{g'} \, P_{gg'}$$

where R_n specifies an overall fractional normalization uncertainty (i.e., complete correlation) for the set of values. The fractional uncertainties, R_g, specify additional random uncertainties for group g that are correlated with a correlation matrix given by:

$$P_{gg'} = [1 - \theta]\delta_{gg'} + \theta \, e^{-H}$$

where:

$$H = \frac{(g - g')^2}{2\gamma^2}$$

The first term in the correlation matrix equation specifies purely random uncertainties, while the second term describes short range correlations over a group range γ (θ specifies the strength of the latter term). The value of δ is 1 when g = g' and 0 otherwise. For the trial spectrum used in the current evaluations, a short range correlation of γ = 6 groups was used. This choice implies that neighboring groups are strongly correlated when θ is close to 1. Strong long-range correlations (or anti-correlations) were justified based on information presented by R. E. Maerker[22]. The uncertainties associated with the measured reaction rates included both statistical (counting) and systematic components. The systematic component of the overall uncertainty accounts for counter efficiency, counter calibrations, irradiation history corrections, and corrections for competing reactions in the individual sensors.

In performing the least squares adjustment with the FERRET code, the input spectra from the reference forward transport calculations were normalized to the absolute calculations from the cycle specific adjoint analyses. The specific normalization factors for individual evaluations depended on the location of the sensor set as well as on the neutron flux level at that location.

The specific assignment of uncertainties in the measured reaction rates and the input (trial) spectra used in the FERRET evaluations was as follows:

Reaction Rate Uncertainty	5%
Flux Normalization Uncertainty	15%
Flux Group Uncertainties	
(E > 0.0055 MeV)	15%
(0.68 eV < E < 0.0055 MeV)	29%
(E < 0.68 eV)	52%
Short Range Correlation	
(E > 0.0055 MeV)	0.9
(0.68 eV < E < 0.0055 MeV)	0.5
(E < 0.68 eV)	0.5
Flux Group Correlation Range	
(E > 0.0055 MeV)	6
(0.68 eV < E < 0.0055 MeV)	3
(E < 0.68 eV)	2

It should be noted that the uncertainties listed for the upper energy ranges extend down to the lower range. Thus, the 29% group uncertainty in the second range is made up of a 15% uncertainty with a 0.9 short-range correlation and a range of 6, and a second part of magnitude 25% with a 0.5 correlation and a range of 3.

These input uncertainty assignments were based on prior experience in using the FERRET least squares adjustment approach in the analysis of neutron dosimetry from surveillance capsule, reactor cavity, and benchmark irradiations. The values are liberal enough to permit adjustment of the input spectrum to fit the measured data for all practical applications.

3.3   DETERMINATION OF BEST ESTIMATE REACTOR VESSEL EXPOSURE

As noted earlier in this report, the best estimate exposure of the reactor vessel was developed using a combination of absolute plant specific transport calculations based on the methodology discussed in Section 3.1 and plant specific measurement data determined using the measurement evaluation techniques described in Section 3.2.

In particular, the best estimate vessel exposure is obtained from the following relationship:

$$\Phi_{Best\ Est.} = K\ \Phi_{Calc.}$$

where: $\Phi_{Best\ Est.} =$ The best estimate fast neutron exposure at the location of interest.

K   =   The plant specific measurement/calculation (BE/C) bias factor derived from all available surveillance capsule and reactor cavity dosimetry data.

$\Phi_{Calc.}$ =   The absolute calculated fast neutron exposure at the location of interest.

The approach defined in the above equation is based on the premise that the measurement data represent the most accurate plant specific information available at the locations of the dosimetry; and, further that the use of the measurement data on a plant specific basis essentially removes biases present in the analytical approach and mitigates the uncertainties that would result from the use of analysis alone. That is, at the measurement points the uncertainty in the best estimate exposure is dominated by the uncertainties in the measurement process. At locations within the reactor vessel wall, additional uncertainty is incurred due to the analytically determined relative ratios among the various measurement points and locations within the reactor vessel wall.

The implementation of this approach acts to remove plant specific biases associated with the definition of the core source, actual vs. assumed reactor dimensions, and operational variations in water density within the reactor. As a result, the overall uncertainty in the best estimate exposure projections within the vessel wall depend on the individual uncertainties in the measurement process, the uncertainty in the dosimetry location, and in the uncertainty in the calculated ratio of the neutron exposure at the point of interest to that at the measurement location.

The uncertainties in the measured flux were derived directly from the results of the least squares evaluation of dosimetry data. The positioning uncertainties were taken from parametric studies of sensor position performed as part of an analytical sensitivity evaluation of the McGuire Unit 2 reactor. The uncertainties in the exposure ratios relating dosimetry results to positions within the vessel wall were based on analytical sensitivity studies of the vessel thickness tolerance for the cavity data and on downcomer water density variations and vessel inner radius tolerance for the surveillance capsule measurements.

4   RESULTS OF NEUTRON TRANSPORT CALCULATIONS

4.1   REFERENCE FORWARD CALCULATION

As noted in Section 3.0 of this report, data from the reference forward transport calculation were used in evaluating dosimetry from both reactor cavity and surveillance capsule irradiations as well as in relating the results of these evaluations to the neutron exposure of the reactor vessel wall. In this section, the key data extracted from the reference forward calculation is presented and its relevance to the dosimetry evaluations and vessel exposure projections is discussed. The reader should recall that the results of the reference forward transport calculation were intended for use on a relative basis and, therefore, should not be used for absolute comparison with measurement. All absolute comparisons were based on the results of the fuel-cycle-specific-adjoint calculations discussed in Section 4.2.

4.1.1   Cavity Sensor Set Locations

Data from the reference forward calculation pertinent to cavity sensor evaluations are provided in Tables 4.1-1 and 4.1-2.

In Table 4.1-1, the calculated neutron energy spectra applicable to the permanent sensor locations at 0.5, 14.5, 29.5 and 44.5 degrees relative to the core cardinal axes are listed. These data represent the trial spectra used as the starting guess in the FERRET least squares adjustment evaluations of the cavity sensor sets. On a relative basis these calculated energy distributions establish a baseline against which adjusted spectra may be compared; and, when coupled with the adjoint results of Section 4.2, provide an analytical prediction of absolute neutron spectra at the sensor set locations for each irradiation period.

In Table 4.1-2, the calculated neutron sensor reaction rates associated with the spectra from Table 4.1-1 are provided along with the reference exposure rates in terms of Φ (E > 1.0 MeV), Φ (E < 0.1 MeV) and dpa/sec. Also listed are the associated exposure rate ratios calculated for each of the cavity sensor set locations.

The reference reaction rates, exposure rates, and exposure rate ratios were used in conjunction with fuel cycle specific adjoint transport calculations from Section 4.2 to provide calculated sensor set reaction rates and to project sensor set exposures in terms of Φ (E > 0.1 MeV) and dpa/sec for each irradiation period.

4.1.2   Surveillance Capsule Locations

Data from the reference forward calculation pertinent to surveillance capsule evaluations are provided in Tables 4.1-3 and 4.1-4.

In Table 4.1-3, the calculated neutron energy spectra at the geometric center of surveillance capsules located at 34 and 31.5 degrees relative to the core cardinal axes are listed. In Table 4.1-4, the calculated neutron sensor reaction rates and exposure rate ratios associated with the spectra from Table 4.1-3 are provided along with the calculated exposure rates in terms of of Φ (E > 1.0 MeV), Φ (E < 0.1 MeV) and dpa/sec. Again, these data are applicable to the

geometric center of each surveillance capsule. These tabulated data were used in the surveillance capsule dosimetry evaluations and exposure calculations in the same fashion as was the case for the cavity sensor sets.

4.1.3   Reactor Vessel Wall

Data from the reference forward calculation pertinent to the reactor vessel wall are provided in Tables 4.1-5 through 4.1-9.

In Table 4.1-5, the calculated azimuthal distribution of fast neutron flux (E > 1.0 MeV) is listed for the center of the vessel cladding, at the reactor vessel clad/base metal interface, and at the center of the first DORT mesh interval in the base metal. The interface information (base metal inner radius) was obtained from a linear interpolation of the two sets of data obtained directly from the reference forward calculation. In this detailed tabulation, calculated flux levels are given for each of the 98 azimuthal mesh intervals included in the analytical model.

In Table 4.1-6, the calculated azimuthal distribution of exposure rates in terms of Φ (E > 1.0 MeV), Φ (E < 0.1 MeV), and dpa/sec are listed at approximately 5 degree intervals over the reactor geometry. These data are applicable to the clad/base metal interface. Also given in Table 4.1-6 are the exposure rate ratios [Φ (E > 0.1 MeV)] / [Φ (E > 1.0 MeV)] and [dpa/sec] / [Φ (E > 1.0 MeV)] that provide an indication of the variation in neutron spectrum as a function of azimuthal angle at the reactor vessel inner radius.

Radial gradient information for Φ(E > 1.0 MeV), Φ(E > 0.1 MeV), and dpa/sec is given in Tables 4.1-7, 4.1-8, and 4.1-9, respectively. These data are presented on a relative basis for each exposure parameter at the 0, 15, 30, and 45-degree azimuthal locations. Exposure rate distributions within the vessel wall were obtained by normalizing the calculated or projected exposure at the vessel inner radius to the gradient data given in Tables 4.1-7 through 4.1-9.

Table 4.1-1   Calculated Reference Neutron Energy Spectra at Cavity Sensor Set Locations
3411 MWt, F_a=1.20

Lower Energy [MeV]	0.5°	14.5°	29.5°	44.5°
1.419E+01	3.33E+05	3.84E+05	3.38E+05	2.59E+05
1.221E+01	9.00E+05	1.06E+06	9.41E+05	7.28E+05
1.000E+01	3.27E+06	3.95E+06	3.58E+06	2.84E+06
8.607E+00	5.76E+06	7.07E+06	6.45E+06	5.13E+06
7.408E+00	8.29E+06	1.05E+07	9.64E+06	7.73E+06
6.065E+00	1.70E+07	2.18E+07	2.00E+07	1.57E+07
4.966E+00	2.23E+07	2.98E+07	2.79E+07	2.22E+07
3.679E+00	3.80E+07	5.31E+07	5.15E+07	4.25E+07
3.012E+00	2.96E+07	4.19E+07	4.16E+07	3.52E+07
2.725E+00	2.30E+07	3.29E+07	3.32E+07	2.88E+07
2.466E+00	2.86E+07	4.14E+07	4.22E+07	3.66E+07
2.365E+00	1.48E+07	2.13E+07	2.19E+07	1.94E+07
2.346E+00	4.39E+06	6.30E+06	6.60E+06	6.16E+06
2.231E+00	2.24E+07	3.19E+07	3.35E+07	3.12E+07
1.921E+00	6.16E+07	8.74E+07	9.21E+07	8.58E+07
1.653E+00	8.65E+07	1.23E+08	1.32E+08	1.26E+08
1.353E+00	1.50E+08	2.19E+08	2.37E+08	2.23E+08
1.003E+00	3.64E+08	5.29E+08	5.85E+08	5.60E+08
8.209E-01	3.60E+08	5.25E+08	5.90E+08	5.71E+08
7.427E-01	1.74E+08	2.79E+08	3.13E+08	2.66E+08
6.081E-01	8.53E+08	1.22E+09	1.40E+09	1.39E+09
4.979E-01	7.59E+08	1.14E+09	1.32E+09	1.24E+09
3.688E-01	8.34E+08	1.27E+09	1.48E+09	1.35E+09
2.972E-01	1.25E+09	1.83E+09	2.14E+09	2.07E+09
1.832E-01	1.53E+09	2.46E+09	2.88E+09	2.46E+09
1.111E-01	1.66E+09	2.57E+09	3.04E+09	2.70E+09
6.738E-02	1.06E+09	1.68E+09	1.99E+09	1.70E+09
4.087E-02	7.86E+08	1.26E+09	1.49E+09	1.24E+09
3.183E-02	2.73E+08	4.54E+08	5.34E+08	4.22E+08
2.606E-02	1.75E+08	3.02E+08	3.56E+08	2.69E+08
2.418E-02	4.36E+08	5.80E+08	7.01E+08	7.31E+08
2.188E-02	2.65E+08	3.90E+08	4.72E+08	4.49E+08
1.503E-02	5.06E+08	8.39E+08	1.01E+09	8.25E+08
7.102E-03	7.44E+08	1.22E+09	1.45E+09	1.16E+09
3.355E-03	7.38E+08	1.20E+09	1.42E+09	1.16E+09
1.585E-03	6.51E+08	1.06E+09	1.26E+09	1.01E+09
4.540E-04	1.03E+08	1.64E+09	1.94E+09	1.57E+09
2.144E-04	5.43E+08	8.69E+08	1.03E+09	8.24E+08
1.013E-04	5.48E+08	8.59E+08	1.02E+09	8.28E+08
3.727E-05	6.93E+08	1.08E+09	1.28E+09	1.04E+09
1.068E-05	8.06E+08	1.24E+09	1.47E+09	1.21E+09
5.043E-06	4.47E+08	6.87E+08	8.12E+08	6.69E+08
1.855E-06	5.54E+08	8.44E+08	9.94E+08	8.22E+08
8.764E-07	3.85E+08	5.81E+08	6.84E+08	5.68E+08
4.140E-07	3.42E+08	5.13E+08	6.02E+08	5.04E+08
1.000E-07	4.63E+08	6.72E+08	7.88E+08	6.81E+08
0.000E+00	2.87E+09	3.30E+09	3.86E+09	4.24E+09

Table 4.1-2   Reference Neutron Sensor Reaction Rates and Exposure Parameters at the
Cavity Sensor Set Locations - 3411 Mwt; $F_a = 1.20$

Reaction Rate	0.5°	14.5°	29.5°	44.5°
^{63}Cu (n,α) (Cd)	7.44E-19	9.34E-19	8.55E-19	6.79E-19
^{46}Ti (n,p) (Cd)	1.01E-17	1.31E-17	1.21E-17	9.68E-18
^{54}Fe (n,p) (Cd)	5.47E-17	7.41E-17	7.13E-17	5.92E-17
^{58}Ni (n,p) (Cd)	7.64E-17	1.04E-16	1.02E-16	8.59E-17
^{238}U (n,f) (Cd)	2.74E-16	3.86E-16	3.98E-16	3.58E-16
^{237}Np (n,f) (Cd)	3.94E-15	5.79E-15	6.49E-15	6.06E-15
^{59}Co (n,γ)	1.48E-13	1.90E-13	2.23E-13	2.20E-13
^{59}Co (n,γ) (Cd)	5.09E-14	7.93E-14	9.37E-14	7.67E-14
^{238}U (γ,f)	1.34E-17	1.58E-17	1.57E-17	1.38E-17
^{237}Np (γ,f)	3.77E-17	4.46E-17	4.42E-17	3.89E-17

Exposure Parameter	Neutron Flux [n/cm²-s]			
ϕ (E > 1.0 MeV)	9.02E+08	1.30E+09	1.39E+09	1.29E+09
ϕ (E > 0.1 MeV)	8.52E+09	1.29E+10	1.49E+10	1.36E+10

	dpa/sec			
Iron Atom Displacement Rate	2.97E-12	4.46E-12	5.05E-12	4.58E-12

ϕ (E > 0.1 MeV) / ϕ (E > 1.0 MeV)	9.45	9.96	10.77	10.61
[dpa/sec] / ϕ (E > 1.0 MeV)	3.30E-21	3.44E-21	3.65E-21	3.56E-21
^{238}U (γ,f) / ^{238}U (n,f)	0.0488	0.0410	0.0393	0.0385
^{237}Np (γ, f) / ^{237}Np (n,f)	0.0096	0.0077	0.0068	0.0064

Table 4.1-3   Calculated Reference Neutron Energy Spectra at Surveillance Capsule Locations - 3411 Mwt; $F_a = 1.2$

	ϕ (E) [n/cm^2-s]				ϕ (E) [n/cm^2-s]		
Lower Energy	Dual Capsule		Single Capsule	Lower Energy	Dual Capsule		Single Capsule
[MeV]	31.5°	34.0°	34.0°	[MeV]	31.5°	34.0°	34.0°
1.419E+01	1.52E+07	1.59E+07	1.56E+07	1.832E-01	7.71E+10	9.37E+10	9.79E+10
1.221E+01	4.92E+07	5.17E+07	5.10E+07	1.111E-01	8.07E+10	9.88E+10	1.06E+11
1.000E+01	2.20E+08	2.34E+08	2.31E+08	6.738E-02	5.22E+10	6.35E+10	6.54E+10
8.607E+00	4.37E+08	4.66E+08	4.60E+08	4.087E-02	4.93E+10	6.01E+10	6.28E+10
7.408E+00	7.80E+08	8.39E+08	8.28E+08	3.183E-02	1.59E+10	1.93E+10	1.96E+10
6.065E+00	1.91E+09	2.07E+09	2.04E+09	2.606E-02	6.15E+09	7.44E+09	7.47E+09
4.966E+00	3.02E+09	3.31E+09	3.26E+09	2.418E-02	1.78E+10	2.19E+10	2.27E+10
3.679E+00	6.43E+09	7.20E+09	7.10E+09	2.188E-02	1.20E+10	1.48E+10	1.59E+10
3.012E+00	5.56E+09	6.36E+09	6.30E+09	1.503E-02	2.06E+10	2.48E+10	2.45E+10
2.725E+00	4.40E+09	5.04E+09	4.99E+09	7.102E-03	4.55E+10	5.48E+10	5.44E+10
2.466E+00	5.45E+09	6.27E+09	6.22E+09	3.355E-03	5.09E+10	6.13E+10	6.08E+10
2.365E+00	2.75E+09	3.16E+09	3.14E+09	1.585E-03	4.74E+10	5.72E+10	5.71E+10
2.346E+00	7.69E+08	8.85E+08	8.79E+08	4.540E-04	7.96E+10	9.64E+10	9.59E+10
2.231E+00	3.93E+09	4.53E+09	4.50E+09	2.144E-04	3.90E+10	4.70E+10	4.60E+10
1.921E+00	1.15E+10	1.33E+10	1.33E+10	1.013E-04	4.64E+10	5.61E+10	5.49E+10
1.653E+00	1.44E+10	1.68E+10	1.69E+10	3.727E-05	6.07E+10	7.35E+10	7.16E+10
1.353E+00	2.35E+10	2.76E+10	2.79E+10	1.068E-05	7.17E+10	8.69E+10	8.38E+10
1.003E+00	5.18E+10	6.18E+10	6.41E+10	5.043E-06	3.90E+10	4.72E+10	4.50E+10
8.209E-01	4.02E+10	4.84E+10	5.06E+10	1.855E-06	4.55E+10	5.49E+10	5.10E+10
7.427E-01	1.87E+10	2.25E+10	2.33E+10	8.764E-07	2.86E+10	3.44E+10	3.11E+10
6.081E-01	6.15E+10	7.47E+10	7.89E+10	4.140E-07	1.94E+10	2.32E+10	2.03E+10
4.979E-01	5.81E+10	7.10E+10	7.58E+10	1.000E-07	2.33E+10	2.78E+10	2.34E+10
3.688E-01	5.92E+10	7.20E+10	7.70E+10	0.000E+00	6.31E+10	7.49E+10	6.33E+10
2.972E-01	6.36E+10	7.83E+10	8.59E+10				

Table 4.1-4   Reference Neutron Sensor Reaction Rates and Exposure Parameters at the Center of the Surveillance Capsules - 3411 Mwt; F_a = 1.20

	Dual Capsule		Single Capsule
Reaction Rate	**31.5°**	**34.0°**	**34.0°**
^{63}Cu (n,α) ^{60}Co	6.90E-17	7.44E-17	7.34E-17
^{54}Fe (n,p) ^{54}Mn	7.95E-15	8.89E-15	8.79E-15
^{58}Ni (n,p) ^{58}Co	1.12E-14	1.26E-14	1.25E-14
^{238}U (n,f) F.P. (Cd)	4.34E-14	5.00E-14	5.00E-14
^{237}Np (n,f) F.P. (Cd)	4.24E-13	5.05E-13	5.21E-13
^{59}Co (n,γ) ^{60}Co	6.12E-12	7.36E-12	7.06E-12
^{59}Co (n,γ) ^{60}Co (Cd)	4.25E-12	5.13E-12	4.98E-12
^{238}U (γ,f) F.P.	1.58E-15	1.85E-15	1.65E-15
^{237}Np (γ,f) F.P.	4.40E-15	5.17E-15	4.59E-15

Exposure Parameter	Neutron Flux [n/cm^2-s]		
ϕ (E > 1.0 MeV)	1.38E+11	1.61E+11	1.63E+11
ϕ (E > 0.1 MeV)	6.07E+11	7.33E+11	7.71E+11
	dpa/sec		
Iron Atom Displacement Rate	2.64E-10	3.14E-10	3.25E-10
	Ratios		
ϕ (E > 0.1 MeV) / ϕ (E > 1.0 MeV)	4.41	4.55	4.73
[dpa/sec] / ϕ (E > 1.0 MeV)	1.92E-21	1.95E-21	1.99E-21
^{238}U (γ,f) / ^{238}U (n,f)	3.64E-02	3.71E-02	3.30E-02
^{237}Np (γ,f) / ^{237}Np (n,f)	1.04E-02	1.02E-02	8.80E-03

Table 4.1-5   Summary of Exposure Rates at the Reactor Vessel Clad/Base Metal Interface
(15° Neutron Pad Octant)

Neutron Flux [n/cm²-sec]

θ (deg)	(E > 1.0 MeV)	(E > 0.1 MeV)	dpa/sec	E > 0.1 MeV / E > 1.0 MeV	dpa/sec / E > 1.0 MeV
0.25	1.76E+10	3.73E+10	2.73E-11	2.12	1.55E-21
5.25	1.88E+10	3.99E+10	2.91E-11	2.12	1.55E-21
10.00	2.19E+10	4.67E+10	3.39E-11	2.13	1.55E-21
15.25	2.72E+10	5.80E+10	4.17E-11	2.14	1.54E-21
20.25	3.14E+10	6.71E+10	4.80E-11	2.14	1.53E-21
25.25	3.05E+10	6.61E+10	4.68E-11	2.17	1.53E-21
30.25	2.59E+10	6.00E+10	4.04E-11	2.32	1.56E-21
35.10	2.58E+10	6.47E+10	4.09E-11	2.51	1.59E-21
40.25	2.95E+10	7.53E+10	4.68E-11	2.55	1.59E-21
44.75	3.12E+10	7.90E+10	4.94E-11	2.53	1.58E-21

Table 4.1-6   Relative Radial Distribution of Neutron Flux (E > 1.0 MeV) Within the
Reactor Vessel Wall (15° Neutron Pad Octant)

Radius	Azimuthal Angle			
[cm]	0.0°	15.0°	30.0°	45.0°
220.35	1.000	1.000	1.000	1.000
221.00	0.959	0.958	0.960	0.957
222.30	0.852	0.851	0.852	0.847
223.60	0.741	0.738	0.739	0.732
224.89	0.636	0.632	0.635	0.625
225.87	0.564	0.559	0.562	0.551
227.01	0.489	0.484	0.488	0.475
228.63	0.398	0.393	0.396	0.384
230.09	0.329	0.324	0.327	0.315
231.39	0.276	0.272	0.276	0.263
232.68	0.232	0.228	0.231	0.220
234.14	0.190	0.187	0.190	0.179
235.76	0.152	0.149	0.152	0.142
236.90	0.130	0.127	0.130	0.120
237.88	0.113	0.110	0.113	0.104
239.18	0.093	0.091	0.093	0.085
240.47	0.077	0.074	0.077	0.069
241.77	0.063	0.060	0.062	0.055
242.42	0.060	0.057	0.060	0.053

Note:
    Base Metal Inner Radius =   220.35 cm.
    Base Metal ¼T =   225.87 cm.
    Base Metal ½T =   231.39 cm.
    Base Metal ¾T =   236.90 cm.
    Base Metal Outer Radius =   242.42 cm.

Table 4.1-7   Relative Radial Distribution of Neutron Flux (E > 0.1 MeV) Within the Reactor Vessel Wall (15° Neutron Pad Octant)

Radius		Azimuthal Angle		
[cm]	0.0°	15.0°	30.0°	45.0°
220.35	1.000	1.000	1.000	1.000
221.00	1.012	1.010	1.013	1.007
222.30	0.997	0.991	0.997	0.983
223.60	0.960	0.950	0.960	0.939
224.89	0.914	0.901	0.914	0.886
225.87	0.876	0.861	0.876	0.844
227.01	0.830	0.814	0.831	0.794
228.63	0.765	0.748	0.767	0.725
230.09	0.707	0.689	0.710	0.664
231.39	0.655	0.637	0.659	0.611
232.68	0.605	0.587	0.609	0.559
234.14	0.550	0.532	0.555	0.503
235.76	0.491	0.475	0.497	0.444
236.90	0.450	0.435	0.457	0.404
237.88	0.415	0.401	0.423	0.369
239.18	0.370	0.357	0.378	0.324
240.47	0.326	0.314	0.334	0.280
241.77	0.284	0.269	0.288	0.236
242.42	0.276	0.260	0.279	0.227

Note:

Base Metal Inner Radius =	220.35 cm.
Base Metal ¼T =	225.87 cm.
Base Metal ½T =	231.39 cm.
Base Metal ¾T =	236.90 cm.
Base Metal Outer Radius =	242.42 cm.

Table 4.1-8   Relative Radial Distribution of Iron Displacement Rate (dpa) Within the
Reactor Vessel Wall (15° Neutron Pad Octant)

Radius	Azimuthal Angle			
[cm]	0.0°	15.0°	30.0°	45.0°
220.35	1.000	1.000	1.000	1.000
221.00	0.964	0.964	0.968	0.965
222.30	0.876	0.875	0.882	0.878
223.60	0.784	0.782	0.793	0.788
224.89	0.698	0.695	0.709	0.703
225.87	0.638	0.634	0.651	0.643
227.01	0.575	0.571	0.589	0.580
228.63	0.496	0.491	0.511	0.501
230.09	0.434	0.429	0.450	0.439
231.39	0.385	0.380	0.402	0.389
232.68	0.342	0.337	0.358	0.345
234.14	0.299	0.294	0.315	0.301
235.76	0.257	0.252	0.272	0.257
236.90	0.230	0.226	0.245	0.229
237.88	0.208	0.204	0.223	0.207
239.18	0.182	0.179	0.196	0.179
240.47	0.158	0.154	0.171	0.153
241.77	0.136	0.131	0.146	0.128
242.42	0.132	0.127	0.142	0.123

Note:

Base Metal Inner Radius =   220.35 cm.
Base Metal ¼T =   225.87 cm.
Base Metal ½T =   231.39 cm.
Base Metal ¾T =   236.90 cm.
Base Metal Outer Radius =   242.42 cm.

4.2   FUEL CYCLE SPECIFIC ADJOINT TRANSPORT CALCULATIONS

Results of the fuel cycle specific adjoint transport calculations for the first 12 cycles of operation at McGuire Unit 2 are summarized in Tables 4.2-1 through 4.2-18. The data listed in these tables establish the means for absolute comparison of analysis and measurement for the Cycle 12 reactor cavity dosimetry irradiation as well as for the six sets of surveillance capsule dosimetry withdrawn to date. These results also provide the fuel cycle specific relationship among the surveillance capsule and reactor cavity measurement locations and key positions at the inner radius of the reactor vessel wall.

The core power distributions used in the cycle specific fast neutron exposure calculations for Cycles 1 through 12 were taken from the fuel cycle design reports applicable to McGuire Unit 2.[23 through 33] The data extracted from the fuel cycle design reports represented cycle averaged relative fuel assembly powers and burnups as well as cycle averaged relative axial distributions. Therefore, the results of the adjoint evaluation provided data in terms of fuel cycle averaged neutron flux which, when multiplied by the appropriate fuel cycle length, produced the incremental fast neutron exposure for the fuel cycle.

The calculated fast neutron flux (E > 1.0 MeV) and cumulative fast neutron fluence at the center of surveillance capsules located at 31.5 and 34.0 degrees are provided for each of the twelve operating fuel cycles in Tables 4.2-1 and 4.2-2, respectively. The data as tabulated are applicable to the axial core midplane. Similar data applicable to the reactor vessel inner radius are given in Tables 4.2-3 and 4.2-4 and data pertinent to the cavity dosimetry sensor locations are listed in Tables 4.2-5 and 4.2-6.

Exposure parameter ratios necessary to convert the cycle specific data listed in Tables 4.2-1 through 4.2-6 to other key fast neutron exposure units are given in Section 4.1 of this report. Application of these ratios to the data from Tables 4.2-1 through 4.2-6 yielded corresponding exposure data in terms of flux or fluence (E > 0.1 MeV) in Tables 4.2-7 through 4.2-12 and iron atom displacements in Tables 4.2-13 through 4.2-18.

Table 4.2-1   Calculated Fast Neutron Flux (E > 1.0 MeV) at the Center of Reactor Vessel Surveillance Capsules

	Neutron Flux [n/cm²-sec]		
	Dual Capsule		Single Capsule
Cycle No.	31.5°	34°	34°
1	9.96E+10	1.15E+11	1.17E+11
2	1.15E+11	1.34E+11	1.36E+11
3	1.01E+11	1.18E+11	1.20E+11
4	8.89E+10	1.02E+11	1.03E+11
5	8.56E+10	9.67E+10	9.80E+10
6	8.28E+10	9.28E+10	9.41E+10
7	8.55E+10	9.63E+10	9.76E+10
8	8.43E+10	9.55E+10	9.68E+10
9	8.39E+10	9.65E+10	9.78E+10
10	7.59E+10	8.67E+10	8.79E+10
11	7.66E+10	8.72E+10	8.84E+10
12	7.48E+10	8.49E+10	8.61E+10

Table 4.2-2   Calculated Fast Neutron Fluence (E > 1.0 MeV) at the Center of Reactor Vessel Surveillance Capsules

		Cumulative Fluence [n/cm^2]		
				Single
	Cycle Length	Dual Capsule		Capsule
Cycle	EFPS	31.5°	34°	34°
1	3.239E+07	3.23E+18	3.74E+18	3.79E+18
2	2.158E+07	5.72E+18	6.64E+18	6.73E+18
3	2.311E+07	8.04E+18	9.36E+18	9.50E+18
4	2.664E+07	1.04E+19	1.21E+19	1.22E+19
5	2.769E+07	1.28E+19	1.47E+19	1.50E+19
6	2.891E+07	1.52E+19	1.74E+19	1.77E+19
7	3.071E+07	1.78E+19	2.04E+19	2.07E+19
8	3.541E+07	2.08E+19	2.38E+19	2.41E+19
9	3.446E+07	2.37E+19	2.71E+19	2.75E+19
10	3.701E+07	2.65E+19	3.03E+19	3.07E+19
11	3.538E+07	2.92E+19	3.34E+19	3.39E+19
12	3.794E+07	3.20E+19	3.66E+19	3.71E+19

Table 4.2-3 Calculated Fast Neutron Flux (E > 1.0 MeV) at the Reactor Vessel Clad/Base Metal Interface (15° Neutron Pad Octant)

	Neutron Flux [n/cm²-sec]			
Cycle	0°	15°	30°	45°
1	1.27E+10	1.92E+10	1.90E+10	2.25E+10
2	1.50E+10	2.28E+10	2.21E+10	2.59E+10
3	1.22E+10	1.89E+10	1.91E+10	2.35E+10
4	1.25E+10	1.87E+10	1.74E+10	1.95E+10
5	1.21E+10	1.85E+10	1.68E+10	1.82E+10
6	1.33E+10	1.93E+10	1.66E+10	1.75E+10
7	1.22E+10	1.87E+10	1.69E+10	1.81E+10
8	1.25E+10	1.84E+10	1.66E+10	1.82E+10
9	1.16E+10	1.68E+10	1.62E+10	1.87E+10
10	1.01E+10	1.48E+10	1.47E+10	1.65E+10
11	1.02E+10	1.50E+10	1.48E+10	1.65E+10
12	9.39E+09	1.40E+10	1.44E+10	1.60E+10

Table 4.2-4   Calculated Fast Neutron Fluence (E > 1.0 MeV) at the Reactor Vessel
                Clad/Base Metal Interface (15° Neutron Pad Octant)

	Cycle Length	Cumulative Fluence [n/cm2]			
Cycle	EFPS	0°	15°	30°	45°
1	3.239E+07	4.12E+17	6.22E+17	6.16E+17	7.27E+17
2	2.158E+07	7.35E+17	1.11E+18	1.09E+18	1.29E+18
3	2.311E+07	1.02E+18	1.55E+18	1.54E+18	1.83E+18
4	2.664E+07	1.35E+18	2.05E+18	2.00E+18	2.35E+18
5	2.769E+07	1.69E+18	2.56E+18	2.46E+18	2.86E+18
6	2.891E+07	2.07E+18	3.12E+18	2.94E+18	3.36E+18
7	3.071E+07	2.45E+18	3.69E+18	3.46E+18	3.92E+18
8	3.541E+07	2.89E+18	4.35E+18	4.05E+18	4.56E+18
9	3.446E+07	3.29E+18	4.93E+18	4.61E+18	5.21E+18
10	3.701E+07	3.66E+18	5.47E+18	5.15E+18	5.82E+18
11	3.538E+07	4.02E+18	6.00E+18	5.68E+18	6.41E+18
12	3.794E+07	4.38E+18	6.54E+18	6.22E+18	7.01E+18

Table 4.2-5   Calculated Fast Neutron Flux (E > 1.0 MeV) at the Cavity Sensor Set
Locations (15° Neutron Pad Octant)

	Neutron Flux [n/cm²-sec]			
Cycle	0.5°	14.5°	29.5°	44.5°
1	6.53E+08	9.37E+08	1.00E+09	9.30E+08
2	7.70E+08	1.11E+09	1.17E+09	1.08E+09
3	6.31E+08	9.20E+08	1.01E+09	9.65E+08
4	6.42E+08	9.07E+08	9.21E+08	8.20E+08
5	6.24E+08	8.91E+08	8.91E+08	7.73E+08
6	6.75E+08	9.31E+08	8.87E+08	7.45E+08
7	6.31E+08	8.99E+08	8.96E+08	7.69E+08
8	6.37E+08	8.92E+08	8.84E+08	7.67E+08
9	5.87E+08	8.21E+08	8.57E+08	7.81E+08
10	5.15E+08	7.24E+08	7.69E+08	6.94E+08
11	5.22E+08	7.35E+08	7.76E+08	6.95E+08
12	4.82E+08	6.88E+08	7.47E+08	6.73E+08

Table 4.2-6   Calculated Fast Neutron Fluence (E > 1.0 MeV) at the Cavity Sensor Set
Locations (15° Neutron Pad Octant)

	Cycle Length	Cumulative Fluence [n/cm^2]			
Cycle	EFPS	0.5°	14.5°	29.5°	44.5°
1	3.239E+07	2.12E+16	3.03E+16	3.25E+16	3.01E+16
2	2.158E+07	3.78E+16	5.42E+16	5.77E+16	5.34E+16
3	2.311E+07	5.24E+16	7.55E+16	8.10E+16	7.57E+16
4	2.664E+07	6.95E+16	9.96E+16	1.06E+17	9.75E+16
5	2.769E+07	8.68E+16	1.24E+17	1.30E+17	1.19E+17
6	2.891E+07	1.06E+17	1.51E+17	1.56E+17	1.40E+17
7	3.071E+07	1.26E+17	1.79E+17	1.83E+17	1.64E+17
8	3.541E+07	1.48E+17	2.10E+17	2.15E+17	1.91E+17
9	3.446E+07	1.68E+17	2.39E+17	2.44E+17	2.18E+17
10	3.701E+07	1.88E+17	2.66E+17	2.73E+17	2.44E+17
11	3.538E+07	2.06E+17	2.92E+17	3.00E+17	2.68E+17
12	3.794E+07	2.24E+17	3.18E+17	3.29E+17	2.94E+17

Table 4.2-7   Calculated Fast Neutron Flux (E > 0.1 MeV) at the Center of Reactor Vessel
Surveillance Capsules

Neutron Flux [n/cm²-sec]

Cycle No.	Dual Capsule 31.5°	Dual Capsule 34°	Single Capsule 34°
1	4.39E+11	5.25E+11	5.33E+11
2	5.10E+11	6.12E+11	6.20E+11
3	4.44E+11	5.37E+11	5.45E+11
4	3.93E+11	4.63E+11	4.69E+11
5	3.78E+11	4.40E+11	4.46E+11
6	3.66E+11	4.23E+11	4.28E+11
7	3.77E+11	4.39E+11	4.45E+11
8	3.72E+11	4.35E+11	4.41E+11
9	3.70E+11	4.39E+11	4.45E+11
10	3.35E+11	3.95E+11	4.00E+11
11	3.38E+11	3.97E+11	4.02E+11
12	3.30E+11	3.87E+11	3.92E+11

Table 4.2-8   Calculated Fast Neutron Fluence (E > 0.1 MeV) at the Center of Reactor Vessel Surveillance Capsules

| | | Cumulative Fluence [n/cm²] | | |
| | | Dual Capsule | | Single Capsule |
Cycle	Cycle Length EFPS	31.5°	34°	34°
1	3.239E+07	1.42E+19	1.70E+19	1.73E+19
2	2.158E+07	2.52E+19	3.02E+19	3.06E+19
3	2.311E+07	3.55E+19	4.26E+19	4.32E+19
4	2.664E+07	4.60E+19	5.49E+19	5.57E+19
5	2.769E+07	5.64E+19	6.71E+19	6.81E+19
6	2.891E+07	6.70E+19	7.93E+19	8.05E+19
7	3.071E+07	7.86E+19	9.28E+19	9.41E+19
8	3.541E+07	9.17E+19	1.08E+20	1.10E+20
9	3.446E+07	1.05E+20	1.23E+20	1.25E+20
10	3.701E+07	1.17E+20	1.38E+20	1.40E+20
11	3.538E+07	1.29E+20	1.52E+20	1.54E+20
12	3.794E+07	1.41E+20	1.67E+20	1.69E+20

Table 4.2-9   Calculated Fast Neutron Flux (E > 0.1 MeV) at the Reactor Vessel Clad/Base Metal Interface (15° Neutron Pad Octant)

	Neutron Flux [n/cm²-sec]			
Cycle	**0°**	**15°**	**30°**	**45°**
1	2.64E+10	4.02E+10	4.32E+10	5.58E+10
2	3.10E+10	4.78E+10	5.01E+10	6.44E+10
3	2.52E+10	3.95E+10	4.34E+10	5.84E+10
4	2.60E+10	3.92E+10	3.94E+10	4.86E+10
5	2.50E+10	3.87E+10	3.82E+10	4.53E+10
6	2.75E+10	4.05E+10	3.76E+10	4.35E+10
7	2.54E+10	3.91E+10	3.83E+10	4.50E+10
8	2.59E+10	3.86E+10	3.77E+10	4.51E+10
9	2.39E+10	3.52E+10	3.68E+10	4.66E+10
10	2.10E+10	3.09E+10	3.33E+10	4.11E+10
11	2.12E+10	3.14E+10	3.37E+10	4.11E+10
12	1.94E+10	2.93E+10	3.27E+10	3.97E+10

Table 4.2-10   Calculated Fast Neutron Fluence (E > 0.1 MeV) at the Reactor Vessel
Clad/Base Metal Interface (15° Neutron Pad Octant)

	Cycle Length	Cumulative Fluence [n/cm^2]			
Cycle	EFPS	0°	15°	30°	45°
1	3.239E+07	1.81E+18	1.40E+18	1.30E+18	8.54E+17
2	2.158E+07	3.20E+18	2.48E+18	2.33E+18	1.52E+18
3	2.311E+07	4.55E+18	3.48E+18	3.25E+18	2.11E+18
4	2.664E+07	5.84E+18	4.53E+18	4.29E+18	2.80E+18
5	2.769E+07	7.10E+18	5.59E+18	5.36E+18	3.49E+18
6	2.891E+07	8.35E+18	6.68E+18	6.53E+18	4.29E+18
7	3.071E+07	9.74E+18	7.86E+18	7.73E+18	5.07E+18
8	3.541E+07	1.13E+19	9.19E+18	9.10E+18	5.98E+18
9	3.446E+07	1.29E+19	1.05E+19	1.03E+19	6.81E+18
10	3.701E+07	1.45E+19	1.17E+19	1.15E+19	7.59E+18
11	3.538E+07	1.59E+19	1.29E+19	1.26E+19	8.34E+18
12	3.794E+07	1.74E+19	1.41E+19	1.37E+19	9.08E+18

Table 4.2-11   Calculated Fast Neutron Flux (E > 0.1 MeV) at the Cavity Sensor Set
Locations (15° Neutron Pad Octant)

	Neutron Flux [n/cm²-sec]			
Cycle	0.5°	14.5°	29.5°	44.5°
1	6.18E+09	9.33E+09	1.08E+10	9.87E+09
2	7.28E+09	1.10E+10	1.26E+10	1.14E+10
3	5.96E+09	9.16E+09	1.09E+10	1.02E+10
4	6.07E+09	9.03E+09	9.92E+09	8.69E+09
5	5.90E+09	8.87E+09	9.60E+09	8.19E+09
6	6.37E+09	9.28E+09	9.56E+09	7.90E+09
7	5.97E+09	8.96E+09	9.65E+09	8.16E+09
8	6.02E+09	8.88E+09	9.52E+09	8.13E+09
9	5.55E+09	8.18E+09	9.23E+09	8.29E+09
10	4.87E+09	7.21E+09	8.28E+09	7.36E+09
11	4.93E+09	7.32E+09	8.36E+09	7.37E+09
12	4.56E+09	6.86E+09	8.05E+09	7.14E+09

Table 4.2-12   Calculated Fast Neutron Fluence (E > 0.1 MeV) at the Cavity Sensor Set
Locations (15° Neutron Pad Octant)

	Cycle Length	Cumulative Fluence [n/cm^2]			
Cycle	EFPS	0.5°	14.5°	29.5°	44.5°
1	3.239E+07	2.00E+17	3.02E+17	3.50E+17	3.20E+17
2	2.158E+07	3.57E+17	5.40E+17	6.22E+17	5.66E+17
3	2.311E+07	4.95E+17	7.52E+17	8.73E+17	8.03E+17
4	2.664E+07	6.57E+17	9.93E+17	1.14E+18	1.03E+18
5	2.769E+07	8.20E+17	1.24E+18	1.40E+18	1.26E+18
6	2.891E+07	1.00E+18	1.51E+18	1.68E+18	1.49E+18
7	3.071E+07	1.19E+18	1.78E+18	1.98E+18	1.74E+18
8	3.541E+07	1.40E+18	2.10E+18	2.31E+18	2.03E+18
9	3.446E+07	1.59E+18	2.38E+18	2.63E+18	2.31E+18
10	3.701E+07	1.77E+18	2.65E+18	2.94E+18	2.59E+18
11	3.538E+07	1.95E+18	2.90E+18	3.23E+18	2.85E+18
12	3.794E+07	2.12E+18	3.16E+18	3.54E+18	3.12E+18

Table 4.2-13   Calculated Iron Displacement Rate at the Center of Reactor Vessel Surveillance Capsules

<u>Displacement Rate [dpa/sec]</u>

Cycle No.	Dual Capsule		Single Capsule
	31.5°	34°	34°
1	1.91E-10	2.25E-10	2.28E-10
2	2.22E-10	2.62E-10	2.66E-10
3	1.93E-10	2.30E-10	2.33E-10
4	1.71E-10	1.98E-10	2.01E-10
5	1.64E-10	1.88E-10	1.91E-10
6	1.59E-10	1.81E-10	1.83E-10
7	1.64E-10	1.88E-10	1.90E-10
8	1.62E-10	1.86E-10	1.89E-10
9	1.61E-10	1.88E-10	1.91E-10
10	1.46E-10	1.69E-10	1.71E-10
11	1.47E-10	1.70E-10	1.72E-10
12	1.43E-10	1.66E-10	1.68E-10

Table 4.2-14   Calculated Iron Displacements at the Center of Reactor Vessel Surveillance Capsules

		Cumulative Displacements [dpa]		
		Dual Capsule		Single Capsule
	Cycle Length			
Cycle	EFPS	31.5°	34°	34°
1	3.239E+07	6.19E-03	7.29E-03	7.39E-03
2	2.158E+07	1.10E-02	1.29E-02	1.31E-02
3	2.311E+07	1.54E-02	1.82E-02	1.85E-02
4	2.664E+07	2.00E-02	2.35E-02	2.39E-02
5	2.769E+07	2.45E-02	2.87E-02	2.91E-02
6	2.891E+07	2.91E-02	3.40E-02	3.44E-02
7	3.071E+07	3.42E-02	3.97E-02	4.03E-02
8	3.541E+07	3.99E-02	4.63E-02	4.70E-02
9	3.446E+07	4.54E-02	5.28E-02	5.35E-02
10	3.701E+07	5.08E-02	5.91E-02	5.99E-02
11	3.538E+07	5.60E-02	6.51E-02	6.60E-02
12	3.794E+07	6.15E-02	7.14E-02	7.23E-02

Table 4.2-15   Calculated Iron Displacement Rate at the Reactor Vessel Clad/Base Metal Interface (15° Neutron Pad Octant)

	Displacement Rate [dpa/sec]			
Cycle	0°	15°	30°	45°
1	1.95E-11	2.92E-11	2.93E-11	3.51E-11
2	2.30E-11	3.46E-11	3.40E-11	4.05E-11
3	1.86E-11	2.86E-11	2.95E-11	3.67E-11
4	1.92E-11	2.84E-11	2.67E-11	3.06E-11
5	1.85E-11	2.81E-11	2.59E-11	2.85E-11
6	2.04E-11	2.93E-11	2.55E-11	2.74E-11
7	1.88E-11	2.83E-11	2.60E-11	2.83E-11
8	1.92E-11	2.80E-11	2.56E-11	2.84E-11
9	1.77E-11	2.55E-11	2.50E-11	2.93E-11
10	1.56E-11	2.24E-11	2.26E-11	2.59E-11
11	1.57E-11	2.28E-11	2.28E-11	2.58E-11
12	1.44E-11	2.13E-11	2.22E-11	2.50E-11

Table 4.2-16   Calculated Iron Displacements at the Reactor Vessel Clad/Base Metal Interface (15° Neutron Pad Octant)

	Cycle Length	Cumulative Displacements [dpa]			
Cycle	EFPS	0°	15°	30°	45°
1	3.239E+07	6.32E-04	9.44E-04	9.49E-04	1.14E-03
2	2.158E+07	1.13E-03	1.69E-03	1.68E-03	2.01E-03
3	2.311E+07	1.56E-03	2.35E-03	2.36E-03	2.86E-03
4	2.664E+07	2.07E-03	3.11E-03	3.08E-03	3.67E-03
5	2.769E+07	2.58E-03	3.89E-03	3.79E-03	4.46E-03
6	2.891E+07	3.17E-03	4.73E-03	4.53E-03	5.26E-03
7	3.071E+07	3.75E-03	5.60E-03	5.33E-03	6.13E-03
8	3.541E+07	4.43E-03	6.60E-03	6.23E-03	7.13E-03
9	3.446E+07	5.04E-03	7.47E-03	7.09E-03	8.14E-03
10	3.701E+07	5.61E-03	8.30E-03	7.93E-03	9.10E-03
11	3.538E+07	6.17E-03	9.11E-03	8.74E-03	1.00E-02
12	3.794E+07	6.71E-03	9.92E-03	9.58E-03	1.10E-02

Table 4.2-17   Calculated Iron Displacement Rate at the Cavity Sensor Set Locations
(15° Neutron Pad Octant)

Displacement Rate [dpa/sec]

Cycle	0.5°	14.5°	29.5°	44.5°
1	2.16E-12	3.22E-12	3.66E-12	3.31E-12
2	2.54E-12	3.81E-12	4.26E-12	3.84E-12
3	2.08E-12	3.16E-12	3.68E-12	3.44E-12
4	2.12E-12	3.12E-12	3.36E-12	2.92E-12
5	2.06E-12	3.06E-12	3.25E-12	2.75E-12
6	2.22E-12	3.20E-12	3.23E-12	2.65E-12
7	2.08E-12	3.09E-12	3.27E-12	2.74E-12
8	2.10E-12	3.07E-12	3.22E-12	2.73E-12
9	1.94E-12	2.82E-12	3.12E-12	2.78E-12
10	1.70E-12	2.49E-12	2.80E-12	2.47E-12
11	1.72E-12	2.53E-12	2.83E-12	2.48E-12
12	1.59E-12	2.37E-12	2.72E-12	2.40E-12

Table 4.2-18   Calculated Iron Displacements at the Cavity Sensor Set Locations
(15° Neutron Pad Octant)

	Cycle Length	Cumulative Displacements [dpa]			
Cycle	EFPS	0.5°	14.5°	29.5°	44.5°
1	3.239E+07	6.98E-05	1.04E-04	1.18E-04	1.07E-04
2	2.158E+07	1.25E-04	1.86E-04	2.10E-04	1.90E-04
3	2.311E+07	1.73E-04	2.59E-04	2.95E-04	2.70E-04
4	2.664E+07	2.29E-04	3.43E-04	3.85E-04	3.47E-04
5	2.769E+07	2.86E-04	4.27E-04	4.75E-04	4.24E-04
6	2.891E+07	3.50E-04	5.20E-04	5.68E-04	5.00E-04
7	3.071E+07	4.14E-04	6.15E-04	6.69E-04	5.85E-04
8	3.541E+07	4.89E-04	7.23E-04	7.83E-04	6.81E-04
9	3.446E+07	5.56E-04	8.21E-04	8.90E-04	7.77E-04
10	3.701E+07	6.18E-04	9.13E-04	9.94E-04	8.69E-04
11	3.538E+07	6.79E-04	1.00E-03	1.09E-03	9.56E-04
12	3.794E+07	7.40E-04	1.09E-03	1.20E-03	1.05E-03

5   EVALUATION OF SURVEILLANCE CAPSULE DOSIMETRY

In this section, the results of the evaluations of the six neutron sensor sets withdrawn as a part of the McGuire Unit 2 Reactor Vessel Materials Surveillance Program[34] are presented. The capsule designation, location within the reactor, and time of withdrawal of each of these dosimetry sets were as follows:

Capsule ID	Azimuthal Location	Withdrawal Time	Irradiation Time (EFPS)
V	31.5° - Dual	End Of Cycle 1	3.239E+07
X	34.0° - Dual	End Of Cycle 5	1.314E+08
U	34.0° - Dual	End Of Cycle 7	1.910E+08
Y	31.5° - Dual	End Of Cycle 8	2.264E+08
Z	34.0° - Single	End Of Cycle 8	2.264E+08
W	34.0° - Single	End Of Cycle 10	2.979E+08

5.1   MEASURED REACTION RATES

The radiometric counting of each of these capsule dosimetry data sets was accomplished by Westinghouse using the procedures discussed in Section 3.0 of this report. The measured specific activities are included in Appendix A to this report.

The irradiation history of the McGuire Unit 2 reactor during the first ten fuel cycles of operation is also listed in Appendix A. The irradiation history was obtained from NUREG-0020, "Licensed Operating Reactors Status Summary Report" and from plant personnel[17] for the applicable operating periods

Based on the irradiation history, the individual sensor characteristics, and the measured specific activities, reaction rates averaged over the appropriate irradiation periods and referenced to a core power level of 3411 MWt were computed for the sensor set removed from Capsules V, X, U, Y, Z, and W. The computed reaction rates for the multiple foil sensor sets from Capsules V, X, U, Y, Z, and W are provided in Table 5.1-1.

In regard to the data listed in Table 5.1-1, the fission rate measurements for the ^{238}U sensors include corrections for ^{235}U impurities, the build-in of plutonium isotopes during the long irradiations, and for the effects of γ,f reactions. Likewise, the fission rate measurements for the ^{237}Np sensors include adjustments for γ,f reactions occurring over the course of the respective irradiation periods.

5.2   RESULTS OF THE LEAST SQUARES ADJUSTMENT PROCEDURE

The results of the application of the least squares adjustment procedure to the six sets of surveillance capsule dosimetry are provided in Tables 5.2-1 through 5.2-5. In these tables, the best estimate exposure experienced by the capsule along with data illustrating the fit of both the trial and best estimate spectra to the measurements are given. Also included in the tabulations are the 1σ uncertainties associated with each of the derived exposure rates.

In Tables 5.2-1 through 5.2-5, the columns labeled "Calculated" were obtained by normalizing the neutron spectral data from Table 4.1-3 to the absolute calculated neutron flux (E > 1.0 MeV) averaged over the applicable irradiation periods (Cycle 1 for Capsule V, Cycles 1 through 5 for Capsule X, Cycles 1 through 7 for Capsule U, Cycles 1 through 8 for Capsules Y and Z, and Cycles 1 though 10 for Capsule W) as discussed in Section 3.0. Thus, the comparisons illustrated in Tables 5.2-1 through 5.2-5 indicate the degree to which the calculated neutron energy spectra matched the measured sensor data before and after adjustment. Absolute comparisons are discussed further in Section 7.0 of this report.

Table 5.1-1   Summary of Reaction Rates Derived from Multiple Foil Sensor Sets Withdrawn from Internal Surveillance Capsules

<div align="center"><u>Reaction Rate [rps/nucleus]</u></div>

Reaction	Capsule V	Capsule X	Capsule U	Capsule Y	Capsule Z	Capsule W
^{63}Cu (n,α) ^{60}Co	5.21E-17	5.43E-17	5.15E-17	4.80E-17	5.00E-17	4.98E-17
^{54}Fe (n,p) ^{54}Mn	5.23E-15	5.48E-15	5.01E-15	4.28E-15	4.83E-15	4.85E-15
^{58}Ni (n,p) ^{58}Co	7.04E-15	7.69E-15	6.98E-15	6.34E-15	6.94E-15	7.08E-15
^{238}U (n,f) ^{137}Cs (Cd)	3.27E-14	3.62E-14	3.43E-14	3.00E-14	3.63E-14	3.40E-14
^{237}Np (n,f) ^{137}Cs (Cd)	3.30E-13	3.27E-13	3.20E-13	2.79E-13	3.28E-13	3.13E-13
^{59}Co (n,γ) ^{60}Co	5.11E-12	5.45E-12	4.72E-12	3.88E-12	4.68E-12	4.69E-12
^{59}Co (n,γ) ^{60}Co (Cd)	2.78E-12	3.11E-12	2.85E-12	2.23E-12	2.69E-12	2.65E-12

Table 5.2.1   Best Estimate Exposure Rates from Surveillance Capsule V Dosimetry
                Withdrawn at the End of Fuel Cycle 1

Reaction Rate (rps/nucleus)

Reaction	Measured	Calculated	Best Estimate	BE / Meas	BE / Calc	Meas / Calc
^{63}Cu (n,α) ^{60}Co	5.21E-17	5.00E-17	5.00E-17	0.96	1.00	1.04
^{54}Fe (n,p) ^{54}Mn	5.23E-15	5.76E-15	5.38E-15	1.03	0.93	0.91
^{58}Ni (n,p) ^{58}Co	7.04E-15	8.09E-15	7.45E-15	1.06	0.92	0.87
^{238}U (n,f) ^{137}Cs (Cd)	3.27E-14	3.14E-14	2.97E-14	0.91	0.95	1.04
^{237}Np (n,f) ^{137}Cs (Cd)	3.30E-13	3.07E-13	3.14E-13	0.95	1.02	1.07
^{59}Co (n,γ) ^{60}Co	5.11E-12	4.43E-12	5.02E-12	0.98	1.13	1.15
^{59}Co (n,γ) ^{60}Co (Cd)	2.78E-12	3.08E-12	2.82E-12	1.01	0.92	0.90

Exposure Rate	Calculated	Best Estimate	BE / Calc	1σ Uncertainty
φ (E > 1.0 MeV) [n/cm²-sec]	9.96E+10	9.50E+10	0.95	6%
φ (E > 0.1 MeV) [n/cm²-sec]	4.40E+11	4.41E+11	1.00	10%
φ (E < 0.414 eV) [n/cm²-sec]	6.18E+10	9.78E+10	1.58	15%
dpa/sec	1.91E-10	1.88E-10	0.99	8%

Table 5.2-2   Best Estimate Exposure Rates from the Surveillance Capsule X Dosimetry Withdrawn at the End of Fuel Cycle 5

Reaction Rate (rps/nucleus)

Reaction	Measured	Calculated	Best Estimate	BE / Meas	BE / Calc	Meas / Calc
^{63}Cu (n,α) ^{60}Co	5.43E-17	5.19E-17	5.19E-17	0.96	1.00	1.05
^{54}Fe (n,p) ^{54}Mn	5.48E-15	6.20E-15	5.70E-15	1.04	0.92	0.88
^{58}Ni (n,p) ^{58}Co	7.69E-15	8.77E-15	8.01E-15	1.04	0.91	0.88
^{238}U (n,f) ^{137}Cs (Cd)	3.62E-14	3.49E-14	3.21E-14	0.89	0.92	1.04
^{237}Np (n,f) ^{137}Cs (Cd)	3.27E-13	3.52E-13	3.27E-13	1.00	0.93	0.93
^{59}Co (n,γ) ^{60}Co	5.45E-12	5.13E-12	5.38E-12	0.99	1.05	1.06
^{59}Co (n,γ) ^{60}Co (Cd)	3.11E-12	3.58E-12	3.16E-12	1.02	0.88	0.87

Exposure Rate	Calculated	Best Estimate	BE / Calc	1σ Uncertainty
ϕ (E > 1.0 MeV) [n/cm^2-sec]	1.12E+11	1.03E+11	0.92	6%
ϕ (E > 0.1 MeV) [n/cm^2-sec]	5.11E+11	4.84E+11	0.95	10%
ϕ (E < 0.414 eV) [n/cm^2-sec]	7.07E+10	9.92E+10	1.40	16%
dpa/sec	2.19E-10	2.06E-10	0.94	8%

Table 5.2-3   Best Estimate Exposure Rates from the Surveillance Capsule U Dosimetry
Withdrawn at the End of Fuel Cycle 7

Reaction Rate (rps/nucleus)

Reaction	Measured	Calculated	Best Estimate	BE / Meas	BE / Calc	Meas / Calc
^{63}Cu (n,α) ^{60}Co	5.15E-17	4.85E-17	4.87E-17	0.95	1.00	1.06
^{54}Fe (n,p) ^{54}Mn	5.01E-15	5.80E-15	5.27E-15	1.05	0.91	0.86
^{58}Ni (n,p) ^{58}Co	6.98E-15	8.20E-15	7.38E-15	1.06	0.90	0.85
^{238}U (n,f) ^{137}Cs (Cd)	3.43E-14	3.26E-14	2.98E-14	0.87	0.91	1.05
^{237}Np (n,f) ^{137}Cs (Cd)	3.20E-13	3.29E-13	3.13E-13	0.98	0.95	0.97
^{59}Co (n,γ) ^{60}Co	4.72E-12	4.80E-12	4.68E-12	0.99	0.98	0.98
^{59}Co (n,γ) ^{60}Co (Cd)	2.85E-12	3.35E-12	2.88E-12	1.01	0.86	0.85

Exposure Rate	Calculated	Best Estimate	BE / Calc	1σ Uncertainty
φ (E > 1.0 MeV) [n/cm²-sec]	1.05E+11	9.60E+10	0.91	6%
φ (E > 0.1 MeV) [n/cm²-sec]	4.78E+11	4.56E+11	0.95	10%
φ (E < 0.414 eV) [n/cm²-sec]	6.61E+10	8.10E+10	1.23	17%
dpa/sec	2.05E-10	1.93E-10	0.94	8%

Table 5.2-4   Best Estimate Exposure Rates from the Surveillance Capsule Y Dosimetry Withdrawn at the End of Fuel Cycle 8

Reaction Rate (rps/nucleus)

Reaction	Measured	Calculated	Best Estimate	BE / Meas	BE / Calc	Meas / Calc
^{63}Cu (n,α) ^{60}Co	4.80E-17	4.61E-17	4.51E-17	0.94	0.98	1.04
^{54}Fe (n,p) ^{54}Mn	4.28E-15	5.31E-15	4.64E-15	1.08	0.87	0.81
^{58}Ni (n,p) ^{58}Co	6.34E-15	7.46E-15	6.58E-15	1.04	0.88	0.85
^{238}U (n,f) ^{137}Cs (Cd)	3.00E-14	2.90E-14	2.59E-14	0.86	0.89	1.03
^{237}Np (n,f) ^{137}Cs (Cd)	2.79E-13	2.83E-13	2.69E-13	0.96	0.95	0.99
^{59}Co (n,γ) ^{60}Co	3.88E-12	4.09E-12	3.84E-12	0.99	0.94	0.95
^{59}Co (n,γ) ^{60}Co (Cd)	2.23E-12	2.84E-12	2.27E-12	1.02	0.80	0.79

Exposure Rate	Calculated	Best Estimate	BE / Calc	1σ Uncertainty
ϕ (E > 1.0 MeV) [n/cm^2-sec]	9.18E+10	8.25E+10	0.90	6%
ϕ (E > 0.1 MeV) [n/cm^2-sec]	4.05E+11	3.84E+11	0.95	10%
ϕ (E < 0.414 eV) [n/cm^2-sec]	5.69E+10	7.10E+10	1.25	16%
dpa/sec	1.76E-10	1.64E-10	0.93	8%

Table 5.2-5   Best Estimate Exposure Rates from the Surveillance Capsule Z Dosimetry
Withdrawn at the End of Fuel Cycle 8

Reaction Rate (rps/nucleus)

Reaction	Measured	Calculated	Best Estimate	BE / Meas	BE / Calc	Meas / Calc
^{63}Cu (n,α) ^{60}Co	5.00E-17	4.78E-17	4.73E-17	0.95	0.99	1.05
^{54}Fe (n,p) ^{54}Mn	4.83E-15	5.73E-15	5.16E-15	1.07	0.90	0.84
^{58}Ni (n,p) ^{58}Co	6.94E-15	8.13E-15	7.30E-15	1.05	0.90	0.85
^{238}U (n,f) ^{137}Cs (Cd)	3.63E-14	3.26E-14	3.00E-14	0.83	0.92	1.11
^{237}Np (n,f) ^{137}Cs (Cd)	3.28E-13	3.40E-13	3.24E-13	0.99	0.95	0.96
^{59}Co (n,γ) ^{60}Co	4.68E-12	4.49E-12	4.60E-12	0.98	1.02	1.04
^{59}Co (n,γ) ^{60}Co (Cd)	2.69E-12	3.25E-12	2.73E-12	1.01	0.84	0.83

Exposure Rate	Calculated	Best Estimate	BE / Calc	1σ Uncertainty
ϕ (E > 1.0 MeV) [n/cm^2-sec]	1.06E+11	9.85E+10	0.93	6%
ϕ (E > 0.1 MeV) [n/cm^2-sec]	5.03E+11	4.88E+11	0.97	10%
ϕ (E < 0.414 eV) [n/cm^2-sec]	5.58E+10	8.30E+10	1.49	16%
dpa/sec	2.12E-10	2.02E-10	0.95	8%

Table 5.2-6   Best Estimate Exposure Rates from the Surveillance Capsule W Dosimetry Withdrawn at the End of Fuel Cycle 10

Reaction Rate (rps/nucleus)

Reaction	Measured	Calculated	Best Estimate	BE / Meas	BE / Calc	Meas / Calc
^{63}Cu (n,α) ^{60}Co	4.98E-17	4.64E-17	4.74E-17	0.95	1.02	1.07
^{54}Fe (n,p) ^{54}Mn	4.85E-15	5.56E-15	5.15E-15	1.06	0.93	0.87
^{58}Ni (n,p) ^{58}Co	7.08E-15	7.88E-15	7.32E-15	1.03	0.93	0.90
^{238}U (n,f) ^{137}Cs (Cd)	3.40E-14	3.16E-14	2.95E-14	0.87	0.93	1.08
^{237}Np (n,f) ^{137}Cs (Cd)	3.13E-13	3.29E-13	3.12E-13	1.00	0.95	0.95
^{59}Co (n,γ) ^{60}Co	4.69E-12	4.35E-12	4.61E-12	0.98	1.06	1.08
^{59}Co (n,γ) ^{60}Co (Cd)	2.65E-12	3.15E-12	2.70E-12	1.02	0.86	0.84

Exposure Rate	Calculated	Best Estimate	BE / Calc	1σ Uncertainty
ϕ (E > 1.0 MeV) [n/cm^2-sec]	1.03E+11	9.64E+10	0.93	6%
ϕ (E > 0.1 MeV) [n/cm^2-sec]	4.87E+11	4.71E+11	0.97	10%
ϕ (E < 0.414 eV) [n/cm^2-sec]	5.40E+10	8.46E+10	1.56	15%
dpa/sec	2.05E-10	1.96E-10	0.96	8%

6   EVALUATION OF REACTOR CAVITY DOSIMETRY

In this section, the results of the evaluations of the neutron sensor sets irradiated since the inception of the Reactor Cavity Measurement Program are presented. At McGuire Unit 2, the program was initiated prior to Cycle 12 operation and includes one set of measurement evaluations at the conclusion of Cycle 12. The evaluation of this set of measured data was accomplished using a consistent approach based on the methodology discussed in Section 3.0, resulting in an accurate database defining the exposure of the reactor vessel wall.

6.1   CYCLE 12 RESULTS

6.1.1   Measured Reaction rates

During the Cycle 12 irradiation, six multiple foil sensor sets and four stainless steel gradient chains were deployed in the reactor cavity as depicted in Figures 2.1-1 through 2.1-3. The capsule identifications associated with each of the multiple foil sensor sets were as follows:

		Capsule Identification	
Azimuth (Degrees)	Top of Core	Core Midplane	Bottom of Core
0.5		G	
14.5		H	
29.5		I	
44.5	J	K	L

The contents of each of these irradiation capsules is specified in Appendix B to this report.

The irradiation history of the McGuire Unit 2 reactor during Cycle 12 is listed in Appendix B. The irradiation history was obtained from plant personnel[17] for the applicable operating period. Based on this reactor operating history, the individual sensor characteristics, and the measured specific activities given in Appendix B, cycle average reaction rates referenced to a core power level of 3411 MWt were computed for each multiple foil sensor and gradient wire segment.

The computed reaction rates for the multiple foil sensor sets irradiated during Cycle 12 are provided in Table 6.1-1. Corresponding ^{54}Fe (n,p) ^{54}Mn, ^{58}Ni (n,p) ^{58}Co, and ^{59}Co (n,γ) ^{60}Co reaction rate data from segments of the four stainless steel gradient chains are recorded in Tables 6.1-2 through 6.1-5 for the 0.5°, 14.5°, 29.5°, and 44.5° chains, respectively. The ^{54}Fe (n,p) ^{54}Mn reaction rates are also shown plotted in Figures 6.1-1 through 6.1-4

In regard to the data listed in Table 6.1-1, the ^{54}Fe (n,p) ^{54}Mn reaction rates represent an average of the bare and cadmium covered measurements for each capsule. The ^{238}U (n,f) F.P. reaction rates include corrections for ^{235}U impurities in the ^{238}U sensors as well as corrections for photofission reactions in both the ^{238}U and ^{237}Np sensors. The ^{238}U and ^{237}Np sensors also include

corrections for the gamma ray self-absorption in the oxide matrix and vanadium capsule as described in Section 3.2.1.2.

6.1.2   Axial Position of Reactor Cavity Dosimetry

An examination of the axial reaction rate distributions shown in Figures 6.1-1 through 6.1-4 shows an unrealistic asymmetry relative to the core midplane. The data suggests that the dosimetry support bar is located at a position lower that the as designed position. In order to estimate the amount of axial mispositioning, these axial distributions were compared to those measured during Cycle 12 at McGuire Unit 1[36]. The data comparison indicates that the dosimetry support bar may be located approximately 12 to 18 inches lower than the intended installation point.

When correctly installed, there is approximately 19 inches of excess support chain between the threaded chain connector that attaches the support chain to the spring hook on the local attachment plate at plant elevation 746☐+10.5☐ (refer to Westinghouse Drawing 6452E95, Revision 1). If, instead of the intended threaded chain connector, a link of the support chain itself were attached to the spring hook on the local attachment plate, this would place the dosimetry support bar lower in the reactor cavity by up to 19 inches. While it was noted that there was difficulty in raising the dosimetry bar into position, there was no mention of anything unusual during the support chain attachment phase of the installation. It is recommended that a visual examination of the support chain attachment configuration be performed during the Cycle 13/14 refueling outage (Fall 2000).

While it appears that the dosimetry support bar is located at a position lower that the as designed position, this has no impact on the interpretation of the midplane dosimetry capsules presented in this report. This is due to the fact that the cycle average axial core power distribution is flat in the central portion of the core.

6.1.3   Results of the Least Squares Adjustment Procedure

The results of the application of the least squares adjustment procedure to the six sets of multiple foil measurements obtained from the Cycle 12 irradiation are provided in Tables 6.1-6 through 6.1-11. In these tables, the best estimate exposure experienced at each sensor set location along with data illustrating the fit of both the trial and best estimate spectra to the measurements are given. Also included in the tabulations are the 1σ uncertainties associated with each of the derived exposure rates.

In Tables 6.1-6 through 6.1-11, the columns labeled "Calculated" were obtained by normalizing the neutron spectral data from Table 4.1-2 to the absolute calculated neutron flux (E > 1.0 MeV) averaged over the Cycle 12 irradiation period as discussed in Section 3.0. Thus, the comparisons illustrated in Tables 6.1-6 through 6.1-11 indicate the degree to which the calculated neutron energy spectra matched the measured data before and after adjustment. Absolute comparisons of calculation and measurement are discussed further in Section 7.0 of this report.

**Table 6.1-1   Summary of Reaction Rates Derived from Multiple Foil Sensor Sets
Cycle 12 Irradiation**

Reaction Rate [rps/nucleus]

Reaction	Capsule G	Capsule H	Capsule I	Capsule K	Capsule J	Capsule L
^{63}Cu (n,α) ^{60}Co (Cd)	3.37E-19	4.34E-19	4.20E-19	3.38E-19	2.30E-19	3.80E-20
^{46}Ti (n,p) ^{46}Sc (Cd)	4.90E-18	6.42E-18	6.35E-18	5.06E-18	3.85E-18	6.37E-19
^{54}Fe (n,p) ^{54}Mn (Cd)	2.42E-17	3.81E-17	3.41E-17	2.83E-17	2.06E-17	3.60E-18
^{58}Ni (n,p) ^{58}Co (Cd)	3.41E-17	5.04E-17	4.89E-17	4.13E-17	3.32E-17	5.48E-18
^{238}U (n,f) ^{137}Cs (Cd)	1.25E-16	1.82E-16	1.96E-16	1.92E-16	1.61E-16	2.33E-17
^{237}Np (n,f) ^{137}Cs (Cd)	2.01E-15	3.05E-15	3.70E-15	1.50E-15	2.86E-15	4.41E-16
^{59}Co (n,γ) ^{60}Co	3.63E-14	4.63E-14	6.87E-14	4.27E-14	2.80E-14	1.12E-14
^{59}Co (n,γ) ^{60}Co (Cd)	1.68E-14	2.77E-14	3.53E-14	2.80E-14	1.81E-14	6.95E-15

Table 6.1-2 ^{54}Fe (n,p), ^{58}Ni (n,p) and ^{59}Co (n,γ) Reaction Rates Derived from the RCND Stainless Steel Gradient Chain at 0.5° - Cycle 12 Irradiation

Distance From Core Midplane (ft)	Reaction Rate [rps/nucleus]		
	^{54}Fe (n,p)	^{58}Ni (n,p)	^{59}Co (n,γ)
5.5	1.88E-17	2.77E-17	1.88E-14
4.5	2.23E-17	3.34E-17	2.24E-14
3.5	2.39E-17	3.62E-17	2.55E-14
2.5	2.56E-17	3.57E-17	2.74E-14
1.5	2.50E-17	3.54E-17	3.51E-14
0.5	2.45E-17	3.47E-17	3.64E-14
-0.5	2.42E-17	3.39E-17	3.55E-14
-1.5	2.40E-17	3.36E-17	3.44E-14
-2.5	2.17E-17	3.23E-17	3.09E-14
-3.5	1.88E-17	2.78E-17	1.99E-14
-4.5	1.11E-17	1.72E-17	1.35E-14
-5.5	4.15E-18	6.43E-18	8.76E-15
-6.5	1.21E-18	2.07E-18	3.94E-15

Table 6.1-3　^{54}Fe (n,p), ^{58}Ni (n,p) and ^{59}Co (n,γ) Reaction Rates Derived from the RCND Stainless Steel Gradient Chain at 14.5° – Cycle 12 Irradiation

Distance From Core Midplane	Reaction Rate [rps/nucleus]		
(ft)	^{54}Fe (n,p)	^{58}Ni (n,p)	^{59}Co (n,γ)
5.5	2.73E-17	4.13E-17	3.87E-14
4.5	3.14E-17	4.79E-17	4.75E-14
3.5	3.35E-17	4.95E-17	5.36E-14
2.5	3.59E-17	4.91E-17	5.26E-14
1.5	3.45E-17	4.87E-17	4.69E-14
0.5	3.43E-17	4.87E-17	4.61E-14
-0.5	3.37E-17	4.79E-17	4.61E-14
-1.5	3.24E-17	4.79E-17	4.41E-14
-2.5	3.11E-17	4.62E-17	4.08E-14
-3.5	2.74E-17	4.04E-17	3.71E-14
-4.5	1.80E-17	2.73E-17	2.67E-14
-5.5	7.23E-18	1.13E-17	1.55E-14
-6.5	2.10E-18	3.29E-18	7.26E-15

Table 6.1-4 ^{54}Fe (n,p), ^{58}Ni (n,p) and ^{59}Co (n,γ) Reaction Rates Derived from the RCND Stainless Steel Gradient Chain at 29.5° - Cycle 12 Irradiation

Distance From Core Midplane	Reaction Rate [rps/nucleus]		
(ft)	^{54}Fe (n,p)	^{58}Ni (n,p)	^{59}Co (n,γ)
5.5	2.70E-17	4.30E-17	5.43E-14
4.5	3.17E-17	4.75E-17	6.82E-14
3.5	3.48E-17	4.99E-17	7.65E-14
2.5	3.60E-17	4.99E-17	7.76E-14
1.5	3.47E-17	4.95E-17	7.37E-14
0.5	3.31E-17	4.95E-17	6.98E-14
-0.5	3.34E-17	4.75E-17	6.43E-14
-1.5	3.35E-17	4.87E-17	6.65E-14
-2.5	3.18E-17	4.71E-17	5.93E-14
-3.5	2.66E-17	4.06E-17	5.40E-14
-4.5	1.76E-17	2.72E-17	4.00E-14
-5.5	7.91E-18	1.21E-17	2.42E-14
-6.5	2.35E-18	3.77E-18	1.02E-14

Table 6.1-5 ^{54}Fe (n,p), ^{58}Ni (n,p) and ^{59}Co (n,γ) Reaction Rates Derived from the RCND Stainless Steel Gradient Chain at 44.5° - Cycle 12 Irradiation

Distance From Core Midplane	Reaction Rate [rps/nucleus]		
(ft)	^{54}Fe (n,p)	^{58}Ni (n,p)	^{59}Co (n,γ)
5.5	2.35E-17	3.76E-17	3.36E-14
4.5	2.97E-17	4.46E-17	4.07E-14
3.5	3.06E-17	4.54E-17	4.52E-14
2.5	3.00E-17	4.58E-17	4.77E-14
1.5	3.10E-17	4.58E-17	4.69E-14
0.5	2.93E-17	4.38E-17	4.50E-14
-0.5	2.85E-17	4.26E-17	4.48E-14
-1.5	2.89E-17	4.22E-17	4.32E-14
-2.5	2.68E-17	4.06E-17	3.90E-14
-3.5	2.25E-17	3.49E-17	3.33E-14
-4.5	1.39E-17	2.23E-17	2.27E-14
-5.5	5.93E-18	9.45E-18	1.59E-14
-6.5	5.54E-19	9.09E-19	1.86E-15

Figure 6.1-1 ^{54}Fe (n,p) ^{54}Mn Reaction Rate Derived from the Stainless Steel Gradient Chain at 0.5 Degrees in the Reactor Cavity - Cycle 12 Irradiation
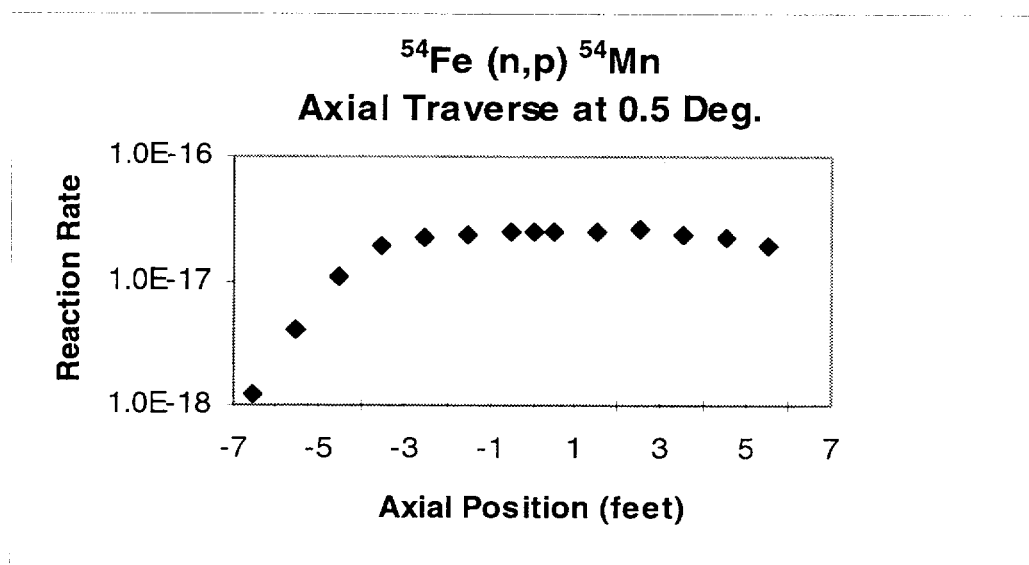
Figure 6.1-2 ^{54}Fe (n,p) ^{54}Mn Reaction Rate Derived from the Stainless Steel Gradient Chain at 14.5 Degrees in the Reactor Cavity - Cycle 12 Irradiation
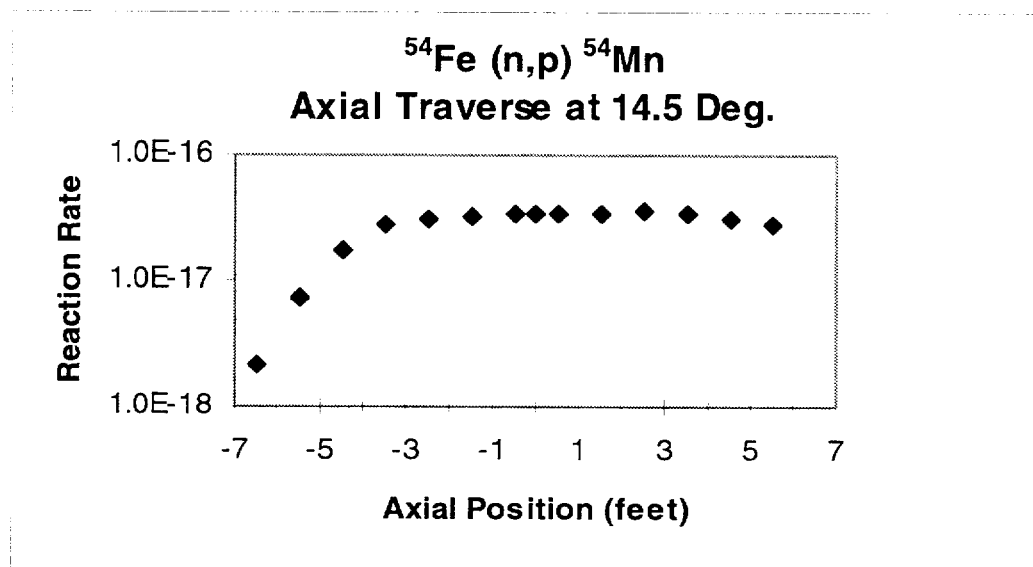
Figure 6.1-3 ^{54}Fe (n,p) ^{54}Mn Reaction Rate Derived from the Stainless Steel Gradient Chain at 29.5 Degrees in the Reactor Cavity - Cycle 12 Irradiation

^{54}Fe (n,p) ^{54}Mn
Axial Traverse at 29.5 Deg.
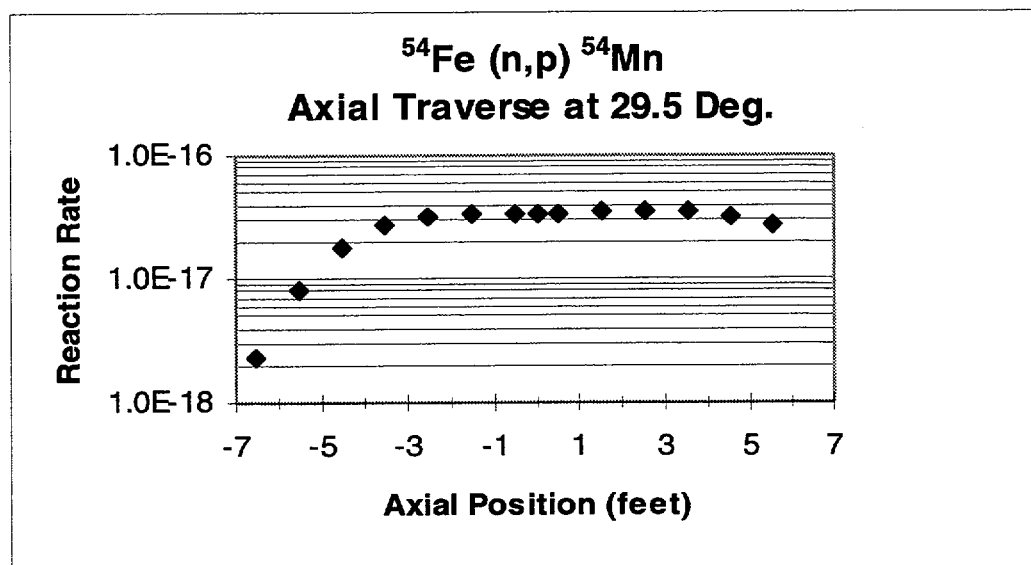
Figure 6.1-4 ^{54}Fe (n,p) ^{54}Mn Reaction Rate Derived from the Stainless Steel Gradient Chain at 44.5 Degrees in the Reactor Cavity - Cycle 12 Irradiation

^{54}Fe (n,p) ^{54}Mn
Axial Traverse at 44.5 Deg.
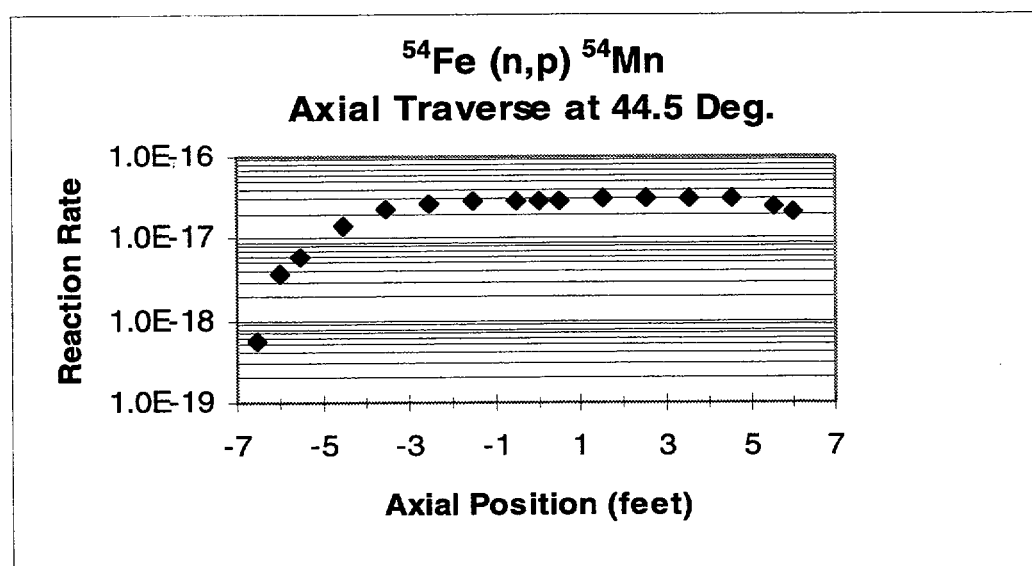
Table 6.1-6   Best Estimate Exposure Rates from the Capsule G Dosimetry Evaluation
                0.5° Azimuth - Core Midplane - Cycle 12 Irradiation

Reaction Rate (rps/nucleus)

Reaction	Measured	Calculated	Best Estimate	BE / Meas	BE / Calc	Meas / Calc
^{63}Cu (n,α) ^{60}Co (cd)	3.37E-19	3.98E-19	3.40E-19	1.01	0.85	0.85
^{46}Ti (n,p) ^{46}Sc (Cd)	4.90E-18	5.42E-18	4.72E-18	0.96	0.87	0.90
^{54}Fe (n,p) ^{54}Mn (Cd)	2.42E-17	2.93E-17	2.48E-17	1.02	0.85	0.83
^{58}Ni (n,p) ^{58}Co (Cd)	3.41E-17	4.08E-17	3.46E-17	1.01	0.85	0.84
^{238}U (n,f) ^{137}Cs (Cd)	1.25E-16	1.46E-16	1.25E-16	1.00	0.86	0.86
^{237}Np (n,f) ^{137}Cs (Cd)	2.01E-15	2.11E-15	1.91E-15	0.95	0.91	0.95
^{59}Co (n,γ) ^{60}Co	3.63E-14	7.91E-14	3.69E-14	1.02	0.47	0.46
^{59}Co (n,γ) ^{60}Co (Cd)	1.68E-14	2.72E-14	1.69E-14	1.01	0.62	0.62

Exposure Rate	Calculated	Best Estimate	BE / Calc	1σ Uncertainty
ϕ (E > 1.0 MeV) [n/cm^2-sec]	4.82E+08	4.14E+08	0.86	6%
ϕ (E > 0.1 MeV) [n/cm^2-sec]	4.56E+09	4.01E+09	0.88	11%
ϕ (E < 0.414 eV) [n/cm^2-sec]	1.77E+09	7.27E+08	0.41	12%
dpa/sec	1.59E-12	1.38E-12	0.87	9%

**Table 6.1-7   Best Estimate Exposure Rates From the Capsule H Dosimetry Evaluation
14.5° Azimuth - Core Midplane - Cycle 12 Irradiation**

<u>**Reaction Rate (rps/nucleus)**</u>

Reaction	Measured	Calculated	Best Estimate	BE / Meas	BE / Calc	Meas / Calc
^{63}Cu (n,α) ^{60}Co (cd)	4.34E-19	4.96E-19	4.43E-19	1.02	0.89	0.88
^{46}Ti (n,p) ^{46}Sc (Cd)	6.42E-18	6.95E-18	6.36E-18	0.99	0.92	0.92
^{54}Fe (n,p) ^{54}Mn (Cd)	3.81E-17	3.94E-17	3.68E-17	0.97	0.93	0.97
^{58}Ni (n,p) ^{58}Co (Cd)	5.04E-17	5.53E-17	5.10E-17	1.01	0.92	0.91
^{238}U (n,f) ^{137}Cs (Cd)	1.82E-16	2.05E-16	1.91E-16	1.05	0.93	0.89
^{237}Np (n,f) ^{137}Cs (Cd)	3.05E-15	3.08E-15	2.94E-15	0.96	0.95	0.99
^{59}Co (n,γ) ^{60}Co	4.63E-14	1.01E-13	4.77E-14	1.03	0.47	0.46
^{59}Co (n,γ) ^{60}Co (Cd)	2.77E-14	4.21E-14	2.75E-14	0.99	0.65	0.66

Exposure Rate	Calculated	Best Estimate	BE / Calc	1σ Uncertainty
φ (E > 1.0 MeV) [n/cm^2-sec]	6.88E+08	6.45E+08	0.94	6%
φ (E > 0.1 MeV) [n/cm^2-sec]	6.86E+09	6.30E+09	0.92	11%
φ (E < 0.414 eV) [n/cm^2-sec]	2.10E+09	7.83E+08	0.37	16%
dpa/sec	2.37E-12	2.17E-12	0.92	9%

Table 6.1-8   Best Estimate Exposure Rates From the Capsule I Dosimetry Evaluation
29.5° Azimuth - Core Midplane - Cycle 12 Irradiation

Reaction Rate (rps/nucleus)

Reaction	Measured	Calculated	Best Estimate	BE / Meas	BE / Calc	Meas / Calc
^{63}Cu (n,α) ^{60}Co (cd)	4.20E-19	4.61E-19	4.23E-19	1.01	0.92	0.91
^{46}Ti (n,p) ^{46}Sc (Cd)	6.35E-18	6.53E-18	6.11E-18	0.96	0.94	0.97
^{54}Fe (n,p) ^{54}Mn (Cd)	3.41E-17	3.85E-17	3.49E-17	1.02	0.91	0.89
^{58}Ni (n,p) ^{58}Co (Cd)	4.89E-17	5.49E-17	4.98E-17	1.02	0.91	0.89
^{238}U (n,f) ^{137}Cs (Cd)	1.96E-16	2.15E-16	1.97E-16	1.01	0.92	0.91
^{237}Np (n,f) ^{137}Cs (Cd)	3.70E-15	3.50E-15	3.47E-15	0.94	0.99	1.06
^{59}Co (n,γ) ^{60}Co	6.87E-14	1.20E-13	6.98E-14	1.02	0.58	0.57
^{59}Co (n,γ) ^{60}Co (Cd)	3.53E-14	5.06E-14	3.54E-14	1.00	0.70	0.70

Exposure Rate	Calculated	Best Estimate	BE / Calc	1σ Uncertainty
φ (E > 1.0 MeV) [n/cm²-sec]	7.47E+08	6.91E+08	0.92	6%
φ (E > 0.1 MeV) [n/cm²-sec]	8.05E+09	7.64E+09	0.95	11%
φ (E < 0.414 eV) [n/cm²-sec]	2.49E+09	1.30E+09	0.52	14%
dpa/sec	2.72E-12	2.56E-12	0.94	9%

Table 6.1-9   Best Estimate Exposure Rates From the Capsule K Dosimetry Evaluation
                 44.5° Azimuth - Core Midplane - Cycle 12 Irradiation

Reaction Rate (rps/nucleus)

Reaction	Measured	Calculated	Best Estimate	BE / Meas	BE / Calc	Meas / Calc
^{63}Cu (n,α) ^{60}Co (cd)	3.38E-19	3.56E-19	3.41E-19	1.01	0.96	0.95
^{46}Ti (n,p) ^{46}Sc (Cd)	5.06E-18	5.07E-18	4.92E-18	0.97	0.97	1.00
^{54}Fe (n,p) ^{54}Mn (Cd)	2.83E-17	3.10E-17	2.87E-17	1.01	0.93	0.91
^{58}Ni (n,p) ^{58}Co (Cd)	4.13E-17	4.50E-17	4.11E-17	1.00	0.91	0.92
^{238}U (n,f) ^{137}Cs (Cd)	1.92E-16	1.87E-16	1.62E-16	0.84	0.87	1.03
^{237}Np (n,f) ^{137}Cs (Cd)	1.50E-15	3.17E-15	1.95E-15	1.30	0.62	0.47
^{59}Co (n,γ) ^{60}Co	4.27E-14	1.15E-13	4.46E-14	1.04	0.39	0.37
^{59}Co (n,γ) ^{60}Co (Cd)	2.80E-14	4.01E-14	2.74E-14	0.98	0.68	0.70

Exposure Rate	Calculated	Best Estimate	BE / Calc	1σ Uncertainty
ϕ (E > 1.0 MeV) [n/cm^2-sec]	6.74E+08	5.49E+08	0.82	6%
ϕ (E > 0.1 MeV) [n/cm^2-sec]	7.14E+09	5.07E+09	0.71	11%
ϕ (E < 0.414 eV) [n/cm^2-sec]	2.56E+09	6.44E+08	0.25	16%
dpa/sec	2.40E-12	1.75E-12	0.73	9%

Table 6.1-10   Best Estimate Exposure Rates From the Capsule J Dosimetry Evaluation
44.5° Azimuth - Top of Core - Cycle 12 Irradiation

<u>Reaction Rate (rps/nucleus)</u>

Reaction	Measured	Calculated	Best Estimate	BE / Meas	BE / Calc	Meas / Calc
^{63}Cu (n,α) ^{60}Co (cd)	2.30E-19	2.59E-19	2.38E-19	1.03	0.92	0.89
^{46}Ti (n,p) ^{46}Sc (Cd)	3.85E-18	3.69E-18	3.62E-18	0.94	0.98	1.04
^{54}Fe (n,p) ^{54}Mn (Cd)	2.06E-17	2.26E-17	2.20E-17	1.07	0.97	0.91
^{58}Ni (n,p) ^{58}Co (Cd)	3.32E-17	3.27E-17	3.30E-17	0.99	1.01	1.02
^{238}U (n,f) ^{137}Cs (Cd)	1.61E-16	1.36E-16	1.43E-16	0.89	1.05	1.18
^{237}Np (n,f) ^{137}Cs (Cd)	2.86E-15	2.31E-15	2.66E-15	0.93	1.15	1.24
^{59}Co (n,γ) ^{60}Co	2.80E-14	8.38E-14	2.94E-14	1.05	0.35	0.33
^{59}Co (n,γ) ^{60}Co (Cd)	1.81E-14	2.92E-14	1.78E-14	0.98	0.61	0.62

Exposure Rate	Calculated	Best Estimate	BE / Calc	1σ Uncertainty
ϕ (E > 1.0 MeV) [n/cm^2-sec]	4.90E+08	5.27E+08	1.08	6%
ϕ (E > 0.1 MeV) [n/cm^2-sec]	5.20E+09	5.54E+09	1.07	11%
ϕ (E < 0.414 eV) [n/cm^2-sec]	1.87E+09	4.37E+08	0.23	16%
dpa/sec	1.75E-12	1.84E-12	1.05	9%

Table 6.1-11   Best Estimate Exposure Rates From the Capsule L Dosimetry Evaluation
44.5° Azimuth - Bottom of Core - Cycle 12 Irradiation

Reaction Rate (rps/nucleus)

Reaction	Measured	Calculated	Best Estimate	BE / Meas	BE / Calc	Meas / Calc
^{63}Cu (n,α) ^{60}Co (cd)	3.80E-20	4.52E-20	4.00E-20	1.05	0.88	0.84
^{46}Ti (n,p) ^{46}Sc (Cd)	6.37E-19	6.45E-19	6.06E-19	0.95	0.94	0.99
^{54}Fe (n,p) ^{54}Mn (Cd)	3.60E-18	3.94E-18	3.69E-18	1.03	0.94	0.91
^{58}Ni (n,p) ^{58}Co (Cd)	5.48E-18	5.72E-18	5.44E-18	0.99	0.95	0.96
^{238}U (n,f) ^{137}Cs (Cd)	2.33E-17	2.38E-17	2.33E-17	1.00	0.98	0.98
^{237}Np (n,f) ^{137}Cs (Cd)	4.41E-16	4.04E-16	4.26E-16	0.97	1.05	1.09
^{59}Co (n,γ) ^{60}Co	1.12E-14	1.46E-14	1.15E-14	1.03	0.79	0.77
^{59}Co (n,γ) ^{60}Co (Cd)	6.95E-15	5.11E-15	6.79E-15	0.98	1.33	1.36

Exposure Rate	Calculated	Best Estimate	BE / Calc	1σ Uncertainty
φ (E > 1.0 MeV) [n/cm²-sec]	8.57E+07	8.52E+07	1.00	6%
φ (E > 0.1 MeV) [n/cm²-sec]	9.08E+08	9.32E+08	1.03	11%
φ (E < 0.414 eV) [n/cm²-sec]	3.26E+08	1.68E+08	0.51	15%
dpa/sec	3.05E-13	3.09E-13	1.01	9%

7 COMPARISON OF CALCULATIONS WITH MEASUREMENTS

As described in Section 3.3, the best estimate neutron exposure projections for the McGuire Unit 2 reactor vessel were based on a combination of plant specific neutron transport calculations and plant specific measurements. Direct comparisons of the transport calculations with the McGuire Unit 2 measurement data base were used to quantify the biases that may exist due to the transport methodology, reactor modeling, and/or reactor operating characteristics over the respective irradiation periods.

In this section, comparisons of the measurement results from surveillance capsule and reactor cavity dosimetry with corresponding analytical predictions at the measurement locations are presented. These comparisons are provided on two levels. In the first instance, predictions of fast neutron exposure rates in terms of ϕ (E > 1.0 MeV), ϕ (E > 0.1 MeV), and dpa/sec are compared with the best estimate results of the FERRET least squares adjustment procedure; while, in the second case, calculations of individual sensor reaction rates are compared directly with the measured data from the counting laboratories. It is shown that these two levels of comparison yield consistent and similar results, indicating that the least squares adjustment methodology is producing accurate exposure results and that the best estimate to calculation (BE/C) comparisons yield an accurate plant specific bias factor that can be applied to neutron transport calculations performed for the McGuire Unit 2 reactor to produce best estimate exposure projections for the reactor vessel wall.

7.1 COMPARISON OF BEST ESTIMATE RESULTS WITH CALCULATION

In Table 7.1-1, comparisons of best estimate and calculated exposure rates for the six surveillance capsule dosimetry sets withdrawn to date as well as for the reactor cavity midplane dosimetry sets irradiated during Cycle 12 are given. In all cases, the calculated values were based on the fuel cycle specific exposure calculations averaged over the appropriate irradiation period. An examination of Table 7.1-1 indicates that, considering all of the available core midplane data, the best estimate integrated exposures were less than calculated values by factors of 0.91, 0.93, and 0.92 for Φ (E > 1.0 MeV), Φ (E > 0.1 MeV), and dpa/sec, respectively. The standard deviations associated with each of the ten-sample-data-sets were 4.6%, 9.4%, and 8.1%, respectively.

7.2 COMPARISONS OF MEASURED AND CALCULATED SENSOR REACTION RATES

In Table 7.2-1, measurement to calculation (M/C) ratios for each fast neutron sensor reaction rate from the surveillance capsule and reactor cavity irradiations are listed. This tabulation provides a direct comparison, on an absolute basis, of calculation and measurement prior to the application of the least squares adjustment procedure as represented in the FERRET evaluations.

An examination of Table 7.2-1 shows consistent behavior for all reactions and all measurement points. The standard deviations observed for the six fast neutron reactions range from 3.2% to 18.1% on an individual reaction basis; whereas, the overall average M/C ratio for the entire data set has an associated 1σ standard deviation of 11.6%. Furthermore, the average M/C bias

of 0.94 observed in the reaction rate comparisons is in excellent agreement with the values observed in the integrated exposure comparisons shown in Table 7.1-1.

Table 7.1-1   Comparison of Best Estimate and Calculated Exposure Rates from
               Surveillance Capsule and Cavity Dosimetry Irradiations

Neutron Fluence (E > 1.0 MeV) [n/cm^2]

	Calculated	Best Estimate	BE/C
Surveillance Capsules			
Capsule V	3.23E+18	3.08E+18	0.95
Capsule X	1.47E+19	1.35E+19	0.92
Capsule U	2.04E+19	1.83E+19	0.90
Capsule Y	2.08E+19	1.87E+19	0.90
Capsule Z	2.41E+19	2.23E+19	0.93
Capsule W	3.07E+19	2.87E+19	0.93
0.5° Cavity			
Cycle 12	1.83E+16	1.57E+16	0.86
14.5° Cavity			
Cycle 12	2.61E+16	2.45E+16	0.94
29.5° Cavity			
Cycle 12	2.84E+16	2.62E+16	0.92
44.5° Cavity			
Cycle 12	2.55E+16	2.08E+16	0.82
Average BE/C Bias Factor			0.91
% Standard Deviation (1σ)			4.6%

Note: The 1σ standard deviation represents the uncertainty associated with the derivation of
       the bias factor from all available measurements. The bias factor uncertainty is just one
       part of the total uncertainty associated with the reactor vessel exposure projections as
       described in Section 8.3.

Table 7.1-1   Comparison of Best Estimate and Calculated Exposure Rates from
(cont.)   Surveillance Capsule and Cavity Dosimetry Irradiations

Neutron Fluence (E > 0.1 MeV) [n/cm^2]

	Calculated	Best Estimate	BE/C
Surveillance Capsules			
Capsule V	1.42E+19	1.43E+19	1.00
Capsule X	6.71E+19	6.36E+19	0.95
Capsule U	9.28E+19	8.71E+19	0.94
Capsule Y	9.17E+19	8.70E+19	0.95
Capsule Z	1.10E+20	1.10E+20	1.01
Capsule W	1.40E+20	1.40E+20	1.00
0.5° Cavity			
Cycle 12	1.73E+17	1.52E+17	0.88
14.5° Cavity			
Cycle 12	2.60E+17	2.39E+17	0.92
29.5° Cavity			
Cycle 12	3.05E+17	2.90E+17	0.95
44.5° Cavity			
Cycle 12	2.71E+17	1.92E+17	0.71
Average BE/C Bias Factor			0.93
% Standard Deviation (1σ)			9.4%

Note: The 1σ standard deviation represents the uncertainty associated with the derivation of the bias factor from all available measurements. The bias factor uncertainty is just one part of the total uncertainty associated with the reactor vessel exposure projections as described in Section 8.3.

Table 7.1-1   **Comparison of Best Estimate and Calculated Exposure Rates from**
(cont.)   **Surveillance Capsule and Cavity Dosimetry Irradiations**

<div align="center">

Iron Displacements [dpa]

</div>

	Calculated	Best Estimate	BE/C
<u>Surveillance Capsules</u>			
Capsule V	6.19E-03	6.10E-03	0.99
Capsule X	2.87E-02	2.70E-02	0.94
Capsule U	3.97E-02	3.68E-02	0.93
Capsule Y	3.99E-02	3.71E-02	0.93
Capsule Z	4.70E-02	4.58E-02	0.97
Capsule W	5.99E-02	5.85E-02	0.98
<u>0.5° Cavity</u>			
Cycle 12	6.03E-05	5.25E-05	0.87
<u>14.5° Cavity</u>			
Cycle 12	8.98E-05	8.24E-05	0.92
<u>29.5° Cavity</u>			
Cycle 12	1.03E-04	9.71E-05	0.94
<u>44.5° Cavity</u>			
Cycle 12	9.10E-05	6.65E-05	0.73
Average BE/C Bias Factor			0.92
% Standard Deviation (1σ)			8.1%

Note: The 1σ standard deviation represents the uncertainty associated with the derivation of the bias factor from all available measurements. The bias factor uncertainty is just one part of the total uncertainty associated with the reactor vessel exposure projections as described in Section 8.3.

Table 7.2-1   Comparison of Measured and Calculated Neutron Sensor Reaction Rates from Surveillance Capsule and Cavity Dosimetry Irradiations

	^{63}Cu (n,α)	^{46}Ti (n,p)	^{54}Fe (n,p)	^{58}Ni (n,p)	^{238}U (n,f)	^{237}Np (n,f)
Surveillance Capsules						
Capsule V	1.04		0.91	0.87	1.04	1.07
Capsule X	1.05		0.88	0.88	1.04	0.93
Capsule U	1.06		0.86	0.85	1.05	0.97
Capsule Y	1.04		0.81	0.85	1.03	0.99
Capsule Z	1.05		0.84	0.85	1.11	0.96
Capsule W	1.07		0.87	0.90	1.08	0.95
0.5° Cavity						
Cycle 12	0.85	0.90	0.83	0.84	0.86	0.95
14.5° Cavity						
Cycle 12	0.88	0.92	0.97	0.91	0.89	0.99
29.5° Cavity						
Cycle 12	0.91	0.97	0.89	0.89	0.91	1.06
44.5° Cavity						
Cycle 12	0.95	1.00	0.91	0.92	1.03	0.47
Average	0.99	0.95	0.88	0.88	1.00	0.93
% Std. Dev. (1σ)	8.5%	4.8%	5.3%	3.2%	8.5%	18.1%

Overall M/C Average   0.94

% Std. Dev. (1σ)   11.0%

8 BEST ESTIMATE NEUTRON EXPOSURE OF REACTOR VESSEL MATERIALS

In this section the measurement results provided in Sections 5.0 and 6.0 are combined with the results of the neutron transport calculations described in Section 4.0 to establish a mapping of the best estimate neutron exposure of the beltline region of the McGuire Unit 2 reactor vessel through the completion of Cycle 12. Based on the continued use of the core power distributions producing the Cycles 10-12 measured results, projections of future vessel exposure to 21, 34, and 51 effective full power years of operation are also provided. In addition to the spatial mapping over the beltline region, data pertinent to the maximum exposure experienced by the intermediate and lower shell plates as well as the beltline circumferential and longitudinal welds are highlighted.

8.1 EXPOSURE DISTRIBUTIONS WITHIN THE BELTLINE REGION

As described in Section 3.3 of this report, the best estimate vessel exposure was determined from the following relationship:

$$\Phi_{Best\ Est.} = K\Phi_{Calc.}$$

where: $\Phi_{Best\ Est.}$ = The best estimate fast neutron exposure at the location of interest.

K = The plant specific best estimate/calculation (BE/C) bias factor derived from all available surveillance capsule and reactor cavity dosimetry data.

$\Phi_{Calc.}$ = The absolute calculated fast neutron exposure at the location of interest.

From the data provided in Table 7.1-1, the plant specific bias factors (K) to be applied to the calculated exposure values given in Section 4.2 were as follows:

Φ (E > 1.0 MeV)	$0.91 \pm 4.6\%$
Φ (E > 0.1 MeV)	$0.93 \pm 9.4\%$
dpa	$0.92 \pm 8.1\%$

These bias factors were based on the results of the continuous monitoring program at McGuire Unit 2 that has provided measured data from six internal surveillance capsules and one reactor cavity sensor set through the first 12 cycles of operation.

The uncertainties listed with the individual bias factors are at the 1σ level. Additional uncertainties associated with the evaluation of the best estimate vessel exposure are discussed in Section 8.3.

8.1.1 Exposure Accumulated During Cycles 1 through 12

To assess the incremental exposure resulting from the Cycles 12 irradiation, the bias factors listed in Section 8.1 were applied directly to the calculated values from Section 4.2 for the vessel clad/base metal interface to produce best estimate fluence levels characteristic of the midplane of the reactor core. The composite axial core power distributions were then used to develop the complete axial traverse along the vessel wall. The best estimate results applicable to the vessel inner surface are incorporated into Tables 8.1-1 through 8.1-12 to establish the exposure accumulated by the reactor vessel through the end of Cycles 10 and 12.

Exposure distributions through the vessel wall can be developed using these surface exposures and radial distribution functions from Section 4.0. This exposure information, applicable through the end of Cycle 12, was derived from an extensive set of measurements and assures that embrittlement gradients can be established with a minimum uncertainty. Further, as the monitoring program continues and additional data become available, the overall plant specific data base for McGuire Unit 2 will expand resulting in reduced uncertainties and an improved accuracy in the assessment of vessel condition.

8.1.2 Projection of Future Vessel Exposure

At the end of Cycle 12, the McGuire Unit 2 reactor had accumulated 11.76 effective full power years (EFPY) of operation. In order to establish a framework for the assessment of the future reactor vessel condition, exposure projections to 21, 34, and 51 EFPY are also included in Tables 8.1-1 through 8.1-12 in addition to the plant specific exposure assessments through the end of Cycle 12.

These extrapolations into the future were based on the assumption that the data from the Cycle 10-12 irradiations were representative of all future fuel cycles. That is, that future fuel designs would incorporate the low leakage fuel management concept employed during Cycles 10 through 12. Examination of these projected exposure levels establishes the long term effectiveness of the low leakage fuel management incorporated to date and can be used as a guide in assessing strategies for future reactor vessel exposure management. The validity of these projections for future operation will be confirmed via the continued reactor cavity neutron monitoring program.

Table 8.1-1   Summary of Best Estimate Fast Neutron (E > 1.0 MeV) Exposure Projections
for the Beltline Region of the McGuire Unit 2 Reactor Vessel -
0° Azimuthal Angle

Distance from Core Midplane	Cycle 10 9.44 EFPY	Cycle 12 11.76 EFPY	Projected Exposures		
			21 EFPY	34 EFPY	51 EFPY
6.00	1.38E+18	1.66E+18	2.75E+18	4.29E+18	6.30E+18
5.00	2.57E+18	3.06E+18	5.08E+18	7.93E+18	1.16E+19
4.00	3.02E+18	3.61E+18	5.99E+18	9.34E+18	1.37E+19
3.00	3.21E+18	3.84E+18	6.37E+18	9.93E+18	1.46E+19
2.00	3.28E+18	3.91E+18	6.50E+18	1.01E+19	1.49E+19
1.00	3.30E+18	3.94E+18	6.54E+18	1.02E+19	1.50E+19
0.00	3.32E+18	3.97E+18	6.59E+18	1.03E+19	1.51E+19
-1.00	3.32E+18	3.98E+18	6.60E+18	1.03E+19	1.51E+19
-2.00	3.28E+18	3.93E+18	6.53E+18	1.02E+19	1.50E+19
-3.00	3.22E+18	3.86E+18	6.41E+18	1.00E+19	1.47E+19
-4.00	3.07E+18	3.70E+18	6.15E+18	9.59E+18	1.41E+19
-5.00	2.66E+18	3.23E+18	5.36E+18	8.36E+18	1.23E+19
-6.00	1.35E+18	1.63E+18	2.70E+18	4.21E+18	6.19E+18

Table 8.1-2   Summary of Best Estimate Fast Neutron (E > 1.0 MeV) Exposure Projections
for the Beltline Region of the McGuire Unit 2 Reactor Vessel -
15° Azimuthal Angle

Distance from Core Midplane	Cycle 10 9.44 EFPY	Cycle 12 11.76 EFPY	Projected Exposures		
			21 EFPY	34 EFPY	51 EFPY
6.00	2.07E+18	2.47E+18	4.08E+18	6.35E+18	9.31E+18
5.00	3.84E+18	4.57E+18	7.54E+18	1.17E+19	1.72E+19
4.00	4.51E+18	5.38E+18	8.89E+18	1.38E+19	2.03E+19
3.00	4.80E+18	5.72E+18	9.45E+18	1.47E+19	2.16E+19
2.00	4.89E+18	5.84E+18	9.64E+18	1.50E+19	2.20E+19
1.00	4.93E+18	5.88E+18	9.71E+18	1.51E+19	2.21E+19
0.00	4.96E+18	5.93E+18	9.78E+18	1.52E+19	2.23E+19
-1.00	4.96E+18	5.93E+18	9.80E+18	1.52E+19	2.23E+19
-2.00	4.90E+18	5.86E+18	9.68E+18	1.51E+19	2.21E+19
-3.00	4.80E+18	5.76E+18	9.51E+18	1.48E+19	2.17E+19
-4.00	4.59E+18	5.53E+18	9.13E+18	1.42E+19	2.08E+19
-5.00	3.98E+18	4.82E+18	7.96E+18	1.24E+19	1.81E+19
-6.00	2.02E+18	2.43E+18	4.00E+18	6.23E+18	9.13E+18

Table 8.1-3   Summary of Best Estimate Fast Neutron (E > 1.0 MeV) Exposure Projections
for the Beltline Region of the McGuire Unit 2 Reactor Vessel -
30° Azimuthal Angle

Distance from Core Midplane	Cycle 10 9.44 EFPY	Cycle 12 11.76 EFPY	Projected Exposures		
			21 EFPY	34 EFPY	51 EFPY
6.00	1.94E+18	2.35E+18	3.97E+18	6.24E+18	9.21E+18
5.00	3.61E+18	4.35E+18	7.33E+18	1.15E+19	1.70E+19
4.00	4.25E+18	5.12E+18	8.64E+18	1.36E+19	2.01E+19
3.00	4.52E+18	5.45E+18	9.18E+18	1.44E+19	2.13E+19
2.00	4.61E+18	5.56E+18	9.37E+18	1.47E+19	2.17E+19
1.00	4.64E+18	5.60E+18	9.44E+18	1.48E+19	2.19E+19
0.00	4.67E+18	5.64E+18	9.51E+18	1.50E+19	2.21E+19
-1.00	4.67E+18	5.65E+18	9.52E+18	1.50E+19	2.21E+19
-2.00	4.61E+18	5.58E+18	9.41E+18	1.48E+19	2.18E+19
-3.00	4.52E+18	5.48E+18	9.25E+18	1.45E+19	2.15E+19
-4.00	4.32E+18	5.26E+18	8.87E+18	1.39E+19	2.06E+19
-5.00	3.75E+18	4.59E+18	7.73E+18	1.22E+19	1.79E+19
-6.00	1.90E+18	2.31E+18	3.89E+18	6.12E+18	9.04E+18

Table 8.1-4   Summary of Best Estimate Fast Neutron (E > 1.0 MeV) Exposure Projections
for the Beltline Region of the McGuire Unit 2 Reactor Vessel -
45° Azimuthal Angle

Distance from Core Midplane	Cycle 10 9.44 EFPY	Cycle 12 11.76 EFPY	Projected Exposures 21 EFPY	34 EFPY	51 EFPY
6.00	2.20E+18	2.65E+18	4.45E+18	6.99E+18	1.03E+19
5.00	4.08E+18	4.90E+18	8.23E+18	1.29E+19	1.91E+19
4.00	4.80E+18	5.78E+18	9.70E+18	1.52E+19	2.25E+19
3.00	5.10E+18	6.14E+18	1.03E+19	1.62E+19	2.39E+19
2.00	5.21E+18	6.26E+18	1.05E+19	1.65E+19	2.43E+19
1.00	5.25E+18	6.31E+18	1.06E+19	1.66E+19	2.45E+19
0.00	5.28E+18	6.36E+18	1.07E+19	1.68E+19	2.47E+19
-1.00	5.28E+18	6.37E+18	1.07E+19	1.68E+19	2.47E+19
-2.00	5.21E+18	6.29E+18	1.06E+19	1.66E+19	2.45E+19
-3.00	5.11E+18	6.18E+18	1.04E+19	1.63E+19	2.40E+19
-4.00	4.88E+18	5.93E+18	9.96E+18	1.56E+19	2.31E+19
-5.00	4.23E+18	5.17E+18	8.68E+18	1.36E+19	2.01E+19
-6.00	2.15E+18	2.60E+18	4.37E+18	6.86E+18	1.01E+19

Table 8.1-5   Summary of Best Estimate Fast Neutron (E > 0.1 MeV) Exposure Projections for the Beltline Region of the McGuire Unit 2 Reactor Vessel - 0° Azimuthal Angle

Distance from Core Midplane	Cycle 10 9.44 EFPY	Cycle 12 11.76 EFPY	Projected Exposures 21 EFPY	34 EFPY	51 EFPY
6.00	2.94E+18	3.52E+18	5.85E+18	9.13E+18	1.34E+19
5.00	5.46E+18	6.51E+18	1.08E+19	1.69E+19	2.48E+19
4.00	6.43E+18	7.67E+18	1.27E+19	1.99E+19	2.92E+19
3.00	6.83E+18	8.16E+18	1.35E+19	2.11E+19	3.10E+19
2.00	6.97E+18	8.32E+18	1.38E+19	2.15E+19	3.17E+19
1.00	7.02E+18	8.38E+18	1.39E+19	2.17E+19	3.19E+19
0.00	7.06E+18	8.45E+18	1.40E+19	2.19E+19	3.21E+19
-1.00	7.06E+18	8.46E+18	1.40E+19	2.19E+19	3.22E+19
-2.00	6.97E+18	8.36E+18	1.39E+19	2.16E+19	3.18E+19
-3.00	6.84E+18	8.21E+18	1.36E+19	2.13E+19	3.13E+19
-4.00	6.54E+18	7.88E+18	1.31E+19	2.04E+19	3.00E+19
-5.00	5.67E+18	6.87E+18	1.14E+19	1.78E+19	2.61E+19
-6.00	2.88E+18	3.46E+18	5.74E+18	8.96E+18	1.32E+19

Table 8.1-6   Summary of Best Estimate Fast Neutron (E > 0.1 MeV) Exposure Projections
for the Beltline Region of the McGuire Unit 2 Reactor Vessel -
15° Azimuthal Angle

Distance from Core Midplane	Cycle 10 9.44 EFPY	Cycle 12 11.76 EFPY	Projected Exposures		
			21 EFPY	34 EFPY	51 EFPY
6.00	4.44E+18	5.31E+18	8.77E+18	1.36E+19	2.00E+19
5.00	8.24E+18	9.82E+18	1.62E+19	2.52E+19	3.70E+19
4.00	9.70E+18	1.16E+19	1.91E+19	2.97E+19	4.36E+19
3.00	1.03E+19	1.23E+19	2.03E+19	3.16E+19	4.63E+19
2.00	1.05E+19	1.25E+19	2.07E+19	3.22E+19	4.72E+19
1.00	1.06E+19	1.26E+19	2.09E+19	3.25E+19	4.76E+19
0.00	1.07E+19	1.27E+19	2.10E+19	3.27E+19	4.80E+19
-1.00	1.07E+19	1.28E+19	2.11E+19	3.27E+19	4.80E+19
-2.00	1.05E+19	1.26E+19	2.08E+19	3.24E+19	4.75E+19
-3.00	1.03E+19	1.24E+19	2.04E+19	3.18E+19	4.66E+19
-4.00	9.87E+18	1.19E+19	1.96E+19	3.05E+19	4.47E+19
-5.00	8.56E+18	1.04E+19	1.71E+19	2.66E+19	3.90E+19
-6.00	4.35E+18	5.21E+18	8.61E+18	1.34E+19	1.96E+19

Table 8.1-7   Summary of Best Estimate Fast Neutron (E > 0.1 MeV) Exposure Projections
for the Beltline Region of the McGuire Unit 2 Reactor Vessel -
30° Azimuthal Angle

Distance from Core Midplane	Cycle 10 9.44 EFPY	Cycle 12 11.76 EFPY	Projected Exposures		
			21 EFPY	34 EFPY	51 EFPY
6.00	4.53E+18	5.48E+18	9.24E+18	1.45E+19	2.15E+19
5.00	8.41E+18	1.01E+19	1.71E+19	2.69E+19	3.96E+19
4.00	9.90E+18	1.19E+19	2.01E+19	3.16E+19	4.67E+19
3.00	1.05E+19	1.27E+19	2.14E+19	3.36E+19	4.97E+19
2.00	1.07E+19	1.29E+19	2.18E+19	3.43E+19	5.07E+19
1.00	1.08E+19	1.30E+19	2.20E+19	3.46E+19	5.10E+19
0.00	1.09E+19	1.31E+19	2.22E+19	3.48E+19	5.14E+19
-1.00	1.09E+19	1.32E+19	2.22E+19	3.49E+19	5.15E+19
-2.00	1.07E+19	1.30E+19	2.19E+19	3.45E+19	5.09E+19
-3.00	1.05E+19	1.28E+19	2.15E+19	3.39E+19	5.00E+19
-4.00	1.01E+19	1.23E+19	2.07E+19	3.25E+19	4.80E+19
-5.00	8.73E+18	1.07E+19	1.80E+19	2.83E+19	4.18E+19
-6.00	4.44E+18	5.38E+18	9.07E+18	1.43E+19	2.11E+19

Table 8.1-8   Summary of Best Estimate Fast Neutron (E > 0.1 MeV) Exposure Projections
for the Beltline Region of the McGuire Unit 2 Reactor Vessel -
45° Azimuthal Angle

Distance from	Cycle 10	Cycle 12	Projected Exposures		
Core Midplane	9.44 EFPY	11.76 EFPY	21 EFPY	34 EFPY	51 EFPY
6.00	5.60E+18	6.76E+18	1.14E+19	1.78E+19	2.63E+19
5.00	1.04E+19	1.25E+19	2.10E+19	3.30E+19	4.86E+19
4.00	1.22E+19	1.47E+19	2.47E+19	3.88E+19	5.73E+19
3.00	1.30E+19	1.57E+19	2.63E+19	4.13E+19	6.09E+19
2.00	1.33E+19	1.60E+19	2.68E+19	4.21E+19	6.21E+19
1.00	1.34E+19	1.61E+19	2.70E+19	4.24E+19	6.26E+19
0.00	1.35E+19	1.62E+19	2.72E+19	4.28E+19	6.30E+19
-1.00	1.35E+19	1.62E+19	2.73E+19	4.28E+19	6.31E+19
-2.00	1.33E+19	1.60E+19	2.70E+19	4.23E+19	6.24E+19
-3.00	1.30E+19	1.58E+19	2.65E+19	4.16E+19	6.13E+19
-4.00	1.25E+19	1.51E+19	2.54E+19	3.99E+19	5.88E+19
-5.00	1.08E+19	1.32E+19	2.21E+19	3.48E+19	5.13E+19
-6.00	5.49E+18	6.64E+18	1.11E+19	1.75E+19	2.58E+19

Table 8.1-9   Summary of Best Estimate Iron Atom Displacement [dpa] Projections for the Beltline Region of the McGuire Unit 2 Reactor Vessel - 0° Azimuthal Angle

Distance from Core Midplane	Cycle 10 9.44 EFPY	Cycle 12 11.76 EFPY	Projected Exposures		
			21 EFPY	34 EFPY	51 EFPY
6.00	2.15E-03	2.57E-03	4.27E-03	6.66E-03	9.79E-03
5.00	3.99E-03	4.76E-03	7.90E-03	1.23E-02	1.81E-02
4.00	4.69E-03	5.60E-03	9.31E-03	1.45E-02	2.13E-02
3.00	4.99E-03	5.96E-03	9.89E-03	1.54E-02	2.27E-02
2.00	5.09E-03	6.08E-03	1.01E-02	1.57E-02	2.31E-02
1.00	5.13E-03	6.12E-03	1.02E-02	1.59E-02	2.33E-02
0.00	5.16E-03	6.17E-03	1.02E-02	1.60E-02	2.35E-02
-1.00	5.16E-03	6.18E-03	1.03E-02	1.60E-02	2.35E-02
-2.00	5.09E-03	6.11E-03	1.01E-02	1.58E-02	2.32E-02
-3.00	4.99E-03	6.00E-03	9.96E-03	1.55E-02	2.28E-02
-4.00	4.77E-03	5.75E-03	9.55E-03	1.49E-02	2.19E-02
-5.00	4.14E-03	5.02E-03	8.33E-03	1.30E-02	1.91E-02
-6.00	2.10E-03	2.53E-03	4.19E-03	6.54E-03	9.61E-03

Table 8.1-10   Summary of Best Estimate Iron Atom Displacement [dpa] Projections for the
Beltline Region of the McGuire Unit 2 Reactor Vessel -
15° Azimuthal Angle

Distance from Core Midplane	Cycle 10 9.44 EFPY	Cycle 12 11.76 EFPY	Projected Exposures		
			21 EFPY	34 EFPY	51 EFPY
6.00	3.18E-03	3.80E-03	6.28E-03	9.76E-03	1.43E-02
5.00	5.90E-03	7.02E-03	1.16E-02	1.80E-02	2.65E-02
4.00	6.94E-03	8.28E-03	1.37E-02	2.13E-02	3.12E-02
3.00	7.38E-03	8.80E-03	1.45E-02	2.26E-02	3.31E-02
2.00	7.53E-03	8.97E-03	1.48E-02	2.30E-02	3.38E-02
1.00	7.59E-03	9.04E-03	1.49E-02	2.32E-02	3.41E-02
0.00	7.63E-03	9.11E-03	1.50E-02	2.34E-02	3.43E-02
-1.00	7.63E-03	9.12E-03	1.51E-02	2.34E-02	3.44E-02
-2.00	7.53E-03	9.02E-03	1.49E-02	2.32E-02	3.40E-02
-3.00	7.39E-03	8.86E-03	1.46E-02	2.27E-02	3.34E-02
-4.00	7.06E-03	8.50E-03	1.40E-02	2.18E-02	3.20E-02
-5.00	6.12E-03	7.41E-03	1.22E-02	1.90E-02	2.79E-02
-6.00	3.11E-03	3.73E-03	6.16E-03	9.58E-03	1.40E-02

Table 8.1-11   Summary of Best Estimate Iron Atom Displacement [dpa] Projections for the
Beltline Region of the McGuire Unit 2 Reactor Vessel -
30° Azimuthal Angle

Distance from Core Midplane	Cycle 10 9.44 EFPY	Cycle 12 11.76 EFPY	Projected Exposures 21 EFPY	34 EFPY	51 EFPY
6.00	3.03E-03	3.67E-03	6.19E-03	9.73E-03	1.44E-02
5.00	5.63E-03	6.79E-03	1.14E-02	1.80E-02	2.65E-02
4.00	6.63E-03	8.00E-03	1.35E-02	2.12E-02	3.13E-02
3.00	7.05E-03	8.50E-03	1.43E-02	2.25E-02	3.33E-02
2.00	7.19E-03	8.67E-03	1.46E-02	2.30E-02	3.39E-02
1.00	7.25E-03	8.74E-03	1.47E-02	2.32E-02	3.42E-02
0.00	7.29E-03	8.80E-03	1.48E-02	2.33E-02	3.44E-02
-1.00	7.29E-03	8.81E-03	1.49E-02	2.34E-02	3.45E-02
-2.00	7.20E-03	8.71E-03	1.47E-02	2.31E-02	3.41E-02
-3.00	7.06E-03	8.56E-03	1.44E-02	2.27E-02	3.35E-02
-4.00	6.74E-03	8.21E-03	1.38E-02	2.18E-02	3.21E-02
-5.00	5.85E-03	7.16E-03	1.21E-02	1.90E-02	2.80E-02
-6.00	2.97E-03	3.60E-03	6.07E-03	9.55E-03	1.41E-02

Table 8.1-12   Summary of Best Estimate Iron Atom Displacement [dpa] Projections for the
Beltline Region of the McGuire Unit 2 Reactor Vessel -
45° Azimuthal Angle

Distance from Core Midplane	Cycle 10 9.44 EFPY	Cycle 12 11.76 EFPY	Projected Exposures		
			21 EFPY	34 EFPY	51 EFPY
6.00	3.48E-03	4.20E-03	7.06E-03	1.11E-02	1.63E-02
5.00	6.46E-03	7.76E-03	1.30E-02	2.05E-02	3.02E-02
4.00	7.61E-03	9.15E-03	1.54E-02	2.41E-02	3.56E-02
3.00	8.08E-03	9.73E-03	1.63E-02	2.56E-02	3.78E-02
2.00	8.25E-03	9.92E-03	1.67E-02	2.62E-02	3.86E-02
1.00	8.31E-03	9.99E-03	1.68E-02	2.64E-02	3.89E-02
0.00	8.36E-03	1.01E-02	1.69E-02	2.66E-02	3.92E-02
-1.00	8.36E-03	1.01E-02	1.69E-02	2.66E-02	3.92E-02
-2.00	8.25E-03	9.96E-03	1.67E-02	2.63E-02	3.87E-02
-3.00	8.09E-03	9.79E-03	1.64E-02	2.58E-02	3.81E-02
-4.00	7.74E-03	9.39E-03	1.58E-02	2.48E-02	3.65E-02
-5.00	6.71E-03	8.19E-03	1.38E-02	2.16E-02	3.18E-02
-6.00	3.41E-03	4.12E-03	6.92E-03	1.09E-02	1.60E-02

8.2   EXPOSURE OF SPECIFIC BELTLINE MATERIALS

As shown in Figure 1.1-1, the beltline region of the McGuire Unit 2 reactor vessel is comprised of three ring forgings (one intermediate shell, one lower shell, and one lower transition shell) and two circumferential welds joining the three shells. The uppermost of the two circumferential welds (W05) is centered just above (~6.94 inches) the axial midplane of the active core at the axial location of the maximum vessel exposure. The intermediate shell extends upward to an elevation well above the active fuel and the lower shell extends downward to an elevation just below (~6.97 inches) the bottom of the active fuel. The lowermost of the two circumferential welds (W04) is located at this point, joining the lower transition shell to the lower shell. The maximum neutron exposure experienced by each of these beltline materials can be extracted from the data provided in Tables 8.1-1 through 8.1-12.

The current (End of Cycle 12) and projected maximum exposures of the beltline region materials are listed in Table 8.2-1 through 8.2-3. In these tables, the weld and forging exposure is expressed in terms of Φ (E > 1.0 MeV), Φ (E > 0.1 MeV), and dpa. Data are also provided at the end of Cycle 10 for ease of comparison to the data in Reference 34.

The peak axial fluence occurs at the 45° azimuth behind the neutron pad throughout the service life of the unit on all three beltline region materials.

Due to the asymmetry of the neutron pads there is variation in the neutron exposure of the reactor vessel from octant to octant. With no surveillance capsule holder present, the neutron pad span ranges from 30° to 45° in the respective octant. Likewise, pad spans of 27.5° to 45° and 25° to 45° exist in octants containing single and double surveillance capsule holders, respectively. The presence of these extended pads acts to reduce the overall neutron exposure at the locations behind the edge of the pad. The data presented in Tables 8.2-1 through 8.2-3 are characteristic of an octant with a 15° pad span and, thus represent the maximum reactor vessel neutron exposure at all azimuthal locations.

Table 8.2-1   Fast Neutron Fluence (E > 1.0 MeV) at Key Forging and Weld Locations of McGuire Unit 2

Best Estimate $\Phi(E>1.0\ MeV)$ [n/cm^2]

Location	Cycle 10 9.44 EFPY	Cycle 12 11.76 EFPY	Projected Exposures 21 EFPY	34 EFPY	51 EFPY
Intermediate Shell Forging - 526840 Circumferential Weld – W05 Lower Shell Forging - 411337					
0°	3.32E+18	3.97E+18	6.59E+18	1.03E+19	1.51E+19
15°	4.96E+18	5.93E+18	9.78E+18	1.52E+19	2.23E+19
30°	4.67E+18	5.64E+18	9.51E+18	1.50E+19	2.21E+19
45°	5.28E+18	6.36E+18	1.07E+19	1.68E+19	2.47E+19
Circumferential Weld – W04 Lower Transition Shell Forging - 527428					
0°	1.35E+18	1.63E+18	2.70E+18	4.21E+18	6.19E+18
15°	2.02E+18	2.43E+18	4.00E+18	6.23E+18	9.13E+18
30°	1.90E+18	2.31E+18	3.89E+18	6.12E+18	9.04E+18
45°	2.15E+18	2.60E+18	4.37E+18	6.86E+18	1.01E+19

Table 8.2-2   Fast Neutron Fluence (E > 0.1 MeV) at Key Plate and Weld Locations of McGuire Unit 2

Best Estimate $\Phi(E{>}0.1\ MeV)$ $[n/cm^2]$

Location	Cycle 10 9.44 EFPY	Cycle 12 11.76 EFPY	Projected Exposures 21 EFPY	34 EFPY	51 EFPY
Intermediate Shell Forging - 526840 Circumferential Weld – W05 Lower Shell Forging - 411337					
0°	7.06E+18	8.45E+18	1.40E+19	2.19E+19	3.21E+19
15°	1.07E+19	1.27E+19	2.10E+19	3.27E+19	4.80E+19
30°	1.09E+19	1.31E+19	2.22E+19	3.48E+19	5.14E+19
45°	1.35E+19	1.62E+19	2.72E+19	4.28E+19	6.30E+19
Circumferential Weld – W04 Lower Transition Shell Forging - 527428					
0°	2.88E+18	3.46E+18	5.74E+18	8.96E+18	1.32E+19
15°	4.35E+18	5.21E+18	8.61E+18	1.34E+19	1.96E+19
30°	4.44E+18	5.38E+18	9.07E+18	1.43E+19	2.11E+19
45°	5.49E+18	6.64E+18	1.11E+19	1.75E+19	2.58E+19

Table 8.2-3   Iron Atom Displacements [dpa] at Key Plate and Weld Locations of McGuire Unit 2

Best Estimate Iron Atom Displacements [dpa]

Location	Cycle 10 9.44 EFPY	Cycle 12 11.76 EFPY	Projected Exposures 21 EFPY	34 EFPY	51 EFPY
Intermediate Shell Forging - 526840 Circumferential Weld – W05 Lower Shell Forging - 411337					
0°	5.16E-03	6.17E-03	1.02E-02	1.60E-02	2.35E-02
15°	7.63E-03	9.11E-03	1.50E-02	2.34E-02	3.43E-02
30°	7.29E-03	8.80E-03	1.48E-02	2.33E-02	3.44E-02
45°	8.36E-03	1.01E-02	1.69E-02	2.66E-02	3.92E-02
Circumferential Weld – W04 Lower Transition Shell Forging - 527428					
0°	2.10E-03	2.53E-03	4.19E-03	6.54E-03	9.61E-03
15°	3.11E-03	3.73E-03	6.16E-03	9.58E-03	1.40E-02
30°	2.97E-03	3.60E-03	6.07E-03	9.55E-03	1.41E-02
45°	3.41E-03	4.12E-03	6.92E-03	1.09E-02	1.60E-02

8.3   UNCERTAINTIES IN EXPOSURE PROJECTIONS

The overall uncertainty in the best estimate exposure projections within the reactor vessel wall arises primarily from two sources; a) the uncertainty in the bias factor (K) derived from the plant specific measurement data base and b) the analytical uncertainty associated with relating the results at the measurement locations to the desired results within the reactor vessel wall. Uncertainty in the bias factor derives directly from the individual uncertainties in the measurement process, in the least squares adjustment procedure, and in the location of the surveillance capsule and cavity dosimetry sensor sets.   The analytical uncertainty in the relationship between the exposure of the reactor vessel and the exposure at the measurement locations is based on the vessel thickness tolerance relative to the cavity data and on the downcomer water density variations and the reactor vessel inner radius tolerance relative to the surveillance capsule data.

The 1σ uncertainties associated with the bias factors applicable to Φ (E > 1.0 MeV), Φ (E > 0.1 MeV), and dpa are given in Section 8.1 of this report.   The additional information pertinent to the required analytical uncertainty for reactor vessel locations has been obtained from benchmarking studies using the Westinghouse neutron transport methodology[35] and from several comparisons of power reactor internal surveillance capsule dosimetry and reactor cavity dosimetry for which the irradiation history of all sensors was the same.

Based on these benchmarking evaluations the additional uncertainty associated with the tolerances in dosimetry positioning, reactor vessel thickness, vessel inner radius, and downcomer temperature was estimated to be approximately 6% for all exposure parameters. These uncertainty components were then combined as follows:

<div align="center">

1σ Uncertainty

</div>

	Φ (E > 1.0 MeV)	Φ (E > 0.1 MeV)	dpa
Bias Factor	4.6%	9.4%	8.1%
Analytical	6.0%	6.0%	6.0%
Combined	7.5%	11.2%	10.1%

These uncertainty values are well within the 20% 1σ uncertainty in vessel fluence projections required by the PTS rule.

9   REFERENCES

1.   "Methodology used to Develop Cold Overpressure Mitigating System Setpoints and RCS Heatup and Cooldown Curves," WCAP-14040-NP-A, January 1996.

2.   "Duke Power Company William B. McGuire Unit No. 2 Reactor Vessel Radiation Surveillance Program", WCAP-9489, K. Koyama and J. A. Davidson, May 1979.

3.   RSICC Computer Code Collection CCC-650, "DOORS 3.1 One-, Two-, and Three-Dimensional Discrete Ordinates Neutron/Photon Transport Code System", August 1996.

4.   RSICC Data Library Collection DLC-185, "BUGLE-96, Coupled 47 Neutron, 20 Gamma-Ray Group Cross Section Library Derived from ENDF/B-VI for LWR Shielding and Pressure Vessel Dosimetry Applications", March 1996.

5.   Maerker, R. E., *et al*, "Accounting for Changing Source Distributions in Light Water Reactor Surveillance Dosimetry Analysis," *Nuclear Science and Engineering*, Volume 94, pp. 291-308, 1986.

6.   ASTM Designation E706-87 (Reapproved 1994), "Standard Master Matrix for Light-Water Reactor Pressure Vessel Surveillance Standards," in *1999 Annual Book of ASTM Standards*, Volume 12.02, ASTM, West Conshohocken, PA, 1999.

7.   ASTM Designation E853-87 (Re-approved 1995), "Standard Practice for Analysis and Interpretation of Light-Water Reactor Surveillance Results," *in 1999 Annual Book of ASTM Standards*, Volume 12.02, ASTM, West Conshohocken, PA, 1999.

8.   ASTM Designation E261-98, "Standard Practice for Determining Neutron Fluence, Fluence Rate, and Spectra by Radioactivation Techniques," in *1999 Annual Book of ASTM Standards*, Volume 12.02, ASTM, West Conshohocken, PA, 1999.

9.   ASTM Designation E262-97, "Standard Test Method for Determining Thermal Neutron Reaction and Fluence Rates by Radioactivation Techniques," in *1999 Annual Book of ASTM Standards*, Volume 12.02, ASTM, West Conshohocken, PA, 1999.

10.   ASTM Designation E263-93, "Standard Test Method for Determining Fast-Neutron Reaction Rates by Radioactivation of Iron," in *1999 Annual Book of ASTM Standards*, Volume 12.02, ASTM, West Conshohocken, PA, 1999.

11.   ASTM Designation E264-92 (Re-approved 1996), "Standard Test Method for Determining Fast-Neutron Reaction Rates by Radioactivation of Nickel," in *1999 Annual Book of ASTM Standards*, Volume 12.02, ASTM, West Conshohocken, PA, 1999.

12.   ASTM Designation E481-97, "Standard Test Method for Measuring Neutron Fluence Rates by Radioactivation of Cobalt and Silver," in *1999 Annual Book of ASTM Standards*, Volume 12.02, ASTM, West Conshohocken, PA, 1999.

13.   ASTM Designation E523-92 (Re-approved 1996), "Standard Test Method for Determining Fast-Neutron Reaction Rates by Radioactivation of Copper," in *1999 Annual Book of ASTM Standards*, Volume 12.02, ASTM, West Conshohocken, PA, 1999.

14.   ASTM Designation E704-96, "Standard Test Method for Measuring Reaction Rates by Radioactivation of Uranium-238," in *1999 Annual Book of ASTM Standards,* Volume 12.02, ASTM, West Conshohocken, PA, 1999.

15.   ASTM Designation E705-96, "Standard Test Method for Measuring Reaction Rates by Radioactivation of Neptunium-237," in *1999 Annual Book of ASTM Standards,* Volume 12.02, ASTM, West Conshohocken, PA, 1999.

16.   ASTM Designation E1005-97, "Standard Test Method for Application and Analysis of Radiometric Monitors for Reactor Vessel Surveillance," in *1999 Annual Book of ASTM Standards,* Volume 12.02, ASTM, West Conshohocken, PA, 1999.

17.   Electronic mail transmissions of "McGuire Unit 2 Thermal Power Production Data" dated October 20, 1999 and October 21, 1999, from R. A. Williams of Duke Power Company to A. H. Fero of Westinghouse.

18.   J.M. Adams, *et al,* "The Materials Dosimetry Reference Facility Round Robin Tests of ^{237}Np and ^{238}U Fissionable Dosimeters," pp. 124-129, *Proceedings of the 9th International Symposium on Reactor Dosimetry,* Prague, Czech Republic, 2-6 September 1996.

19.   Schmittroth, E. A., "FERRET Data Analysis Code", HEDL-TME-79-40, Hanford Engineering Development Laboratory, Richland, Washington, September 1979.

20.   McElroy, W. N., et. al., "A Computer-Automated Iterative Method of Neutron Flux Spectra Determined by Foil Activation," AFWL-TR-67-41, Volumes I-IV, Air Force Weapons Laboratory, Kirkland AFB, NM, July 1967.

21.   RSICC Data Library Collection DLC-178, "SNLRML Recommended Dosimetry Cross-Section Compendium", July 1994.

22.   Maerker, R. E. as reported by Stallman, F. W., "Workshop on Adjustment Codes and Uncertainties," *Proceedings of the 4th ASTM/EURATOM Symposium on Reactor Dosimetry,* NUREG/CP-0029, NRC, Washington, D.C., July 1982.

23.   "The Nuclear Design and Core Physics Characteristics of the W. B. McGuire Unit 2 Nuclear Power Plant Cycle 1," WCAP-10182, September 1982. [Westinghouse Proprietary Class 2]

24.   "The Nuclear Design of the W. B. McGuire Unit 2 Nuclear Power Plant Cycle 2", WCAP-10747, March 1985. [Westinghouse Proprietary Class 2]

25.   "The Nuclear Design of the W. B. McGuire Unit 2 Nuclear Power Plant Cycle 3", WCAP-11048, March 1986. [Westinghouse Proprietary Class 2]

26.   "The Nuclear Design of the W. B. McGuire Unit 2 Nuclear Power Plant Cycle 4", WCAP-11530, June 1987. [Westinghouse Proprietary Class 2]

27.   "The Nuclear Design of the W. B. McGuire Unit 2 Nuclear Power Plant Cycle 5", WCAP-11891, July 1988. [Westinghouse Proprietary Class 2]

28.   "The Nuclear Design of the W. B. McGuire Unit 2 Nuclear Power Plant Cycle 6", WCAP-12316, August 1989. [Westinghouse Proprietary Class 2]

29.   "The Nuclear Design of the W. B. McGuire Unit 2 Nuclear Power Plant Cycle 7", WCAP-12736, July 1990. [Westinghouse Proprietary Class 2]

30. K. Naugle, "Transmittal of the McGuire Unit 2 Cycle 8 Core Inventory, Average Assembly Burnups, and Average Axial Power Conditions, October 10, 1996. [DPC Proprietary Information from DPC Calc. Files: MCC-1553.05-00-0083, Rev. 3, June 1993 and MCC-1553.05-00-0155, February 1994]

31. K. Naugle, "Transmittal of the McGuire Unit 2 Cycle 9 Core Inventory, Average Assembly Burnups, and Average Axial Power Conditions, October 10, 1996. [DPC Proprietary Information from DPC Calc. Files: MCC-1553.05-00-0123, Rev. 3, June 1993 and MCC-1553.05-00-0183, December 1994]

32. K. Naugle, "Transmittal of the McGuire Unit 2 Cycle 10 Core Inventory, Average Assembly Burnups, and Average Axial Power Conditions, October 10, 1996. [DPC Proprietary Information from DPC Calc. Files: MCC-1553.05-00-0154, December 1993 and MCC-1553.05-00-0185, Rev. 1, April 1996]

33. T. E. Foley, "Core Power Distribution Information for McGuire Unit 2 Neutron Dosimetry Analysis," November 11, 1999. [DPC Proprietary Information]

34. "Analysis of Capsule W from the Duke Power Company McGuire Unit 2 Reactor Vessel Radiation Surveillance Program," WCAP-14799, March 1997.

35. "Westinghouse Fast Neutron Exposure Methodology for Pressure Vessel Fluence Determination and Dosimetry Evaluation," WCAP-13362, May 1992. [Westinghouse Proprietary Class 2].

36. "Duke Power Company Reactor Cavity Neutron Measurement program for William B. McGuire Unit 1 Cycle 12," WCAP-15253, July 1999.

APPENDIX A

SPECIFIC ACTIVITIES AND IRRADIATION HISTORY OF SENSORS
FROM SURVEILLANCE CAPSULES V, X, U, Y, Z, AND W

In this Appendix, the irradiation history, as extracted from NUREG-0020 and Reference 17, and the measured specific activities of radiometric sensors irradiated in Surveillance Capsules V, X, U, Y, Z, and W are provided.

The startup and shutdown dates for each fuel cycle comprising the irradiation history of the surveillance capsules are listed below. Data for the two fuel cycles following the withdrawal of Capsule W are also included for ease of reference.

Cycle	Startup	Shutdown	
1	05/07/83	01/25/85	**Capsule V Withdrawn**
2	05/08/85	03/14/86	
3	06/27/86	05/01/87	
4	07/05/87	05/27/88	
5	07/27/88	07/05/89	**Capsule X Withdrawn**
6	09/19/89	09/01/90	
7	12/29/90	01/09/92	**Capsule U Withdrawn**
8	03/17/92	07/01/93	**Capsules Y & Z Withdrawn**
9	09/14/93	11/24/94	
10	01/12/95	04/05/96	**Capsule W Withdrawn**
11	05/14/96	10/03/97	
12	12/18/97	03/12/99	

The detailed operating history of the reactor over the course of these twelve fuel cycles is provided in Table A-1. Note that the reference full power for McGuire Unit 2 is 3411 MWt.

The measured specific activities of the monitors removed from Capsules V, X, U, Y, Z, and W are provided in Tables A-2 through A-7, respectively. The locations of the various monitors within the surveillance capsules may be obtained from Reference 2.

Table A-1   McGuire Unit 2 Operating History - Cycles 1 Through 12

Cycle 1		Cycle 2		Cycle 3		Cycle 4	
Date	MWt-hr	Date	MWt-hr	Date	MWt-hr	Date	MWt-hr
May-83	29,804	May-85	1,613,921	Jun-86	98,860	Jul-87	1,968,987
Jun-83	281,343	Jun-85	2,080,510	Jul-86	2,419,839	Aug-87	2,304,777
Jul-83	503	Jul-85	949,838	Aug-86	2,295,334	Sep-87	2,209,664
Aug-83	713,998	Aug-85	1,698,280	Sep-86	2,455,840	Oct-87	2,534,464
Sep-83	1,283,803	Sep-85	2,451,943	Oct-86	2,268,723	Nov-87	2,091,145
Oct-83	1,407,029	Oct-85	2,342,207	Nov-86	834,670	Dec-87	2,449,205
Nov-83	1,677,739	Nov-85	2,366,518	Dec-86	2,539,926	Jan-88	2,375,936
Dec-83	1,637,288	Dec-85	1,328,243	Jan-87	1,942,205	Feb-88	2,372,171
Jan-84	430,628	Jan-86	2,284,248	Feb-87	2,094,930	Mar-88	2,528,325
Feb-84	1,908,578	Feb-86	2,262,594	Mar-87	2,537,082	Apr-88	2,446,326
Mar-84	2,306,794	Mar-86	1,070,655	Apr-87	2,391,293	May-88	1,965,065
Apr-84	2,301,882			May-87	20,798		
May-84	2,131,577						
Jun-84	2,382,476						
Jul-84	1,558,900						
Aug-84	614,384						
Sep-84	2,272,550						
Oct-84	2,260,438						
Nov-84	1,822,772						
Dec-84	1,719,551						
Jan-85	1,948,246						
MWt-hr	30,690,283		20,448,957		21,899,500		25,246,065
EFPS	3.239E+07		2.158E+07		2.311E+07		2.664E+07

Table A-1   McGuire Unit 2 Operating History - Cycles 1 Through 12 (continued)

Cycle 5		Cycle 6		Cycle 7		Cycle 8	
Date	**MWt-hr**	**Date**	**MWt-hr**	**Date**	**MWt-hr**	**Date**	**MWt-hr**
Jul-88	182,814	Sep-89	745,948	Dec-90	55,107	Mar-92	846,822
Aug-88	2,312,603	Oct-89	2,483,669	Jan-91	2,425,825	Apr-92	2,321,028
Sep-88	2,447,331	Nov-89	2,400,111	Feb-91	2,231,028	May-92	1,624,848
Oct-88	2,518,180	Dec-89	2,469,574	Mar-91	2,538,082	Jun-92	403,108
Nov-88	2,395,542	Jan-90	2,458,034	Apr-91	2,444,210	Jul-92	2,529,061
Dec-88	2,528,858	Feb-90	2,283,648	May-91	2,523,168	Aug-92	2,074,181
Jan-89	2,475,080	Mar-90	2,469,938	Jun-91	2,372,591	Sep-92	2,449,036
Feb-89	2,280,475	Apr-90	2,446,697	Jul-91	2,191,309	Oct-92	2,531,961
Mar-89	2,248,654	May-90	2,474,847	Aug-91	2,528,077	Nov-92	2,449,669
Apr-89	1,929,466	Jun-90	2,359,097	Sep-91	2,315,536	Dec-92	2,533,105
May-89	2,259,109	Jul-90	2,492,907	Oct-91	2,156,131	Jan-93	2,525,260
Jun-89	2,365,375	Aug-90	2,298,172	Nov-91	2,185,092	Feb-93	2,016,910
Jul-89	290,705	Sep-90	5,074	Dec-91	2,500,590	Mar-93	2,369,376
				Jan-92	628,307	Apr-93	2,452,571
						May-93	2,465,261
						Jun-93	1,947,721
						Jul-93	7,767
MWt-hr	26,234,192		27,387,716		29,095,053		33,547,685
EFPS	2.769E+07		2.891E+07		3.071E+07		3.541E+07

Table A-1 McGuire Unit 2 Operating History - Cycles 1 Through 12 (continued)

Cycle 9		Cycle 10		Cycle 11		Cycle 12	
Date	MWt-hr	Date	MWt-hr	Date	MWt-hr	Date	MWt-hr
Sep-93	914,446	Jan-95	1,510,651	May-96	413,906	Dec-97	815,605
Oct-93	1,265,251	Feb-95	2,286,904	Jun-96	0	Jan-98	2,531,723
Nov-93	2,422,534	Mar-95	2,445,829	Jul-96	2,302,509	Feb-98	2,123,326
Dec-93	2,077,334	Apr-95	1,953,193	Aug-96	2,530,734	Mar-98	2,486,372
Jan-94	2,018,852	May-95	2,534,654	Sep-96	2,451,632	Apr-98	2,445,127
Feb-94	2,283,841	Jun-95	2,404,622	Oct-96	2,477,019	May-98	2,534,880
Mar-94	2,533,507	Jul-95	2,534,676	Nov-96	1,487,425	Jun-98	2,452,802
Apr-94	2,445,941	Aug-95	2,516,579	Dec-96	2,529,393	Jul-98	2,535,620
May-94	2,529,621	Sep-95	2,451,456	Jan-97	2,521,053	Aug-98	2,534,604
Jun-94	2,452,082	Oct-95	2,536,146	Feb-97	2,288,023	Sep-98	2,445,546
Jul-94	2,535,315	Nov-95	2,452,222	Mar-97	2,070,129	Oct-98	2,538,199
Aug-94	2,469,538	Dec-95	1,767,303	Apr-97	2,356,756	Nov-98	2,451,324
Sep-94	2,444,624	Jan-96	2,526,107	May-97	2,532,084	Dec-98	2,535,549
Oct-94	2,533,244	Feb-96	2,366,757	Jun-97	1,141,152	Jan-99	2,527,869
Nov-94	1,726,862	Mar-96	2,452,599	Jul-97	1,562,319	Feb-99	2,190,213
		Apr-96	325,181	Aug-97	2,526,832	Mar-99	797,901
				Sep-97	2,165,325		
				Oct-97	161,797		
MWt-hr	32,652,992		35,064,879		33,518,088		35,946,660
EFPS	3.446E+07		3.701E+07		3.538E+07		3.794E+07

Table A-2   Radiometric Counting Results For Sensors Removed From Capsule V

CHEMICAL ANALYSIS REPORT	WESTINGHOUSE ADVANCED ENERGY SYSTEMS DIVISION ANALYTICAL LABORATORIES WALTZ MILL SITE	ANAL. SERV. REQUEST NO. 12160

ORIGINATOR: S. L. ANDERSON   DEPT. & GRP.   FACILITY: MNC

APPROVAL SIGNATURE: C. A. Blackburn   DATE RECEIVED: 8-22-85   DATE REPORTED: 9-18-85

METHOD	ANALYST	REFERENCE	METHOD	ANALYST	REFERENCE
GAMMA SPEC	WTF	WB #10 Pg 118			
		Pg 119			

RESULTS OF ANALYSIS

ORIGINATOR'S SAMPLE NO.	ANAL. SERV. LAB. NO.	DOSIMETRY MATERIAL		ISOTOPE	ACTIVITY	SEPT. 16, 1985 12:0	
U #345	85-2422	U_3O_8		Cs-137	136	dps/mg of U-238	
Np #20/210	-2423	NpO_2		Cs-137	1196	dps/mg of Np-237	
TOP WIRES 1	-2424	Co Al		Co-60	10060	dps/mg of WIRE	
2	-2425	Co Al cd		Co-60	5043		
3	-2426	Cu		Co-60	38.4		
4	-2427	Ni		Co-58	3958		
5	-2428	Fe		Mn-54	969		
MID WIRES 1	-2429	Co Al		Co-60	8832		
2	-2430	Co Al		Co-60	7833		
3	-2431	Co Al cd		Co-60	4723		
4	-2432	Cu		Co-60	40.3		
5	-2433	Ni		Co-58	3574		
6	-2434	Fe		Mn-54	1010		
BOTTOM WIRES 1	-2435	Co Al		Co-60	9489		
2	-2436	Co Al		Co-60	8747		
3	-2437	Co Al		Co-60	8336		
REMARKS: 4	-2438	Co Al cd		Co-60	4742		
5	-2439	Cu		Co-60	37.6		
6	-2440	Ni		Co-58	4042		
7	-2441	Fe		Mn-54	987		

McGUIRE UNIT #2 "V" CAPSULE DOSIMETRY.

Table A-3   Radiometric Counting Results For Sensors Removed From Capsule X

Table A-4   Radiometric Counting Results For Sensors Removed From Capsule U

REVISED
REPORT

Westinghouse Electric Corporation
Advanced Programs - Analytical Laboratory
Waltz Mill Site

Request# 14675

Originator: Ed Terek (V)NATD
Structural Reliability & Plant Life Optimization
Westinghouse Electric Corporation

Received: 5/6/92
Reported: 8/18/92

[RESULTS OF ANALYSIS]

Dosimetry: McGuire Unit #2 "U" Capsule

Originator ID	Lab. Sample #	Dosimeter Material	Nuclide	(May 15,1992) dps/mg *		2 sigma
FISSON MONITORS						
U-238	92-1350	U-238	Cs-137	8.67E+03	+/-	8.31E+00
Np-237	92-1351	Np-237	Cs-137	6.48E+03	+/-	4.24E-01
TOP WIRES						
AlCo	92-1352	AlCo	Co-60	3.38E+04	+/-	2.97E-02
AlCo	92-1353	AlCo	Co-60	3.75E+04	+/-	2.76E-02
AlCo(Cd)	92-1354	AlCo	Co-60	2.11E+04	+/-	1.89E-02
Cu	92-1355	Cu	Co-60	1.34E+02	+/-	1.52E-00
Fe	92-1356	Fe	Mn-54	1.75E+03	+/-	2.20E+01
Ni	92-1357	Ni	Co-58	1.16E+04	+/-	9.98E+01
MID WIRES						
AlCo	92-1358	AlCo	Co-60	3.38E+04	+/-	2.38E+02
AlCo	92-1359	AlCo	Co-60	3.15E+04	+/-	3.39E-02
AlCo(Cd)	92-1360	AlCo	Co-60	1.93E+04	+/-	1.64E-02
Cu	92-1361	Cu	Co-60	1.63E+02	+/-	1.67E+00
Fe	92-1362	Fe	Mn-54	1.86E+03	+/-	2.14E+01
Ni	92-1363	Ni	Co-58	1.19E+04	+/-	7.91E+01
BOTTOM WIRES						
AlCo	92-1364	AlCo	Co-60	3.04E+04	+/-	2.21E+02
AlCo	92-1365	AlCo	Co-60	3.57E+04	+/-	2.47E+02
AlCo(Cd)	92-1366	AlCo	Co-60	2.05E+04	+/-	1.63E-02
Cu	92-1367	Cu	Co-60	1.56E+02	+/-	1.49E+00
Fe	92-1368	Fe	Mn-54	1.70E+03	+/-	1.38E+01
Ni	92-1369	Ni	Co-58	1.18E+04	+/-	8.32E+01

Remarks: * Results are in units of dps/(mg of Dosimeter Material).
            Cu Co-60 efficiency corrected

AL File: 14675
References: Lab.Book# 51 pages 40: Lab. Book# 53 page 90
Procedures:A-812,A-813,A-824
Analyst:WTF,FRC

Approved: _____

Table A-5 Radiometric Counting Results For Sensors Removed From Capsule Y

REPORT

Westinghouse Electric Corporation
CNSD - Analytical Laboratory
Waltz Mill Site

Request# 15388

Originator: R.Torok   (W)NATD, Energy Center (X4708)

Received: 4/27/94
Reported: 5/18/94

[RESULTS OF ANALYSIS]

Dosimetry: McGuire Unit #2 "Y" Capsule

Originator ID	Lab. Sample #	Dosimeter Material	Nuclide	(May 6, 1994) dpa/mg *		2 sigma
FISSION MONITORS						
U-238	94-1815	U-238	Co-137	8.52E+02	+/-	5.5E+00
Np-237	94-1816	Np-237	Cs-137	6.41E+03	+/-	4.6E+01
TOP WIRES						
AlCo(Cd)	94-1817	AlCo	Co-60	1.62E+04	+/-	2.2E+02
AlCo	94-1818	AlCo	Co-60	3.25E+04	+/-	3.2E+02
AlCo	94-1819	AlCo	Co-60	2.77E+04	+/-	2.7E+02
Ni	94-1822	Ni	Co-58	1.71E+03	+/-	1.2E+01
Cu	94-1821	Cu	Co-60	1.45E+02	+/-	2.5E+00
Fe	94-1820	Fe	Mn-54	1.04E+03	+/-	1.1E+01
MID WIRES						
AlCo(Cd)	94-1823	AlCo	Co-60	1.53E+04	+/-	2.1E+02
AlCo	94-1824	AlCo	Co-60	2.46E+04	+/-	2.5E+02
AlCo	94-1825	AlCo	Co-60	2.95E+04	+/-	2.9E+02
Ni	94-1826	Ni	Co-58	1.53E+03	+/-	1.1E+01
Cu	94-1827	Cu	Co-60	1.54E+02	+/-	2.7E+00
Fe	94-1828	Fe	Mn-54	1.07E+03	+/-	1.1E+01
BOTTOM WIRES						
AlCo(Cd)	94-1829	AlCo	Co-60	1.59E+04	+/-	2.1E+02
AlCo	94-1830	AlCo	Co-60	2.54E+04	+/-	2.5E+02
Ni	94-1834	Ni	Co-58	1.70E+03	+/-	1.2E+01
Cu	94-1833	Cu	Co-60	1.45E+02	+/-	2.9E+00
Fe	94-1832	Fe	Mn-54	1.02E+03	+/-	1.1E+01

Remarks: * Results are in units of dpa/(mg of Dosimeter Material).

AL File:15388
References: Lab.Book# 54 page 134.
Procedures: A-512, A-513
Analyst: WTF, FRC

Approved: _____

Table A-6   Radiometric Counting Results For Sensors Removed From Capsule Z

REPORT

Westinghouse Electric Corporation
WNATD - Analytical Laboratory
Waltz Mill Site

Request: 15388

Originator: E.Terek (W)NATD, Energy Center (84702)

Received: 4/27/94
Reported: 5/13/94

[RESULTS OF ANALYSIS]

Dosimetry: McGuire Unit #2 "Z" - Capsule

Originator ID	Lab. Sample #	Dosimeter Material	Nuclide	(May 6,1994) dps/mg *		2 sigma
FISSION MONITORS						
U-238	94-1838	U-238	Cs-137	1.04E+03	+/-	9.0E+00
Np-237	94-1835	Np-237	Cs-137	7.53E+03	+/-	4.3E+01
TOP WIRES						
AlCo(Cd)	94-1837	AlCo	Co-60	1.99E+04	+/-	2.3E+02
AlCo	94-1838	AlCo	Co-60	3.30E+04	+/-	2.5E+02
AlCo	94-1839	AlCo	Co-60	3.79E+04	+/-	3.3E+02
Ni	94-1840	Ni	Co-58	1.92E+03	+/-	1.6E+01
Cu	94-1841	Cu	Co-60	1.65E+02	+/-	2.7E+00
Fe	94-1842	Fe	Mn-54	1.12E+03	+/-	2.0E+01
MID WIRES						
AlCo(Cd)	94-1843	AlCo	Co-60	1.89E+04	+/-	2.3E+02
AlCo	94-1844	AlCo	Co-60	3.64E+04	+/-	3.1E+02
AlCo	94-1845	AlCo	Co-60	3.01E+04	+/-	2.9E+02
Ni	94-1846	Ni	Co-58	1.97E+03	+/-	1.5E+01
Cu	94-1847	Cu	Co-60	1.55E+02	+/-	2.5E+00
Fe	94-1848	Fe	Mn-54	1.15E+03	+/-	2.1E+01
BOTTOM WIRES						
AlCo(Cd)	94-1849	AlCo	Co-60	1.94E+04	+/-	2.3E+02
AlCo	94-1850	AlCo	Co-60	3.17E+04	+/-	2.5E+02
Ni	94-1851	Ni	Co-58	1.99E+03	+/-	1.6E+01
Cu	94-1853	Cu	Co-60	1.55E+02	+/-	2.7E+00
Fe	94-1852	Fe	Mn-54	1.14E+03	+/-	1.9E+01

Remarks: * Results are in units of dps/mg of Dosimeter Material).

AL File:15388
References: Lab.Book# 84 page 134.
Procedures:A-512, A-513
Analyst:WTF, FRC

Approved: [signature]

Westinghouse Electric Corporation
Chemistry & Materials - Analytical Laboratory
Waltz Mill Site

REPORT
REVISED*   Request# 16138

Originator: I.Terek   (W)ENPD, Energy Center (E476E)

Received: 9-12-96
Reported: 10-28-96

[RESULTS OF ANALYSIS]

Dosimetry: McGuire Unit #2 "W" - Capsule   Block #362

Originator ID	Lab. Sample #	Dosimeter Material	Nuclide	(Sept.26,1996) dps/mg * 2 sigma
FISSION MONITORS				
U-238	96-1856	U	Cs-137	1.29E+03 +/- 1.4E-01
Np-237	96-1857	Np	Cs-137	9.22E-03 +/- 5.3E-01
TOP WIRES				
AlCo	96-1858	AlCo	Co-60	4.47E+04 +/- 3.4E-02
AlCo	96-1859	AlCo	Co-60	4.84E+04 +/- 3.0E-02
AlCo(Cd)	96-1860	AlCo	Co-60	2.34E+04 +/- 1.7E-02
Cu	96-1861	Cu	Co-60	1.84E+02 +/- 2.3E+00
Ni	96-1862	Ni	Co-58	7.15E+03 +/- 3.6E-01
Fe	96-1863	Fe	Mn-54	1.59E+03 +/- 2.1E-01
MID WIRES				
AlCo	96-1864	AlCo	Co-60	4.16E+04 +/- 3.4E-02
AlCo	96-1865	AlCo	Co-60	3.51E+04 +/- 2.9E-02
AlCo(Cd)	96-1866	AlCo	Co-60	2.23E+04 +/- 2.4E-02
Cu	96-1867	Cu	Co-60	1.89E+02 +/- 2.3E+00
Ni	96-1868	Ni	Co-58	7.38E+03 +/- 3.9E-01
Fe	96-1869	Fe	Mn-54	1.63E+03 +/- 2.0E-01
BOTTOM WIRES				
AlCo	96-1870	AlCo	Co-60	3.89E+04 +/- 3.2E-02
AlCo	96-1871	AlCo	Co-60	4.45E+04 +/- 3.4E-02
AlCo(Cd)	96-1872	AlCo	Co-60	2.35E+04 +/- 2.5E-02
Cu	96-1873	Cu	Co-60	1.84E+02 +/- 2.3E+00
Ni	96-1874	Ni	Co-58	7.29E+03 +/- 3.6E-01
Fe	96-1875	Fe	Mn-54	1.60E+03 +/- 1.9E-01

Remarks: * Results are in units of dps/(mg of Dosimeter Material).
          * Calculation error on wire dosimetry.

AL File: 16138
Procedures: A-512, A-513
Analyst: MT?

Approved: _(signature)_

APPENDIX B

SPECIFIC ACTIVITIES AND IRRADIATION HISTORY OF REACTOR CAVITY SENSOR SETS IRRADIATED DURING CYCLE 12

In this appendix, the irradiation history, as extracted from Reference 17, and the measured specific activities of radiometric sensors irradiated in reactor cavity during Cycle 12 are provided.

The startup and shutdown dates for Cycle 12 were as follows:

Cycle	Startup	Shutdown	
12	12/18/97	03/12/99	RCND Set 2S-1 irradiated

The detailed operating history of the reactor over the course of Cycle 12 is provided in Table B-1. Note that the reference full power for McGuire Unit 2 is 3411 MWt.

The capsule loading table for the RCND Set 2S-1 irradiated during Cycle 12 is provided in Table B-2. The measured specific activities of the monitors removed from RCND Set 2S-1 are provided in Table B-3. For the multiple foil sensor sets, the individual foil ID can be correlated with the capsule position description in Section 6.1.1 in order to determine the location of the foil within the reactor cavity.

Table B-1   McGuire Unit 2 Operating History - Cycle 12

<u>Cycle 12</u>

<u>Date</u>	<u>MWt-hr</u>
Dec-97	815,605
Jan-98	2,531,723
Feb-98	2,123,326
Mar-98	2,486,372
Apr-98	2,445,127
May-98	2,534,880
Jun-98	2,452,802
Jul-98	2,535,620
Aug-98	2,534,604
Sep-98	2,445,546
Oct-98	2,538,199
Nov-98	2,451,324
Dec-98	2,535,549
Jan-99	2,527,869
Feb-99	2,190,213
Mar-99	797,901

MWt-hr	**35,946,660**
EFPS	**3.794E+07**

Table B-2   McGuire Unit 2 Dosimeter Capsule Contents for Cycle 12

Capsule ID and Position	Bare or Cadmium Shielded	Radiometric Monitor ID						
		Fe	Ni	Cu	Ti	Co	U-238	Np-237
G-1	B	G				G	—	—
G-2	Cd	CG	G	G	G	CG	—	—
G-3	Cd	—	—	—	—	—	46	42
H-1	B	H	—	—	—	H	—	—
H-2	Cd	CH	H	H	H	CH	—	—
H-3	Cd	—	—	—	—	—	47	43
I-1	B	I	—	—	—	I	—	—
I-2	Cd	C	I	I	I	C	—	—
I-3	Cd	—	—	—	—	—	48	44
J-1	B	J	—	—	—	J	—	—
J-2	Cd	CJ	J	J	J	CJ	—	—
J-3	Cd	—	—	—	—	—	49	45
K-1	B	AA	—	—	—	AA	—	—
K-2	Cd	DA	AA	AA	AA	DA	—	—
K-3	Cd	—	—	—	—	—	50	46
L-1	B	AB	—	—	—	AB	—	—
L-2	Cd	DB	AB	AB	AB	DB	—	—
L-3	Cd	—	—	—	—	—	51	47

Note: Each capsule contains two iron foils, one nickel foil, one copper foil, one titanium foil, two cobalt-aluminum foils, one vanadium encapsulated ^{238}U oxide detector, one vanadium encapsulated ^{237}Np oxide detector, and two cadmium covers.

Table B-3   **Radiometric Counting Results For Sensors Removed From Cycle 12 Cavity Dosimetry Set 2S-1 Capsules G, H, I, J, K, and L**

Antech Ltd.

July 8, 1999

Certificate of Conformance

Mr. Larry Becker
Westinghouse Electric Company
CD&ME Department
F Building, MS 60
Madison, PA 15663
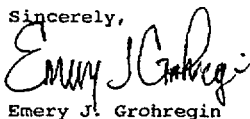
           Dosimetry Characterization; Purchase Order No. DIPP-7500
      McGuire Unit #2 Cycle #12; Duke Power; Nuclear Service Division
               Antech Ltd. Project No. 99-0326W

Dear Mr. Becker:

Enclosed are analytical results for samples submitted by Westinghouse Electric Company. Samples were received and logged in for analysis on May 28, 1999.

Appropriate methods were used and are indicated accordingly on the data tables. Appropriate quality assurance/quality control measures were performed in accordance with Antech Ltd.'s Quality Assurance Plan and 10 CFR, part 50 Appendix B. If you have any questions, please call me at 724-722-5219.

Sincerely,

Emery J. Grohregin
Supervisor

Brian M. Carson
QA/QC Coordinator

EJG:rks

Enclosures

Table B-3   Radiometric Counting Results For Sensors Removed From Cycle 12 Cavity Dosimetry Set 2S-1 Capsules G, H, I, J, K, and L (continued)

ANTECH LTD.
CASE NARRATIVE

I.   PROJECT LOGIN INFORMATION:

A: PROJECT NUMBERS:

ANTECH LTD.:   99-0326W

CLIENT: Purchase Order Number: DIPP-7500

B: SAMPLE IDENTIFICATIONS:

Antech ID	Client ID	Antech ID	Client ID
9905-0279W	G-Fe Bare	9905-0280W	GC-Fe Cd
9905-0281W	G-Ni Cd	9905-0282W	G-Cu Cd
9905-0283W	G-Ti Cd	9905-0284W	G-CoAl Bare
9905-0285W	CG CoAl Cd	9905-0286W	U-238 46 Cd
9905-0287W	NP-237 42 Cd	9905-0288W	H-Fe Bare
9905-0289W	CH-Fe Cd	9905-0290W	H-Ni Cd
9905-0291W	H-Cu Cd	9905-0292W	H-Ti Cd
9905-0293W	H-CoAl Bare	9905-0294W	CH-CoAl Cd
9905-0295W	U-238 47 Cd	9905-0296W	NP-237-43 Cd
9905-0297W	I-Fe Bare	9905-0298W	CI-Fe Cd
9905-0299W	I-Ni Cd	9905-0300W	I-Cu Cd
9905-0301W	I-Ti Cd	9905-0302W	I-CoAl Bare
9905-0303W	CI-CoAl Cd	9905-0304W	U-238 48 Cd
9905-0305W	Np-237 44 Cd	9905-0306W	J-Fe Bare
9905-0307W	CJ-Fe Cd	9905-0308W	J-Ni Cd
9905-0309W	J-Cu Cd	9905-0310W	J-Ti Cd
9905-0311W	J-CoAl Bare	9905-0312W	CJ-CoAl Cd
9905-0313W	U-238 49 Cd	9905-0314W	NP-237 45 Cd
9905-0315W	AA-Fe Bare	9905-0316W	DA-Fe Cd
9905-0317W	AA-Ni Cd	9905-0318W	AA-Cu Cd
9905-0319W	AA-Ti Cd	9905-0320W	AA-CoAl Bare
9905-0321W	DA-CoAl Cd	9905-0322W	U-238 50 Cd
9905-0323W	NP-237 46 Cd	9905-0324W	AB-Fe Bare
9905-0325W	DB-Fe Cd	9905-0326W	AB-Ni Cd
9905-0327W	AB-Cu Cd	9905-0328W	AB-Ti Cd
9905-0329W	AB-CoAl Bare	9905-0330W	DB-CoAl Cd
9905-0331W	U-238 51 Cd	9905-0332W	NP-237 47 Cd
9905-0333W	CHAIN 2S-1(0)	9905-0334W	+5.5(0)
9905-0335W	+4.5(0)	9905-0336W	+3.5(0)
9905-0337W	+2.5(0)	9905-0338W	+1.5(0)
9905-0339W	+0.5(0)	9905-0340W	-0.5(0)
9905-0341W	-1.5(0)	9905-0342W	-2.5(0)
9905-0343W	-3.5(0)	9905-0344W	-4.5(0)
9905-0345W	-5.5(0)	9905-0346W	-6.5(0)
9905-0347W	CHAIN 2S-1 (15)	9905-0348W	+5.5 (15)
9905-0349W	+4.5 (15)	9905-0350W	+3.5 (15)
9905-0351W	+2.5 (15)	9905-0352W	+1.5 (15)

Table B-3   Radiometric Counting Results For Sensors Removed From Cycle 12 Cavity Dosimetry Set 2S-1 Capsules G, H, I, J, K, and L (continued)

ANTECH LTD.
CASE NARRATIVE

(Continued)

9905-0353W	+0.5 (15)		9905-0354W	-0.5 (15)
9905-0355W	-1.5 (15)		9905-0356W	-2.5 (15)
9905-0357W	-3.5 (15)		9905-0358W	-4.5 (15)
9905-0359W	-5.5 (15)		9905-0360W	-6.5 (15)
9905-0361W	CHAIN 2 S-1 (30)		9905-0362W	+5.5 (30)
9905-0363W	+4.5 (30)		9905-0364W	+3.5 (30)
9905-0365W	+2.5 (30)		9905-0366W	+1.5 (30)
9905-0367W	+0.5 (30)		9905-0368W	-0.5 (30)
9905-0369W	-1.5 (30)		9905-0370W	-2.5 (30)
9905-0371W	-3.5 (30)		9905-0372W	-4.5 (30)
9905-0373W	-5.5 (30)		9905-0374W	-6.5 (30)
9905-0375W	CHAIN 2S-1 (45)		9905-0376W	+5.5 (45)
9905-0377W	+4.5 (45)		9905-0378W	+3.5 (45)
9905-0379W	+2.5 (45)		9905-0380W	+1.5 (45)
9905-0381W	+0.5 (45)		9905-0382W	-0.5 (45)
9905-0383W	-1.5 (45)		9905-0384W	-2.5 (45)
9905-0385W	-3.5 (45)		9905-0386W	-4.5 (45)
9905-0387W	-5.5 (45)		9905-0388W	-6.5 (45)
9905-0390W	Nist 101E		9905-0391W	True Value NIST 101E

    C: SHIPPING/RECEIVING COMMENTS:

          Final Report: 07/07/99
II.   PREPARATION/ANALYSIS COMMENTS:

    A: METALS:
          NONE
    B: RADIOLOGICAL:
          Decay correct date for gamma analysis is 6/11/99.
III.   GENERAL COMMENTS:

          Trailing zeroes and decimal places appearing on the data should not
          be interpreted as precision of the analytical procedure, but rather
          as a result of reporting format.

Table B-3   Radiometric Counting Results For Sensors Removed From Cycle 12 Cavity Dosimetry Set 2S-1 Capsules G, H, I, J, K, and L (continued)

Table 1
General Data Table
Westinghouse Electric Company
Antech Ltd. Project No. 99-0326W
Dosimetry Characterization; McGuire Unit #2 Cycle #12
Charge Order No. DIPP-7500; Duke Power

Page 1 of 3

Antech Sample ID	Client Sample ID	Sampling Location	Sc-46 A-524 dps/mg	Mn-54 A-524 dps/mg	Co-58 A-524 dps/mg	Co-60 A-524 dps/mg
9905-0279W	G-Fe Bare	G-CAPSULE	NA	7.78E0 ± 8.1E-1	NA	NA
9905-0280W	GC-Fe Cd	G-CAPSULE	NA	7.61E0 ± 7.9E-1	NA	NA
9905-0281W	G-Ni Cd	G-CAPSULE	NA	NA	9.33E1 ± 7.6E0	NA
9905-0282W	G-Cu Cd	G-CAPSULE	NA	NA	NA	3.12E-1 ± 7.9E-3
9905-0283W	G-Ti Cd	G-CAPSULE	2.27E0 ± 9.4E-2	NA	NA	NA
9905-0284W	G-CoAl Bare	G-CAPSULE	NA	NA	NA	2.53E2 ± 5.1E0
9905-0285W	CG CoAl Cd	G-CAPSULE	NA	NA	NA	1.17E2 ± 2.4E0
9905-0288W	H-Fe Bare	H-CAPSULE	NA	1.08E1 ± 4.2E-1	NA	NA
9905-0289W	CH-Fe Cd	H-CAPSULE	NA	1.34E1 ± 5.2E-1	NA	NA
9905-0290W	H-Ni Cd	H-CAPSULE	NA	NA	1.38E2 ± 1.7E1	NA
9905-0291W	H-Cu Cd	H-CAPSULE	NA	NA	NA	4.02E-1 ± 1.4E-2
9905-0292W	H-Ti Cd	H-CAPSULE	2.97E0 ± 1.1E-1	NA	NA	NA
9905-0293W	H-CoAl Bare	H-CAPSULE	NA	NA	NA	3.23E2 ± 6.2E0
9905-0294W	CH-CoAl Cd	H-CAPSULE	NA	NA	NA	1.93E2 ± 3.8E0

Table B-3   Radiometric Counting Results For Sensors Removed From Cycle 12 Cavity Dosimetry Set 2S-1 Capsules G, H, I, J, K, and L (continued)

Table 1
(Continued)

Page 2 of 3

Antech Sample ID	Client Sample ID	Sampling Location	Parameter Identification			
			Sc-46 A-524 dps/mg	Mn-54 A-524 dps/mg	Co-58 A-524 dps/mg	Co-60 A-524 dps/mg
9905-0297W	I-Fe Bare	I-CAPSULE	NA	1.08E1 ± 3.7E-1	NA	NA
9905-0298W	CI-Fe Cd	I-CAPSULE	NA	1.09E1 ± 3.4E-1	NA	NA
9905-0299W	I-Ni Cd	I-CAPSULE	NA	NA	NA	NA
9905-0300W	I-Cu Cd	I-CAPSULE	NA	NA	1.34E2 ± 9.4E0	NA
9905-0301W	I-Ti Cd	I-CAPSULE	2.94E0 ± 1.1E-1	NA	NA	3.89E-1 ± 1.1E-2
9905-0302W	I-CoAl Bare	I-CAPSULE	NA	NA	NA	NA
9905-0303W	CI-CoAl Cd	I-CAPSULE	NA	NA	NA	4.79E2 ± 1.0E1
9905-0306W	J-Fe Bare	J-CAPSULE	NA	NA	NA	2.46E2 ± 5.8E0
9905-0307W	CJ-Fe Cd	J-CAPSULE	NA	6.40E0 ± 6.7E-1	NA	NA
9905-0308W	J-Ni Cd	J-CAPSULE	NA	6.68E0 ± 7.0E-1	NA	NA
9905-0309W	J-Cu Cd	J-CAPSULE	NA	NA	9.10E1 ± 7.2E0	NA
9905-0310W	J-Ti Cd	J-CAPSULE	1.78E0 ± 8.6E-2	NA	NA	2.13E-1 ± 4.9E-3
9905-0311W	J-CoAl Bare	J-CAPSULE	NA	NA	NA	1.95E2 ± 3.8E0
9905-0312W	CJ-CoAl Cd	J-CAPSULE	NA	NA	NA	1.26E2 ± 2.5E0

Table B-3   Radiometric Counting Results For Sensors Removed From Cycle 12 Cavity Dosimetry Set 2S-1 Capsules G, H, I, J, K, and L (continued)

Table 1
(Continued)

Page 3 of 3

Antech Sample ID	Client Sample ID	Sampling Location	Parameter Identification			
			Sc-46 A-524 dps/mg	Mn-54 A-524 dps/mg	Co-58 A-524 dps/mg	Co-60 A-524 dps/mg
9905-0315W	AA-Fe Bare	K-CAPSULE	NA	9.01E0 ± 9.3E-1	NA	NA
9905-0316W	DA-Fe Cd	K-CAPSULE	NA	8.99E0 ± 9.3E-1	NA	NA
9905-0317W	AA-Ni Cd	K-CAPSULE	NA	NA	1.13E2 ± 3.1E0	NA
9905-0318W	AA-Cu Cd	K-CAPSULE	NA	NA	NA	3.13E-1 ± 1.3E-2
9905-0319W	AA-Ti Cd	K-CAPSULE	2.34E0 ± 7.2E-2	NA	NA	NA
9905-0320W	AA-CoAl Bare	K-CAPSULE	NA	NA	NA	2.98E2 ± 5.4E0
9905-0321W	DA-CoAl Cd	K-CAPSULE	NA	NA	NA	1.95E2 ± 3.6E0
9905-0324W	AB-Fe Bare	L-CAPSULE	NA	1.19E0 ± 7.2E-2	NA	NA
9905-0325W	DB-Fe Cd	L-CAPSULE	NA	1.10E0 ± 6.0E-2	NA	NA
9905-0326W	AB-Ni Cd	L-CAPSULE	NA	NA	1.50E1 ± 1.5E0	NA
9905-0327W	AB-Cu Cd	L-CAPSULE	NA	NA	NA	3.52E-2 ± 2.2E-3
9905-0328W	AB-Ti Cd	L-CAPSULE	2.95E-1 ± 2.3E-2	NA	NA	NA
9905-0329W	AB-CoAl Bare	L-CAPSULE	NA	NA	NA	7.83E1 ± 1.6E0
9905-0330W	DB-CoAl Cd	L-CAPSULE	NA	NA	NA	4.85E1 ± 1.1E0

Table 2
General Data Table
Westinghouse Electric Company
Antech Ltd. Project No. 99-0326W
Dosimetry Characterization; McGuire Unit #2 Cycle #12
Charge Order No. DIPP-7500; Duke Power

Page 1 of 2

Antech Sample ID	Client Sample ID	Parameter Identification		
		Mn-54 A-524 dps/mg	Co-58 A-524 dps/mg	Co-60 A-524 dps/mg
9905-0333W	CHAIN 2S-1(0)	.(1)	-	-
9905-0334W	+5.5(0)	3.89E0 ± 2.8E-1	6.77E0 ± 5.0E-1	3.39E1 ± 7.8E-1
9905-0335W	+4.5(0)	4.62E0 ± 3.3E-1	8.15E0 ± 5.9E-1	4.04E1 ± 9.2E-1
9905-0336W	+3.5(0)	4.96E0 ± 2.6E-1	8.84E0 ± 3.5E-1	4.60E1 ± 9.9E-1
9905-0337W	+2.5(0)	5.31E0 ± 2.7E-1	8.73E0 ± 3.6E-1	4.95E1 ± 1.1E0
9905-0338W	+1.5(0)	5.19E0 ± 2.8E-1	8.64E0 ± 3.6E-1	6.34E1 ± 1.3E0
9905-0339W	+0.5(0)	5.08E0 ± 2.7E-1	8.47E0 ± 3.7E-1	6.56E1 ± 1.4E0
9905-0340W	-0.5(0)	5.01E0 ± 2.7E-1	8.28E0 ± 3.6E-1	6.40E1 ± 1.4E0
9905-0341W	-1.5(0)	4.97E0 ± 2.6E-1	8.22E0 ± 3.6E-1	6.21E1 ± 1.3E0
9905-0342W	-2.5(0)	4.51E0 ± 2.5E-1	7.88E0 ± 3.5E-1	5.57E1 ± 1.2E0
9905-0343W	-3.5(0)	3.90E0 ± 2.1E-1	6.79E0 ± 3.0E-1	3.59E1 ± 7.8E-1
9905-0344W	-4.5(0)	2.30E0 ± 1.2E-1	4.20E0 ± 1.6E-1	2.44E1 ± 5.2E-1
9905-0345W	-5.5(0)	8.60E-1 ± 7.1E-2	1.57E0 ± 1.2E-1	1.58E1 ± 3.7E-1
9905-0346W	-6.5(0)	2.50E-1 ± 3.6E-2	5.05E-1 ± 5.3E-2	7.11E0 ± 1.7E-1
9905-0347W	CHAIN 2S-1 (15)	-	-	-
9905-0348W	+5.5 (15)	5.67E0 ± 2.7E-1	1.01E1 ± 3.9E-1	6.99E1 ± 1.47E0
9905-0349W	+4.5 (15)	6.51E0 ± 3.4E-1	1.17E1 ± 4.5E-1	8.57E1 ± 1.8E0
9905-0350W	+3.5 (15)	6.95E0 ± 3.5E-1	1.21E1 ± 5.1E-1	9.67E1 ± 2.0E0
9905-0351W	+2.5 (15)	7.45E0 ± 3.5E-1	1.20E1 ± 4.8E-1	9.49E1 ± 2.0E0
9905-0352W	+1.5 (15)	7.16E0 ± 3.2E-1	1.19E1 ± 4.8E-1	8.47E1 ± 1.8E0
9905-0353W	+0.5 (15)	7.12E0 ± 3.3E-1	1.19E1 ± 4.7E-1	8.31E1 ± 1.8E0
9905-0354W	-0.5 (15)	7.00E0 ± 3.3E-1	1.17E1 ± 4.4E-1	8.31E1 ± 1.7E0
9905-0355W	-1.5 (15)	6.71E0 ± 3.0E-1	1.17E1 ± 4.4E-1	7.95E1 ± 1.7E0
9905-0356W	-2.5 (15)	6.45E0 ± 2.8E-1	1.13E1 ± 4.2E-1	7.36E1 ± 1.6E0
9905-0357W	-3.5 (15)	5.69E0 ± 2.9E-1	9.87E0 ± 4.0E-1	6.70E1 ± 1.4E0
9905-0358W	-4.5 (15)	3.73E0 ± 2.0E-1	6.66E0 ± 3.0E-1	4.81E1 ± 1.0E0
9905-0359W	-5.5 (15)	1.50E0 ± 1.0E-1	2.77E0 ± 1.4E-1	2.80E1 ± 6.1E-1
9905-0360W	-6.5 (15)	4.36E-1 ± 5.2E-2	8.05E-1 ± 6.6E-2	1.31E1 ± 2.9E-1

See footnotes at end of table.

Table 2
(Continued)

Page 2 of 2

| | | Parameter Identification | | |
| | | Mn-54
A-524
dps/mg | Co-58
A-524
dps/mg | Co-60
A-524
dps/mg |
Antech Sample ID	Client Sample ID			
9905-0361W	CHAIN 2 S-1 (30)	-	-	-
9905-0362W	+5.5 (30)	5.60E0 ± 2.8E-1	1.05E1 ± 4.3E-1	9.80E1 ± 2.1E0
9905-0363W	+4.5 (30)	6.58E0 ± 3.4E-1	1.16E1 ± 4.9E-1	1.23E2 ± 2.6E0
9905-0364W	+3.5 (30)	7.22E0 ± 3.9E-1	1.22E1 ± 5.2E-1	1.38E2 ± 2.9E0
9905-0365W	+2.5 (30)	7.47E0 ± 3.9E-1	1.22E1 ± 5.2E-1	1.40E2 ± 2.9E0
9905-0366W	+1.5 (30)	7.19E0 ± 3.8E-1	1.21E1 ± 4.8E-1	1.33E2 ± 2.8E0
9905-0367W	+0.5 (30)	6.87E0 ± 3.7E-1	1.21E1 ± 5.0E-1	1.26E2 ± 2.6E0
9905-0368W	-0.5 (30)	6.92E0 ± 4.0E-1	1.16E1 ± 4.8E-1	1.16E2 ± 2.4E0
9905-0369W	-1.5 (30)	6.94E0 ± 3.7E-1	1.19E1 ± 4.9E-1	1.20E2 ± 2.5E0
9905-0370W	-2.5 (30)	6.59E0 ± 3.6E-1	1.15E1 ± 4.8E-1	1.07E2 ± 2.3E0
9905-0371W	-3.5 (30)	5.51E0 ± 2.8E-1	9.91E0 ± 4.4E-1	9.75E1 ± 2.1E0
9905-0372W	-4.5 (30)	3.66E0 ± 2.6E-1	6.65E0 ± 3.3E-1	7.22E1 ± 1.5E0
9905-0373W	-5.5 (30)	1.64E0 ± 1.6E-1	2.96E0 ± 1.9E-1	4.36E1 ± 9.3E-1
9905-0374W	-6.5 (30)	4.88E-1 ± 5.7E-2	9.20E-1 ± 8.6E-2	1.84E1 ± 4.3E-1
9905-0375W	CHAIN 2S-1 (45)	-	-	-
9905-0376W	+5.5 (45)	4.87E0 ± 3.5E-1	9.18E0 ± 6.7E-1	6.06E1 ± 1.4E0
9905-0377W	+4.5 (45)	6.16E0 ± 3.1E-1	1.09E1 ± 4.4E-1	7.34E1 ± 1.6E0
9905-0378W	+3.5 (45)	6.35E0 ± 3.0E-1	1.11E1 ± 4.4E-1	8.16E1 ± 1.7E0
9905-0379W	+2.5 (45)	6.23E0 ± 3.1E-1	1.12E1 ± 4.6E-1	8.60E1 ± 1.8E0
9905-0380W	+1.5 (45)	6.43E0 ± 3.3E-1	1.12E1 ± 4.5E-1	8.46E1 ± 1.8E0
9905-0381W	+0.5 (45)	6.07E0 ± 3.2E-1	1.07E1 ± 4.4E-1	8.12E1 ± 1.7E0
9905-0382W	-0.5 (45)	5.91E0 ± 3.3E-1	1.04E1 ± 4.2E-1	8.09E1 ± 1.7E0
9905-0383W	-1.5 (45)	5.99E0 ± 3.1E-1	1.03E1 ± 4.2E-1	7.80E1 ± 1.7E0
9905-0384W	-2.5 (45)	5.56E0 ± 2.8E-1	9.93E0 ± 3.9E-1	7.03E1 ± 1.5E0
9905-0385W	-3.5 (45)	4.67E0 ± 2.6E-1	8.53E0 ± 3.7E-1	6.01E1 ± 1.3E0
9905-0386W	-4.5 (45)	2.88E0 ± 2.1E-1	5.44E0 ± 4.0E-1	4.09E1 ± 9.4E-1
9905-0387W	-5.5 (45)	1.23E0 ± 1.0E-1	2.31E0 ± 1.8E-1	2.87E1 ± 6.6E-1
9905-0388W	-6.5 (45)	1.15E-1 ± 1.7E-2	2.22E-1 ± 2.6E-2	3.35E0 ± 2.3E-1

(1)Dash denotes not analyzed.

Table B-3   **Radiometric Counting Results For Sensors Removed From Cycle 12 Cavity Dosimetry Set 2S-1 Capsules G, H, I, J, K, and L (continued)**

Table 3
U/Np Capsules
Westinghouse Electric Company
Antech Ltd. Project No. 99-0326W
Dosimetry Characterization; McGuire Unit #2 Cycle #12
Charge Order No. DIPP-7500; Duke Power

Antech Sample ID	Client Sample ID	Parameter Identification		
		Zr-95 A-524 dps/mg	Ru-103 A-524 dps/mg	Cs-137 A-524 dps/mg
9905-0286W	U-238 46 Cd	5.22E0 ± 5.4E-1	3.35E0 ± 5.4E-1	4.27E-1 ± 9.1E-2
9905-0287W	NP-237 42 Cd	8.57E1 ± 2.8E0	4.60E1 ± 3.6E0	7.05E0 ± 4.3E-1
9905-0295W	U-238 47 Cd	7.32E0 ± 1.9E-1	4.80E0 ± 3.7E-1	6.45E-1 ± 4.7E-2
9905-0296W	NP-237-43 Cd	1.25E2 ± 7.9E0	7.42E1 ± 5.8E0	1.03E1 ± 1.0E0
9905-0304W	U-238 48 Cd	8.49E0 ± 8.7E-1	5.55E0 ± 9.1E-1	5.87E-1 ± 1.2E-1
9905-0305W	NP-237 44 Cd	1.55E2 ± 5.0E0	8.48E1 ± 5.0E0	1.30E1 ± 6.8E-1
9905-0313W	U-238 49 Cd	6.44E0 ± 2.4E-1	4.30E0 ± 3.6E-1	5.57E-1 ± 8.9E-2
9905-0314W	NP-237 45 Cd	1.24E2 ± 7.9E0	6.92E1 ± 7.0E0	9.16E0 ± 9.1E-1
9905-0322W	U-238 50 Cd	7.66E0 ± 2.6E-1	5.19E0 ± 4.1E-1	6.63E-1 ± 7.8E-2
9905-0323W	NP-237 46 Cd	6.14E1 ± 6.2E0	3.79E1 ± 5.4E0	4.87E0 ± 8.3E-1
9905-0331W	U-238 51 Cd	1.05E0 ± 8.5E-2	6.72E-1 ± 8.5E-2	6.37E-2 ± 4.9E-2
9905-0332W	NP-237 47 Cd	2.14E1 ± 1.4E0	1.18E1 ± 1.2E0	1.04E0 ± 1.6E-1

Table B-3   Radiometric Counting Results For Sensors Removed From Cycle 12
Cavity Dosimetry Set 2S-1 Capsules G, H, I, J, K, and L (continued)

B-13

Table 4
General Data Table
Westinghouse Electric Company
Antech Ltd. Project No. 99-0326W
Dosimetry Characterization; McGuire Unit #2 Cycle #12
Charge Order No. DIPP-7500; Duke Power

Antech Sample ID	Client Sample ID	Date Collected	Parameter Identification		
			Cobalt (Total) 6010[1] mg/kg	Iron (Total) 6010[1] mg/kg	Nickel (Total) 6010[1] mg/kg
9905-0333W	CHAIN 2S-1(0)		1600	720000	97000
9905-0347W	CHAIN 2S-1 (15)		1600	750000	100000
9905-0361W	CHAIN 2 S-1 (30)		1700	720000	98000
9905-0375W	CHAIN 2S-1 (45)		1700	750000	100000
9905-0389W	Method Blank		<2.0	<10.00	<10.00
9905-0390W	Nist 101E		2000	708300	96360
9905-0391W	True Value NIST 101E		1800	690000	94800

[1] U.S. Environmental Protection Agency, 1987, Test Methods for Evaluating Solid Waste, SW-846, 3rd ed., Office of Solid Waste and Emergency Response, Washington, DC.